Persistent Anti-nociceptive Effect with Nitrous Oxide: A DNA Methylome and Transcriptome Analysis

KOU, Shanglong

A Thesis Submitted in Partial Fulfilment

of the Requirements for the Degree of

Doctor of Philosophy

in

Anaesthesia and Intensive Care

The Chinese University of Hong Kong

September 2017

Thesis Assessment Committee

Professor Tony GIN (Chair)

Professor CHAN Tak Vai (Thesis Supervisor)

Professor WU Ka Kei (Committee Member)

Professor CHENG Hon Ki (Committee Member)

Professor Grocott Hilary (External Examiner)

Declaration of origination

The work contained in this thesis is the original research carried out by the author in the Department of Anaesthesia and Intensive Care, Faculty of medicine, The Chinese University of Hong Kong. No part of the work described in this dissertation has already been or is being submitted to any other degree, diploma or other qualification at this or any other institution.

_____

KOU, Shanglong

Abstract

Persistent Anti-nociceptive Effect with Nitrous Oxide: A DNA Methylome and Transcriptome Analysis

Submitted by KOU, Shanglong

for the degree of Doctor of Philosophy in Anaesthesia and Intensive Care

at The Chinese University of Hong Kong in September 2017.

Previous experiments have shown that single exposure of nitrous oxide produced persistent antinociceptive effect in rats with chronic neuropathic pain. However, the mechanisms for this effect is unknown. We hypothesized that the persistent antinociception after nitrous oxide is due to prolonged effect on *N*-methyl-D-aspartate receptor (NMDA) receptor blockade, or as a result of irreversibly inhibition of methionine synthase leading to DNA demethylation and alteration of downstream pain gene expression. In this thesis, four experiments were conducted to test this hypothesis.

In the first experiment, we confirmed the persistent antinociceptive effect in rats with chronic constriction injury (CCI) to the sciatic nerve. More importantly, nitrous oxide reduced the global methylation level in ipsilateral lumbar spinal cord.

In the second experiment, we performed the transcriptome RNA sequencing in tissue harvested from ipsilateral lumbar spinal cord. The analysis showed that nitrous oxide attenuated global expression levels of CCI-induced dysregulated genes. Furthermore, functional clustering and transcription factor motif enrichment analysis revealed that activating transcription factor 3 (Atf3), was a differentially expressed gene specifically altered by nitrous oxide administration and was therefore a potentially target

responsible for the persistent antinociception. Besides, RNA profiling indicated that NMDA receptors were not involved in the transcriptional regulation of pain related pathways. This was confirmed with Western blotting.

In the third experiment, by genome-wide methylated DNA immunoprecipitation sequencing, we confirmed that nitrous oxide decreased DNA methylation, and identified some nitrous oxide-susceptible differentially methylated regions, which could control the transcriptional activity, including Atf3.

In the last experiment, the function of Atf3 in neuropathic pain modulation was evaluated *in vivo* rat model of chronic neuropathic pain by CCI to the sciatic nerve. Knockdown of Atf3 in spinal dorsal horn of rat attenuated CCI-induced hyperalgesia.

In conclusion, we showed that the underlying mechanism of nitrous oxide-mediated persistent antinociception was associated with hypo-methylation at the lumbar spinal cord level. Atf3 was identified as a transcriptional regulator that attenuated CCI-induced hyperalgesia. Our findings form the basis for the development of preventive and therapeutic strategies in preventing the development of chronic pain.

中文摘要

前期研究表明，在大鼠慢性痛模型中，单一使用一氧化二氮 (N_2O，俗稱笑氣) 就能持續產生緩解疼痛的效應。然而這其中的機制卻不為人知。我們推測，產生這種持續緩解疼痛的效應機制可能有三種：包括 NMDA 受體的持續阻斷，甲硫氨酸合成酶不可逆抑制導致的 DNA 去甲基化和對下游疼痛的表達調控。圍繞上述推測，我們設計了如下四部分實驗。

首先，我們證實了慢性損傷模型中長效延緩疼痛的表型。更重要的，我們發現笑氣能夠抑制脊髓組織的甲基化水準。

通過轉錄組 RNA 測序分析發現，術間使用笑氣能廣泛降低固有疼痛相關基因的表達水準。進一步的功能聚類和轉錄因子富集分析顯示，Atf3 可能是長效疼痛緩解的關鍵靶基因。

進一步，我們通過差異表達基因基本分析和 DNA 甲基化關聯分析，我們發現 Atf3 是最出眾的差異表達基因。此外，轉錄組数据顯示，NMDA 受體並沒有參與到疼痛基因的轉錄調節過程中。

另一方面，我們通過全基因組的 DNA 染色質免疫沉澱測序技術，證實笑氣引起

的區甲基化作用，並鑒定出笑氣敏感的甲基化差異性區域。該區域涉及的轉錄調控作用，能解釋包括 Atf3 在內的差異性轉錄調控。

最後，我們在慢性痛模型裡對 Atf3 基因做功能驗證。我們證實，Atf3 在慢性痛模型裡高表達。並且发现，通過脊髓注射敲降 Atf3 基因能顯著緩解慢性痛模型的痛覺過敏。

綜上，我們發現術間笑氣的疼痛緩解現象，並鑒定出之於相關的轉錄調控機制。進一步發現笑氣扮演表觀調控的角色，能減低甲基化。我們筛选的調控因子 Atf3 能減緩慢性痛的痛覺過敏症狀，從而對慢性痛發生過程起重要作用。

Acknowledgements

I would like to express my sincere appreciation to Professor Matthew Chan to give me the precious opportunity to study in Hong Kong. Thanks very much for his inspiring guidance, enduring patience and responsible supervision through the stages of my PhD study. Without his sustained support, I would not have the opportunity to undertake this study. Also, I would like to extend my thanks to Professor William Wu for his valuable suggestions throughout my study.

Besides, I wish to thank all my colleagues and fellow students in the Department of Anaesthesia and Intensive Care for their technical support and sharing. I am grateful to all of them: Dr Xiaodong Liu, Dr Yuanyuan Tian, Dr. Xiaojie Cheng, Dr Lin Zhang, Dr Shan Zhao, Miss Idy Ho and Mr Hung Chan. I would like to thank Professor Kevin Yip and Mr Alexander Fu from the Department of Computer Science and Engineering, The Chinese University of Hong Kong for their kindly help in bio-information analysis.

This study was supported by a project grant project grant (14/009) and academic enhancement grant (AEG13/001), from the Anaesthesia and Pain Medicine Foundation, Australian and New Zealand College of Anaesthetists (Melbourne, Victoria, Australia).

Conference Presentations:

1. Shanglong KOU, William K.K. WU, Matthew T.V. CHAN. "An Integrated Analysis of Transcriptome and DNA Methylome in Neuropathic Pain" the Five Minute Science Competition (FMSC) in the 5th Australia-China Biomedical Research Conference, Oct 30 – Nov 1 2015, Melbourne, Australia.
2. Shanglong KOU, William K.K. WU, Matthew T.V. CHAN. "Genome-wide analysis of DNA methylation and gene expression defines the analgesia role of nitrous oxide in neuropathic pain" poster presentation in the 4th Annual Congress of the European Society for Translational Medicine, 17th to 20th October, 2016, Prague, Czech Republic.

Table of Contents

List of Figures

List of Tables and Appendixes

List of Abbreviations

Atf3	Activating Transcription Factor 3
CCI	Chronic constriction injury
cDNA	Complimentary DNA
Ct	Cycle threshold
DEGs	Differentially expressed genes
DMRs	Differentially methylated regions
DNA	Deoxyribonucleic acid
DNMT	DNA (cytosine-5)-methyltransferase
FDR	False discovery rate
FPKM	Fragments per kilobase of exon model per million mapped reads
GO	Gene Ontology
KEGG	Kyoto Encyclopedia of Genes and Genomes
MeDIP	Methylated DNA immunoprecipitation sequencing
mCs	Methylated cytosines
mRNA	Messenger RNA
N_2O	Nitrous oxide
NMDA	*N*-methyl-D-aspartate
TFs	Transcription factors
TFBS	Transcription factors -binding site
PPI	Protein-protein interaction
dNTP	Deoxyribonucleotide triphosphaste
5mC	5-methylcytosine

PART I INTRUDUCTION

Chapter1 Literature Review

I. Chronic Postsurgical Pain: Definition, Epidemiology and Impact

Chronic postsurgical pain is defined as pain that persisted for more than three months after index surgery and that is not associated with recurrence of disease or due to pre-existing pain syndrome (Niraj et al., 2011; Crombie et al., 1999; Werner et al., 2014). Chronic postsurgical pain has been reported to affect about 10% of patients having common surgical operations (Katz et al., 2009; Johansen et al., 2012; Montes et al., 2015; Liu et al., 2015).

Several risk factors, including younger age, female, current smokers, preoperative anxiety, preoperative pain syndrome and type of surgical procedure, have been shown to increase the risk of chronic postsurgical pain (Hinrichs-Rocker et al., 2009; Steyaert et al., 2012; Liu et al., 2015; Johansen et al., 2012; Montes et al., 2015; Chan et al., 2011; Chan et al., 2016). Table 1 shows the incidence rates for chronic pain development after various kinds of surgery. Notably, chronic postsurgical pain has been reported that up to 80% of patients having limb amputation surgery (5% - 80%, n = 552) (Jensen, et al. 1985; Sherman, et al. 1984). Interestingly, many patients experienced neuropathic symptoms, such as dysesthesia or allodynia, indicating the possibility of nerve injury during many surgical procedures (Chan et al., 2011; Chan et al., 2016; Liu et al., 2015).

Table 1. Incidence rate of chronic postsurgical pain.

Surgery	No. of studies	No. of Patients	Incidence	References
Cesarean section	2	611	9-19%	Nikolajsen et al. 2004; Eisenacg et al. 2008
Cardiac surgery	3	2,293	15-59%	Bruce et al. 2003; Meyerson 2001; Mueller 2000
Limb amputation	2	552	5-80%	Ephraim 2005
Hernia repair	2	1,440	2-19%	Cunningham et al. 1996
Hysterectomy	2	1,173	22-32%	Gilron et al. 2005; Ilias and Jansen 1996; Rorarius 2004
Thoracotomy	2	204	10-42%	Conacher 1992; Richardson and Sabanathan 1994
Breast surgery	3	3,253	5-47%	Kroner et al. 1989; Stevens 1995; Wallace et al. 1996

Chronic postsurgical pain has a negative impact on quality of life and adversely affects daily activities of patients including general activity, mood, walking, relations with others, sleep and enjoyment of life (Chan et al., 2011; Chan et al., 2016; Liu et al., 2015). Consequently, there is a loss of productivity at work, an increase in medical expenses for both in-patient and out-patient services and the development of potential complications, such as dependency and addiction to drug treatments (Hojsted et al., 2010; O'Connor et al., 2009).

Several treatment strategies have been evaluated to prevent chronic postsurgical pain. These include methylprednisolone (Turan et al., 2015), gabapentin and pregabalin (Schmidt et al., 2013; Chaparro et al., 2013; Konstantatos et al., 2016) and other non-steroidal anti-inflammatory drugs. Other treatments include membrane stabilizers, such as gabapentin, tiagabine and topiramate. These drugs block the transmission of ectopic nerve impulses and may improve quality of life for patients with chronic pain in non-operative setting (Backonja M et al., 1998; Sachin B et al., 2016). These treatments have produced mixed results (Chaparro et al., 2013; Humble et al., 2015), therefore, a search for an effective treatment to prevent chronic postsurgical pain is therefore highly desired.

1. Mechanism of Chronic Postsurgical Pain

Inflammatory reaction is considered as an important event during the development of chronic postsurgical pain. Injury to peripheral nerve and other tissues during surgery produces neuro-inflammation in the dorsal root ganglia and dorsal horn of the spinal cord. Current evidence suggested that the interaction between the immune system and the ascending neural circuitry is crucial for the development and maintenance of

chronic pain (Bliss et al., 1993; Sandkuhler et al., 2009). Figure 1.1 shows that damaged sensory neurons activate microglial cells via toll-like and fractalkine receptors (e.g. CX3C chemokine receptor 1, CX3CR1) to initiate neuron-to-glia signaling (Verge et al., 2004; Kim et al., 2007; Tanga et al., 2005). A large body of evidence also indicates that non-neural cells actively contribute to the development of neurodegenerative diseases. In this respect, microglial P2X purinoceptor 4 receptor (P2X4R) is one of the most important microglia–neuronal signaling pathways by mediating the release of brain-derived neurotrophic factor (BDNF). In addition, the adenosine triphosphate (ATP) binds to spinal P2X4R and stimulates microglia, resulting in the release of calcium ions. The P2X4 receptor then activates intracellular p38-mitogen-activated protein kinase, leading to the accumulation of brain-derived neurotrophic factor (BDNF). This promotes phosphorylation of the NR1 subunit of N-methyl-d-aspartate (NMDA) receptors in the dorsal horn (Tsuda et al., 2003; Ulmann et al., 2008; Trang et al., 2009). In animal experiments, drugs modifying functions of glial cells, including interleukin (IL)-1β antagonist (Binshtok et al., 2008), tumor-necrosis factor (TNF)-α inhibitor and cannabinoid agonists (Verri et al., 2006), have been reported to reduce neuropathic pain.

Taken together, these studies indicate that multiple cellular and molecular sites are involved in the development of chronic postsurgical pain. A master transcriptional regulator on controlling pain-related signaling pathways may be responsible for the chronic pain development.

Figure1.1 Schematic diagram showing the interactions between neuron and microglia at initiation of chronic pain.

Microglial cells are activated by factors such as fractalkine, as well as adenosine triphosphate (ATP) through neurotransmission. ATP binding to the purinergic receptor P2RX4 triggers microglial activation after nerve injury. The activation of P2X purinoceptor 4 receptor (P2X4R) and CX3C chemokine receptor 1 (CX3CR1) on microglia then causes phosphorylation of p38, leading to increased synthesis and release of brain-derived neurotrophic factor (BDNF). The increased BDNF promotes the inhibition of GABAergic currents in dorsal neuron. In addition.

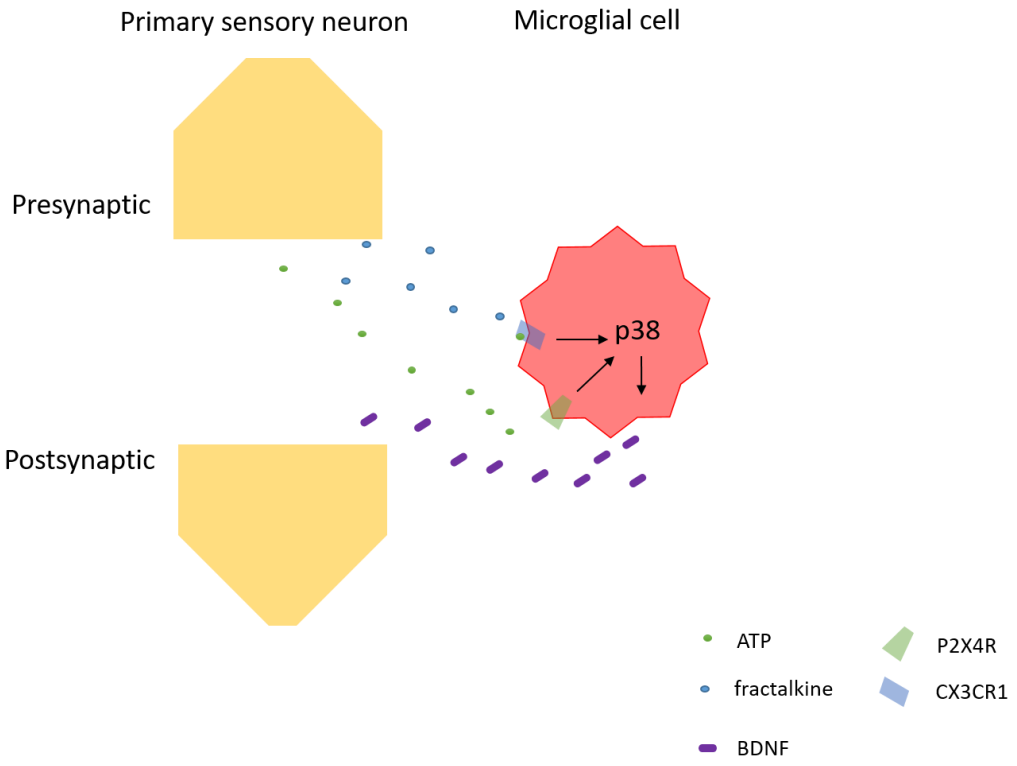

2. Neuropathic Pain and DNA Methylation

DNA methylation is the process by which methyl groups are added to the DNA molecule (Suzuki et al., 2008). DNA methylation exhibits specificity with respect to cells, tissues and diseases due to the differences in differentially methylated regions (DMRs) (Bird et al., 2002). The first study that highlighted the effect of DNA methylation on neuropathic pain showed that intrathecal injection of 5-azacytidine (a drug used to remove methyl groups from DNA) inhibited global DNA methylation and MeCP2 expression, resulting in a decrease of mechanical allodynia in chronic constriction injury (CCI) of the sciatic nerve (Wang et al., 2011). CCI is a partial nerve injury, which is produced by placing several ligatures around the sciatic nerve, to induce constriction of the nerve (Sugimoto et al., 1990). In addition, DNA methylation was increased in the promoter region of secreted protein acidic and cysteine rich (SPARC) gene and was associated with the development of chronic pain in both mice and humans (Tajerian et al., 2011). This gene encodes a cysteine-rich acidic matrix-associated protein and is also involved in extracellular matrix synthesis and promotion of changes to cell shape. Similarly, methylation of endothelial receptor type B (encoded by the EDNRB gene, a G protein-coupled receptor which activates the phosphatidylinositol-calcium) attenuated cancer-induced pain in mice (Viet et al., 2011). Another nociceptive gene cystathionine-β-synthase (CBS) is a major contributor to cellular hydrogen sulfide production and was shown to be upregulated with DNA demethylation in an inflammatory pain model of rats (Qi, et al., 2013). Recent studies showed that the expression of P2X3R was markedly enhanced in animals with demethylated CpG islands in the promoters. This was accompanied with the down-regulation of DNA methyltransferase (DNMT) 3b, which may also alter transcriptional regulation (Zhang et al., 2015). More recently, blood samples from 12

chronic pain patients showed a decrease in messenger RNA (mRNA) of transient receptor potential ankyrin 1 gene (TRPA1, a member of the transient receptor potential superfamily of ion channels) and an increase in methylation of CpG islands, correlated with the onset of neuropathic pain (Sukenaga, et al.,2016). Taken together, these findings showed that DNA demethylation may up-regulate pain-related genes and disrupt subsequent expression of DNA methyltransferases.

II. Nitrous Oxide and Chronic Postsurgical Pain

Nitrous oxide is a commonly used analgesic and anesthetic agent for over 150 years. In animal experiments using Fischer (F244) rats, nitrous oxide exposure for 30 minutes demonstrated a profound antinociceptive effect. (Stevens et al., 1983; Quock et al., 1993). Similarly, a single administration of nitrous oxide 50% produced a significant reduction in nociception as measured by paw pressure vocalization test in adult male Sprague-Dawley rats. In addition, nitrous oxide prevented fentanyl-induced hyperalgesia (Bessiere et al., 2007). More importantly, 50% of nitrous oxide did not only provide antinociceptive effect during exposure, but also relieved heat hyperalgesia and mechanical allodynia that lasted for more than a month after chronic constriction injury to the sciatic nerve (Bessiere et al., 2010; Ben Boujema et al., 2015). These findings suggested that nitrous oxide may provide long-term antinociception and would be convenient to administer during anesthesia for the prevention of chronic postsurgical pain.

Our group has investigated the potential long-term analgesic effect of nitrous oxide. In a long-term follow-up study of 640 patients enrolled to the Evaluation of Nitrous Oxide in General Anesthesia (ENIGMA) trial, administration of nitrous oxide 70% for

more than 2 hours during the index surgery decreased the risk of chronic postsurgical pain compared with oxygen 80% (12.9% versus 5.6%). After the adjusting for wound size, acute pain severity, preoperative anxiety and presence of wound complication or not, the odds ratio was 0.38 [95% confidence intervals (CI): 0.14–0.98, $p = 0.04$] (Chan et al., 2011). Since this is a single-center study with a limited number of patients and a long-term follow-up (median 4.5 years), our group has conducted a more extensive investigation in 2,924 patients recruited to the ENIGMA-II trial (Chan et al., 2016). At one-year after surgery, we collected responses from patients by structured phone interview to seek if there was a pain over the wound that persisted from the index surgery using the modified Brief Pain Inventory (Wang et al., 1996). A total of 12.1% of patients experienced chronic postsurgical pain. In ENIGMA-II, 11.8% of patient in the nitrous oxide group and 12.5% in the no-nitrous oxide group experienced chronic postsurgical pain, while the relative risk after the adjusting for missing data was 0.92 [95% CI: 0.74–1.15, $p = 0.47$]. However, in a sub-group analysis, we found Asian patients had a lower risk of chronic postsurgical pain after nitrous oxide administration [adjusted relative risk (95% CI) = 0.70 (0.50–0.97), $p = 0.048$]. Interestingly, the effect of nitrous oxide on preventing chronic postsurgical pain seemed to be influenced by methylenetetrahydrofolate reductase (MTHFR) gene polymorphisms, such that a decreased enzyme activity with homozygous gene polymorphism was associated with the greater effect on nitrous oxide (Weisberg et al., 1998; Shan et al., 1999; Nagele et al., 2008). The gene MTHFR encodes a cosubstrate for homocysteine remethylation to methionine. Nature variances have been reported in this gene which influence susceptibility to mangy diseases, such as neural tube defects, Alzheimer's disease and acute leukemia (Födinger et al., 2000; Trimmer EE, 2013). Since the genetic basis for individual variations has been reported to associate with pain perception and even the

development of a chronic pain condition among different populations (Luda Diatchenko et al., 2005; Klepstad P et al., 2011), these findings suggested that nitrous oxide may prevent the development of chronic postsurgical pain through the folate and methylation cycles, as well as DNA demethylation. Nevertheless, there may be other mechanisms contributing to the lower risk of chronic postsurgical pain with nitrous oxide.

Table 2. Association between methylenetetrahydrofolate reductase gene polymorphisms and chronic postsurgical pain in the ENIGMA-II Trial.

Genotypes	No Pain (%)	Chronic pain (%)	Odds ratio (95%CI)	*p* value
1298A>C				
All patients				
Wild-type (AA)	86.3%	13.7%	Reference	
Heterozygous (AC)	91.5%	8.5%	0.58 (0.34-1.03)	0.082
Homozygous (CC)	94.8%	5.2%	0.35 (0.14-0.85)	0.025
No-Nitrous oxide				
Wild-type (AA)	85.4%	14.6%	Reference	
Heterozygous (AC)	87.7%	12.3%	0.82 (0.41-1.65)	0.706
Homozygous (CC)	91.8%	8.2%	0.52 (0.17-1.61)	0.366
Nitrous oxide				
Wild-type (AA)	87.2%	12.8%	Reference	
Heterozygous (AC)	94.9%	5.1%	0.37 (0.15-0.89)	0.037
Homozygous (CC)	97.0%	3.0%	0.21 (0.05-0.96)	0.043
667C>T				
All patients				
Wild-type (CC)	85.4%	14.6%	Reference	
Heterozygous (CT)	91.3%	8.7%	0.56 (0.33-0.95)	0.043
Homozygous (TT)	96.2%	3.8%	0.23 (0.08-0.67)	0.007
No-Nitrous oxide				
Wild-type (CC)	84.8%	15.2%	Reference	
Heterozygous (CT)	87.2%	12.8%	0.82 (0.41-1.65)	0.121
Homozygous (TT)	94.6%	5.4%	0.32 (0.09-1.13)	0.110
Nitrous oxide				
Wild-type (CC)	86.0%	14.0%	Reference	
Heterozygous (CT)	94.7%	5.3%	0.35 (0.150-0.80)	0.019
Homozygous (TT)	98.0%	2.0%	0.13 (0.016-0.99)	0.044

CI = confidence intervals

1. The mechanism of nitrous oxide-mediated analgesia

1.1 Adrenoceptor

Previous studies have shown that nitrous oxide increased norepinephrine concentration in the spinal cord, while intrathecal administration of α_2-adrenoceptor antagonists attenuated the release of norepinephrine (Zhang et al., 1999) and produced antinociceptive effects (Guo et al., 1996). Similarly, a subsequent study found that nitrous oxide activated c-Fos labeled neurons and inhibited noradrenergic cells. These effects resulted in an impairment of nitrous oxide-associated antinociceptive effect (Awamura et al., 2000). In addition, studies using knockout mice of various α_2-adrenoceptor subtypes identified that α_{2B} subtype was responsible for nitrous oxide associated antinociception (MacMillan et al., 1996; Link et al., 1996).

1.2 Opioid receptor

As early as 1970s, researchers had reported that nitrous oxide produced a dose-dependent antinociceptive effect which was attenuated by subcutaneous injection of opioid receptor antagonists (Berkowitz et al., 1976; Berkowitz et al., 1977). Numerous studies have identified that specific opioid receptor subtypes were involved in nitrous oxide-associated antinociceptive effect. Interestingly, it is dependent on the species and strains studied and on the behavioral paradigms tested (Quock et al., 1993; Smith et al., 1978; Willer et al., 1985; Quock et al., 1990; Quock et al., 1991; Quock et al., 1990; Gillman et al., 1986). In the Sprague-Dawley rats, κ- and μ- opioid receptor subtypes exerted inhibitory effects against nitrous oxide-associated antinociception (Quock et al., 1990; Hodges et al., 1994; Hara et al., 1994).

1.3 NMDA receptor

Nitrous oxide has long been regarded as a NMDA antagonist that inhibited calcium current for neuronal protection (Jevtovic-Todorovic et al., 1998). Nitrous oxide reduced NMDA receptor-mediated excitatory postsynaptic currents (Mennerick et al., 1998; Ranft et al., 2007) and selectively blocked T-type calcium currents on histidine 191, resulting in a decrease in inflammatory pain processing (Todorovic et al., 2001; Orestes et al., 2011).

Interestingly, a previous study showed that the null mutant of *nmr-1* gene, which encodes the NMDA receptor in Caenorhabditis elegans, was completely resistant to the nitrous oxide-induced behavioral effects (Nagele et al., 2004). The inhibitory effect of nitrous oxide was not affected by the mutation of residues in the transmembrane segment 3 of the NR1 subunit (F639A) or in TM4 of the NR2A subunit (A825W) (Ogata et al., 2006). Recent studies showed that GluR1 subunit knockout or GluN2A subunit knockout mice exhibited resistance to nitrous oxide (Petrenko et al., 2010; Petrenko et al., 2013). Besides, E subunit of NMDA receptor was also reported to mediate the anesthetic effect of nitrous oxide (Sato et al., 2005). All these studies suggested that NMDA receptors are involved in the nitrous oxide-induced antinociception.

Others have investigated the effects of isoflurane/nitrous oxide anesthesia on protein expression of NMDA receptor subunits. In their study, a persistent increase in NR2B protein expression was found at 3 months after anesthesia in the hippocampus and cortex (Mawhinney et al., 2012). In this regard, prolonged (4 hours) treatment with nitrous oxide significantly increased MK801 binding to NMDA receptor (Stover et al.,

2004). Similarly, pretreatment with MK801 significantly enhanced the discriminative effects of nitrous oxide (Richardson et al., 2015).

Taken together, these studies showed that neuronal receptor-mediated interaction are involved in nitrous oxide-associated antinociceptive effect. Antagonists of opioid receptor and adrenoceptor attenuate the antinociceptive actions of nitrous oxide. Nitrous oxide *per se* antagonizes NMDA receptor activity. Interestingly, some work even reported that DNA methylation in these receptor gene regions correlates with clinical pain syndrome (Parrish et al., 2013). This study implies that DNA methylation may be an early event triggered by nerve injury that persists into the development of chronic pain.

2. Possible mechanisms for nitrous oxide-associated persistent antinociception

Based on our literature review, there are at least three mechanisms that contribute to persistent antinociception with nitrous oxide administration.

2.1 Transcriptional regulation of NMDA signaling pathway

A large body of evidence showed that nitrous oxide produced acute antinociception by blocking the NMDA receptor, in mRNA expression level (Dickenson et al., 1997; Gao et al., 2005; Ultenius et al., 2006), as well as in protein phosphorylation level (Jevtovic-Todorovic et al., 1998). The later blockage may attenuate the development of chronic pain (Dickenson et al., 1997). It is therefore hypothesized that persistent influence on the expression or cellular activity of NMDA subunits may contribute to the long-term antinociception by nitrous oxide administration.

2.2 Nitrous oxide-impaired DNA methylation

It is well-known that nitrous oxide inactivates methionine synthase which resulted in an elevation of plasma homocysteine (Deacon et al., 1980). The effect on methylation cycle disrupts the folate and vitamin B12 metabolism (Wilson et al., 1986), resulting in DNA demethylation and the development of chronic pain (Bell et al., 2014) (Figure1.2). Given that global DNA demethylation attenuated hypersensitivity to nociception (Wang et al., 2011), we hypothesized that nitrous oxide inhibits global DNA methylation. The DNA demethylation-mediated transcriptional regulation of pain-related genes may contribute to the long-term antinociception.

Figure1. 2 Schematic diagram showing of nitrous oxide inhibits folate and vitamin B12 metabolism.

Nitrous oxide inhibits methionine synthase (MS) by oxidizing the cobalt atom of cobalamin (Cbl). This reaction converts monovalent cobalamin (Cbl^{I}) to trivalent cobalamin (Cbl^{III}). The results are a decrease in tetrahydrofolate (THF) and nucleotide production in the folate cycle. MS inhibition also decreases S-adenosyl methionine (SAM) concentration, a methyl donor for DNA methylation and accumulation of homocysteine.

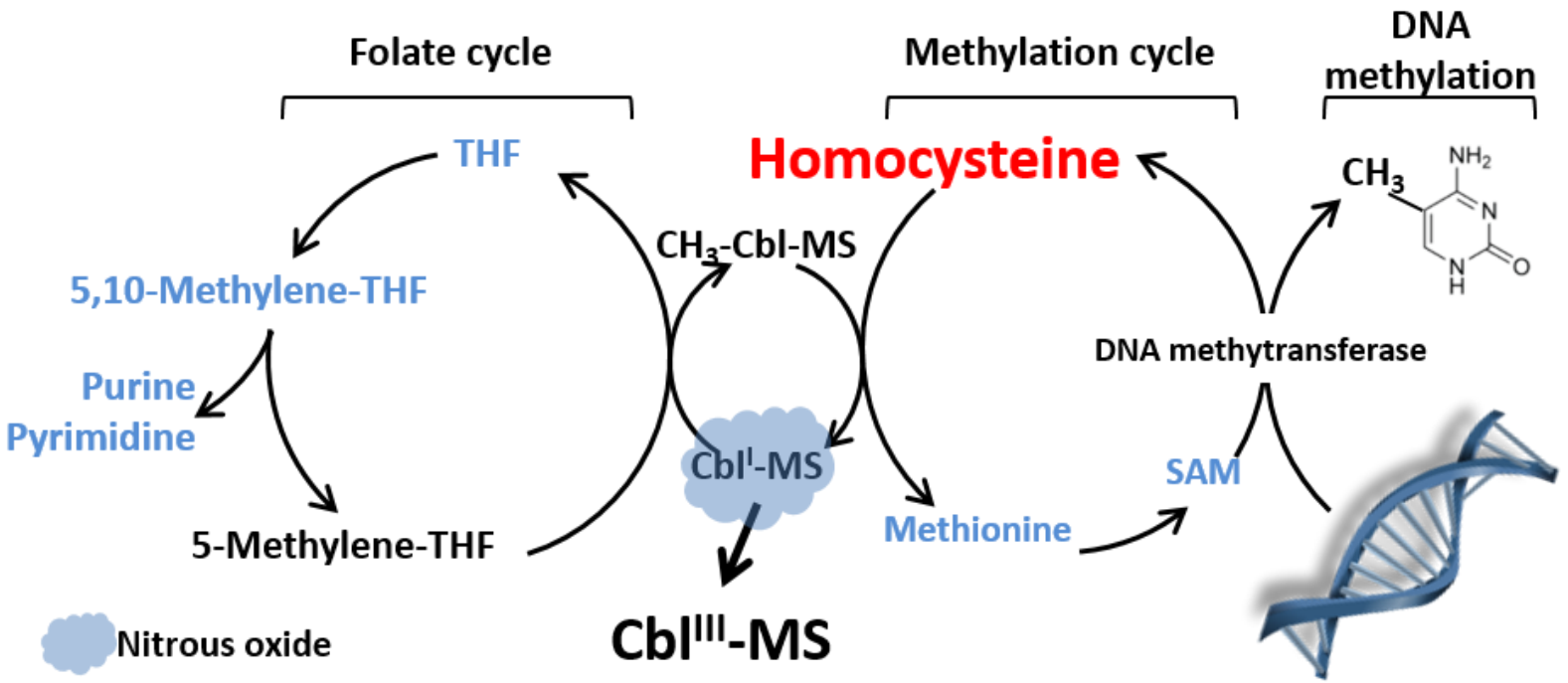

2.3 The transcription factor-centered regulatory network

Although there are evidences to suggest that nitrous oxide produced long-term antinociception by the blockade of NMDA receptor and DNA methylation, it is possible that other signaling pathways are involved in the control of neuronal excitability during the development of chronic pain (Baranauskas et al., 1998; Woolf et al., 2011). This may be derived from the crosstalk between the immune system and neural circuitry (Bliss et al., 1993; Sandkuhler et al., 2009) induced by the inflammatory response to surgical trauma. Nitrous oxide has been reported to impair the activity of neutrophil granulocytes (Lehmberg et al., 2008), indicating that it has an influence on the inflammatory response in central nervous system. Therefore, we hypothesized that transcription factor-based regulation of pain-related genes is another potential mechanism for nitrous oxide induced long-term antinociception.

In summary, our clinical studies showed that nitrous oxide exhibited preventive analgesic effect for chronic postsurgical pain. Furthermore, Asian patients had a lower risk of chronic postsurgical pain after nitrous oxide administration. Previously functional studies suggested that DNA methylation-mediated modification, or transcriptional regulation of pain-related pathways, such as NMDA receptor, may explain for the persistent antinociceptive / analgesic effect of nitrous oxide.

Chapter 2 Hypothesis & Study Design

I. Hypothesis

This study aims to explore the molecular mechanism of nitrous oxide-induced persistent analgesic effect. We hypothesized that transcriptional regulation of nitrous oxide-susceptible pain-related genes are involved in the persistent analgesic action.

There are four specific hypotheses include:

(1) Intraoperative administration of nitrous oxide has a prolonged analgesic/antinociceptive effect on the development of chronic pain.

(2) Nitrous oxide-triggered DNA demethylation contributes to the persistent analgesic actions.

(3) Transcriptional activated NMDA receptor signaling is correlated with the prolonged antinociception.

(4) Transcriptional regulator-mediated alteration on pain-related signaling pathways is responsible for the attenuated hyperalgesia.

II. Study design

To test the above hypotheses, three parts of experiments are included. Firstly, we established the chronic pain model, and confirmed the long-term antinociceptive effect with administration of nitrous oxide. We then performed the RNA and DNA methylation sequencing to explore the potential targets. Finally, we conducted *in vivo* study to clarify the functions of potentially targeted molecule.

1. Experimental Procedures

Outline of the experimental procedures is shown in Figure 2.1. Four groups of 10 rats

each were included as follow: They received 70% nitrous oxide or nitrogen; having CCI or sham surgery to sciatic nerve. We then measured heat hyperalgesia and mechanical allodynia to evaluate the effects of prolonged antinociception. After collection and extraction of spinal dorsal horn, RNA sequencing and MeDIP sequencing was performed for further detection and analysis.

Figure 2. 1 Schematic diagram of experimental procedures

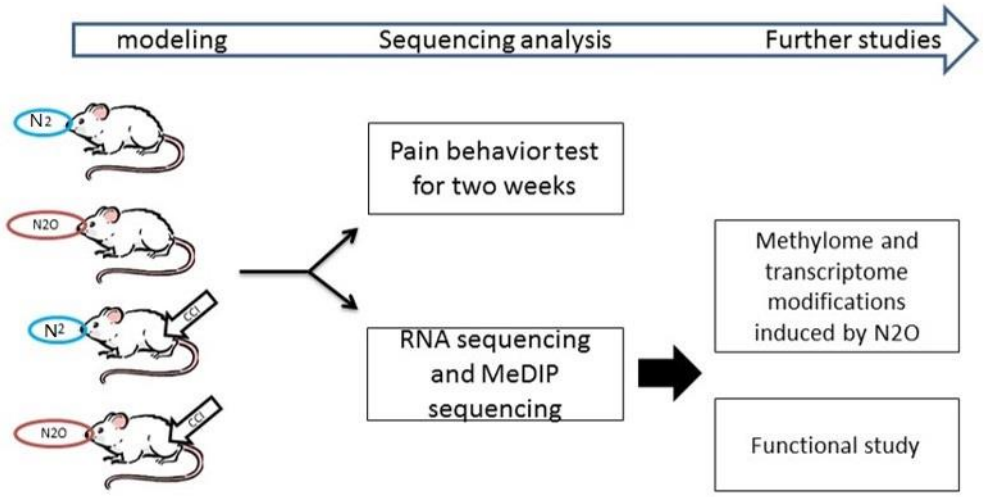

2. Methylome and Transcriptome Studies

The following methylome and transcriptome analyses were performed:

(1) Differentially expression genes (DEGs) analysis,

(2) Functional clustering enrichment analysis,

(3) Transcription factor motif enrichment analysis,

(4) Differentially methylated regions (DMRs) analysis, and

(5) DMR-DEG paired analysis

To delineate the mechanism, we explored the transcriptional changes by nitrous oxide. We first identified the transcriptional changes associated with the development

of chronic pain. In order to characterize and provide an overview of the biological functions of genes involved in the protection against chronic pain by nitrous oxide, we performed Gene Ontology (GO) enrichment analysis and KEGG annotation analysis. To further uncover the potential regulatory role of nitrous oxide in the development of neuropathic pain, TF-binding site (TFBS) enrichment analysis was performed with previously common dysregulated genes in two CCI groups. Finally, we further defined the differentially methylated regions and correlated them with associated DEGs.

3. Functional Verification of Targeted Gene

Figure 2.2 outlines the *in vivo* functional testing of targeted gene. We first conducted spinal injection of lentivirus-based shRNA to inhibit the expression of targeted gene. Then CCI surgery was done to evaluate the effects of knockdown on pain-like responses, just after confirmation of the knockdown efficiency.

Figure 2. 2 Schematic diagram of functional study

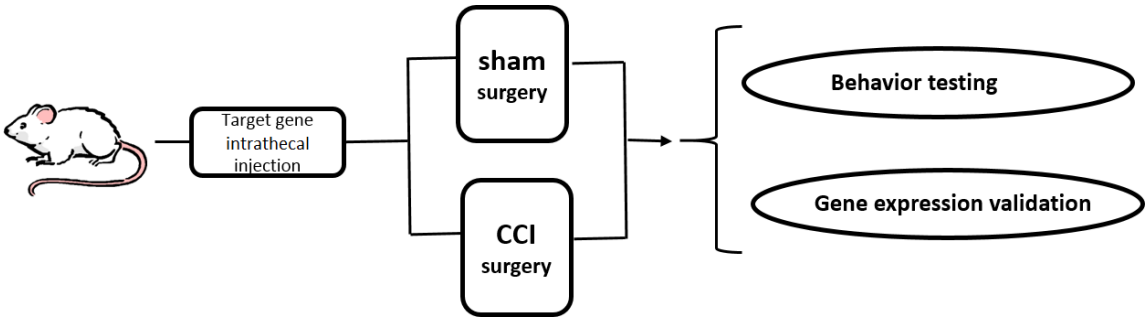

PART II EXPERIMENTS

Chapter 3 Prolonged Antinociception with Nitrous Oxide in Experimental Neuropathic Pain

3.1 Introduction

Nitrous oxide is widely used as an anesthetic-analgesic agent during surgery. Nitrous oxide reduced nociception to pain stimulus through its action on the brain and spinal cord (Luginbuehl et al., 2000; Fujinaga et al., 2002). It is commonly believed that the antinociceptive effect diminished rapidly with the cessation of administration when nitrous oxide is eliminated from the body. This traditional view is however challenged by a rat experiment (Bessiere et al., 2010). In this experiment, 50% of nitrous oxide given for 1 hour and 15 minutes produced a prolonged antinociceptive effect in a neuropathic pain model of CCI to the sciatic nerve. One week after CCI, rats received nitrous oxide during surgery showed a 37 - 45% reduction in hyperalgesia and allodynia. This effect was exaggerated with repeated treatments of nitrous oxide.

In this experiment, we explored the analgesic effect of intraoperative administration of nitrous oxide. We hypothesized that nitrous oxide administration attenuated nociception with CCI of the sciatic nerve for the initiation of chronic neuropathic pain. in rats.

3.2 Materials and methods

3.2.1 Animals

Adult male Sprague Dawley rats, weighing 220 - 250 g, were used in our experiments. The animals were housed in a 12-hour alternating light-dark cycles, at 22 ± 2 °C, in

the animal room of the Prince of Wales Hospital. Rats were provided with standard rodent chow and tap water. The experimental protocol was approved by the Animal Experimentation Ethics Committee of the Chinese University of Hong Kong, and the experimental procedures were complied with the Hong Kong Animals Act [no. (14-867) in DH/HA&P/8/2/1 Pt.44].

3.2.2 Induction of neuropathic pain by chronic constriction injury

Animals were anesthetized with 2% isoflurane under 70% nitrous oxide and 30% oxygen or 70% nitrogen and 30% oxygen. The left sciatic nerve was exposed at mid-thigh level by blunt dissection (Figure 3.1.B). Three 4-0 chromic catgut (U203H, Ethicon Inc., Somerville, NJ) ligatures were loosely placed around the dissected nerve. The wound was then closed in layers. Sham rats were subjected to surgical procedure to expose left sciatic nerve without nerve ligation.

3.2.3 Mechanical allodynia - Electronic von Frey withdrawal threshold

Each rat was placed in a small plastic cage on the metal mesh floor to acclimate to the surroundings for 15 min. Nociception was then measured using von Frey filaments (Stoelting, Wood Dale, IL, USA) or electronic von Frey anesthesiometer (IITC Inc., Life Science Instruments, Woodland Hills, CA, USA). We applied the filaments or the polypropylene tip perpendicularly to the central area of the hindpaw with a gradual increase in pressure. Mechanical sensitivity of the hind paw was measured on each other day after surgery. For baseline testing, animals were weighed and placed into the behavior test room for 2 hours on alternate day for three times to allow familiarization with the room environment and test apparatus. Using the von Frey hairs, each tip of a series of von Frey filaments was applied to the hind paw five times at intervals of 5

seconds and the threshold was taken as the lowest force that evoked a brisk withdrawal response to one of the five repetitive stimuli (Eliav et al., 1999). Each filament was applied five times for 2 seconds. After using the traditional von Frey hairs in our initial study to confirm the CCI-induced chronic pain model, we switched to the electronic von Frey anesthesiometer because it provides wider range of measurements. Using the electronic von Frey anesthesiometer, the threshold was recorded and repeated three times with an interval of 5 min between stimuli (Figure3.1.C). The paw withdrawal threshold (PWT) for each rat was determined from three to five measurements of positive responses. Measurements were performed one week before surgery (baseline) and then on day 1, 3, 5, 7, 10 and 14 after surgery.

3.2.2 Heat hyperalgesia - noxious heat stimulus withdrawal latency

A plantar analgesimeter (IITC Life Science, Woodland Hills, CA) was used to measure the latency of response to noxious heat stimulus. Laser radiant heat source was projected to the plantar surface of the ipsilateral paw after acclimatization (Figure3.1.D). Three latency measurements were taken to calculate the average paw withdrawal latency (PWL) for each testing on the same day with the withdrawal threshold test. The baseline values were tested three times one week before the surgery and then on day 1, 3, 5, 7, 10 and 14 after surgery.

3.2.3 Nitrous oxide administration

A total of 40 rats were divided randomly into the four experimental groups. In each occasion, two rats were taken from each group for nitrous oxide or nitrogen in oxygen administration and CCI or sham surgery. We repeated the experiments 5 times, so that a total of 10 rats per group was included.

Rats were placed in a plexiglas chamber for drug administration (Figure 3.1.A). The gas mixture of 70% nitrous oxide and 30% oxygen was delivered to the chamber at 3 L/min for a total of 2 hours. It should be noted that the minimum alveolar concentration (MAC) for nitrous oxide is 104% in humans (Hombein et al., 1982), but the MAC is 2 atmosphere in Sprague-Dawley rats (Charles et al., 1994). Inspired concentrations of oxygen and nitrous oxide were measured by a built-in gas analyzer, calibrated with a commercially available gas standard (Scott Medical, Plumsteadville, PA).

3.2.4 Statistical Analysis

Mechanical nociceptive threshold (PWT) and the withdrawal latency (PWL) were expressed as means ± standard errors of the mean. Average of 10 rats were included in the study. Differences in PWT or PWL between groups were tested using analysis of variance (ANOVA) for repeated measures. *Post-hoc* intergroup differences were tested with unpaired *t* test.

Figure3. 1 Experimental setup of (A) nitrous oxide administration and (B) surgery of chronic constriction injury - left sciatic nerve was exposed (arrows), with loose ligatures placed around the nerve. Diagrams of the electronic von Frey withdrawal threshold testing (C) and noxious heat stimulus withdrawal latency testing (D).

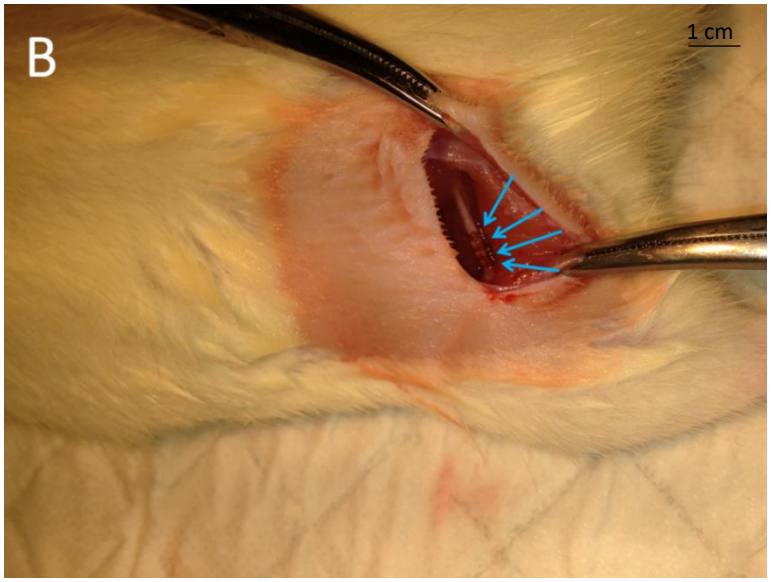

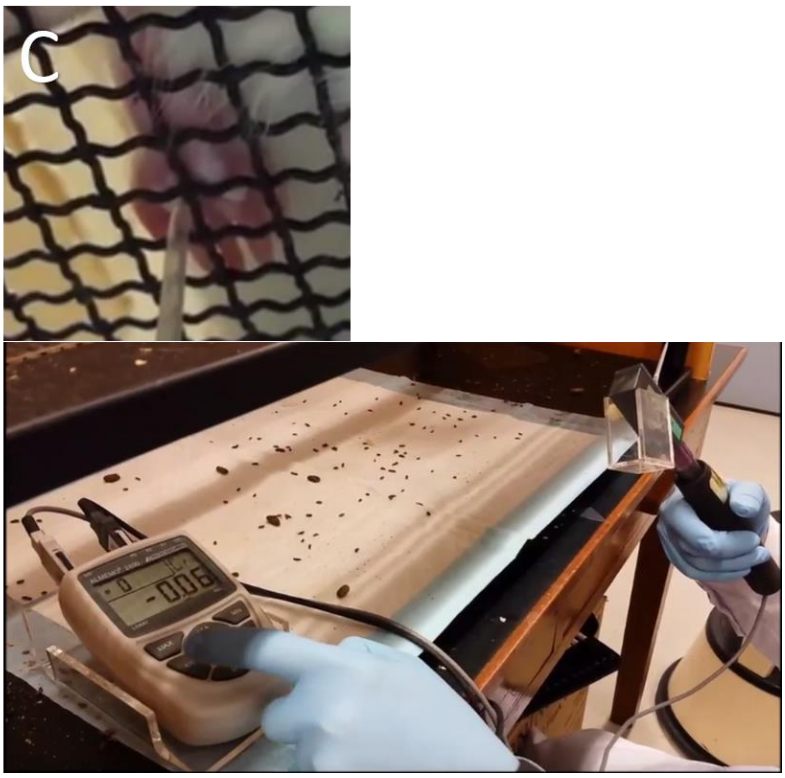

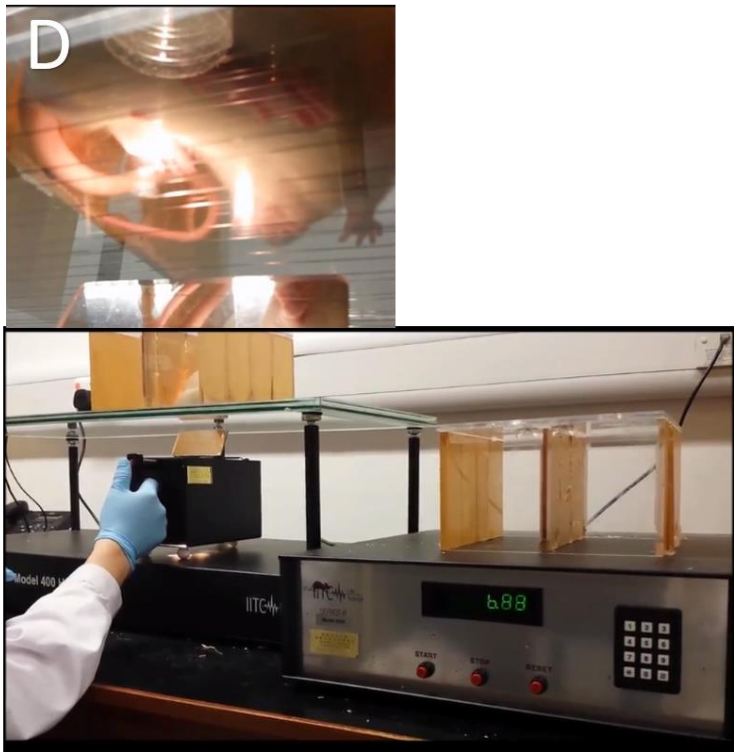

3.3 Results

3.3.1 Nitrous oxide administration reduces mechanical allodynia

Four groups of 10 rats receiving nitrous oxide or nitrogen; having CCI or sham surgery to sciatic nerve (named as N_2O/CCI, N_2/CCI, N_2O/Sham, N_2/Sham, respectively) were used to study the influence of nitrous oxide administration on the development of neuropathic pain. Figure 3.2 showed that CCI produced a significant decrease in PWT compared with the sham surgery group throughout the study period ($p < 0.001$; ANOVA), indicating the well-established chronic neuropathic pain model. Furthermore 70% nitrous oxide had no effect on PWT in rats having sham surgery. However, nitrous oxide attenuated mechanical allodynia. In this respect, PWT was higher in rats receiving nitrous oxide compared with no-nitrous group (N_2/CCI), $p < 0.01$.

3.3.2 Nitrous oxide administration alleviates heat hyperalgesia

Figure 3.3 showed the changes in PWL after latent heat exposure to the ipsilateral paw. PWL was significantly lower in CCI groups compared with sham surgery ($p < 0.001$ ANOVA). While nitrous oxide had no effect on PWL in animals receiving sham surgery, nitrous oxide increased PWL compared with no-nitrous group (N_2/CCI) in rats receiving CCI surgery. It should be noted that the antinociceptive effect persisted for another 7 days (raw data are displayed in Table 3).

Table 3. Raw data of behavior testing results

MECHANICAL ALLODYNIA

	No-nitrous oxide/Sham surgery									
BASELINE	35.94	37.23	37.41	38.50	38.52	38.52	39.43	40.27	41.10	41.31
DAY 1	36.63	40.63	40.56	40.49	39.99	38.87	38.39	37.64	37.18	36.92
DAY 3	37.71	38.05	38.50	39.51	39.72	40.04	36.40	36.61	37.35	37.35
DAY 5	41.89	42.08	35.98	36.51	37.55	37.71	38.84	39.05	36.95	41.21
DAY 7	41.34	41.77	43.41	35.80	37.11	39.63	40.31	40.55	40.67	40.94
DAY 10	42.81	37.33	37.96	38.17	38.40	38.40	39.23	39.26	41.40	42.75
DAY 14	33.03	33.03	33.89	37.03	37.05	38.53	40.08	40.76	41.18	41.72
	Nitrous oxide/Sham surgery									
BASELINE	35.25	41.34	36.82	37.97	38.93	39.79	40.21	40.67	40.96	42.88
DAY 1	40.35	32.02	35.64	36.35	36.71	38.08	38.61	38.70	40.04	40.15
DAY 3	41.86	34.44	34.60	34.86	36.67	36.95	37.58	38.51	38.87	40.76
DAY 5	42.08	36.06	36.06	40.87	43.56	41.21	41.89	38.84	39.05	36.95
DAY 7	38.52	36.32	36.68	39.11	38.52	39.43	35.94	37.23	37.41	38.50
DAY 10	37.55	38.64	39.09	40.43	39.99	38.87	38.39	37.64	37.18	36.92
DAY 14	38.65	39.95	41.34	37.71	38.05	38.50	39.51	36.61	37.35	37.35
	No-nitrous oxide /Chronic constrictive injury to sciatic nerve									
BASELINE	38.01	38.55	38.64	39.52	41.20	36.28	36.60	36.82	37.31	37.58
DAY 1	17.11	17.31	18.39	19.83	24.08	24.40	27.09	28.98	32.66	38.55
DAY 3	16.02	18.60	8.10	9.36	9.73	13.20	13.86	15.19	15.33	15.60
DAY 5	19.43	20.22	9.94	11.01	11.43	14.82	16.53	16.81	19.20	19.24
DAY 7	9.67	9.79	10.13	13.87	14.54	14.80	15.19	16.17	17.59	17.66
DAY 10	18.65	12.20	12.37	13.53	13.66	13.80	14.53	14.80	14.85	15.72
DAY 14	9.18	9.60	10.08	11.07	11.09	11.79	11.93	13.84	14.24	14.90
	Nitrous oxide/Chronic constrictive injury to sciatic nerve									
BASELINE	37.72	39.03	40.55	40.88	40.88	41.77	35.75	36.28	37.20	37.54
DAY 1	33.69	15.07	17.61	19.16	19.49	20.24	20.68	22.34	26.20	31.62
DAY 3	17.28	17.35	18.66	18.68	18.87	13.24	13.52	14.53	14.65	16.26
DAY 5	22.24	23.17	24.98	14.48	14.77	16.78	17.39	20.35	20.95	21.90
DAY 7	15.24	23.43	14.60	16.62	18.21	19.34	20.04	20.41	20.96	21.12
DAY 10	20.94	21.66	15.36	16.17	16.28	16.57	17.43	17.56	17.67	20.52
DAY 14	11.53	11.55	11.82	12.18	13.57	13.84	15.17	15.24	15.94	17.87

THERMAL ALLODYNIA

	No-nitrous oxide/Sham surgery									
BASELINE	11.54	11.63	11.93	11.95	12.01	12.40	12.61	12.77	12.81	13.77
DAY 1	11.08	11.20	11.25	11.30	11.35	11.51	12.40	12.90	13.33	13.76
DAY 3	9.88	10.87	11.76	12.00	13.06	13.60	13.64	13.70	13.73	13.77
DAY 5	10.41	11.01	12.23	12.55	12.79	12.81	12.86	13.17	13.22	13.28
DAY 7	10.65	10.71	10.84	10.89	11.23	11.71	12.18	12.21	12.71	12.87
DAY 10	9.94	11.53	11.82	13.41	13.69	13.71	13.73	14.05	14.29	8.25
DAY 14	11.71	12.18	12.21	12.71	12.87	12.92	13.20	13.82	13.67	13.69
	Nitrous oxide/Sham surgery									
BASELINE	11.10	11.37	12.03	12.54	13.67	13.69	13.70	12.77	12.81	13.77
DAY 1	10.76	11.46	11.69	11.96	12.83	13.63	14.94	15.31	15.32	15.88
DAY 3	10.76	11.46	10.87	9.91	11.31	13.18	13.49	13.68	13.70	13.77
DAY 5	10.00	10.12	10.76	11.90	13.15	13.43	13.43	11.53	11.82	13.41
DAY 7	11.57	11.71	13.63	13.10	11.10	11.37	12.03	12.54	13.67	13.69
DAY 10	13.73	14.05	14.29	10.91	12.03	11.69	10.00	10.12	10.76	11.46
DAY 14	13.70	13.79	13.08	10.76	11.46	11.69	11.96	12.83	13.63	12.54
	No-nitrous oxide /Chronic constrictive injury to sciatic nerve									
BASELINE	12.19	12.26	12.34	12.35	12.36	12.70	13.39	13.56	13.65	13.70
DAY 1	8.39	8.61	8.81	8.90	9.56	10.26	10.56	10.97	11.29	10.30
DAY 3	7.39	7.54	7.63	7.87	8.53	8.89	8.99	9.27	9.46	9.60
DAY 5	6.39	6.59	6.68	6.90	6.93	7.05	7.09	7.34	7.48	7.51
DAY 7	6.12	6.41	6.69	6.85	6.90	7.05	7.16	7.70	7.82	7.91
DAY 10	8.79	7.07	7.11	7.42	7.57	7.74	7.78	7.90	8.45	8.62
DAY 14	6.53	6.75	8.31	8.65	8.98	9.17	9.44	9.51	10.09	6.07
	Nitrous oxide /Chronic constrictive injury to sciatic nerve									
BASELINE	12.96	13.07	11.63	11.66	11.84	11.86	11.98	12.27	12.69	12.93
DAY 1	11.27	8.22	8.55	8.68	9.55	10.18	10.20	10.56	11.00	11.15
DAY 3	9.78	9.79	10.11	10.22	10.56	10.64	11.01	11.07	11.26	11.31
DAY 5	8.70	8.70	8.82	8.93	9.15	9.57	9.76	10.32	10.86	11.09
DAY 7	9.45	10.49	8.17	8.40	8.60	8.73	8.95	9.01	9.03	9.23
DAY 10	10.57	8.24	9.25	9.25	9.35	9.47	9.73	9.79	9.95	7.72
DAY 14	12.27	6.76	6.82	7.64	7.90	8.04	8.81	9.29	9.46	10.06

Figure3. 2 Effect of nitrous oxide on mechanical allodynia in rats with chronic constrictive injury (CCI) to the sciatic nerve.

Paw withdrawal threshold was evaluated using von Frey filaments on day 1 to 14 after CCI or sham surgery with perioperative administration of nitrous oxide (N_2O) or nitrogen (N_2) in 30% oxygen. Each point indicates group mean ± standard error of mean (SEM); n = 10 animals per group, $p < 0.001$ ANOVA with repeated measures. Student t test: *$p < 0.05$ and **$p < 0.01$ (N_2O/CCI rats versus N_2/CCI rats).

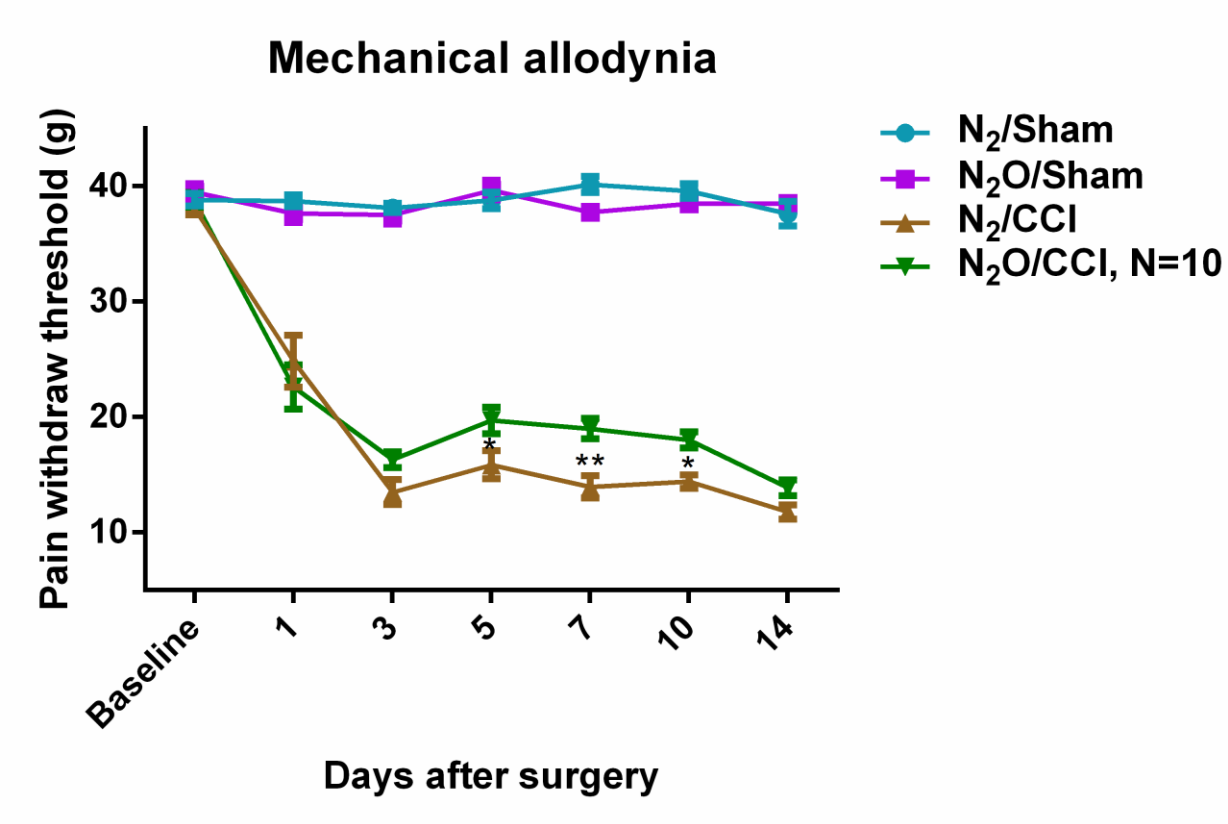

Figure3. 3 Effect of nitrous oxide on thermal hyperalgesia in rats with chronic constrictive injury (CCI) to the sciatic nerve

Withdrawal latency to plantar heat measured on baseline and days 0, 1, 3, 5, 7, 10 and 14 after surgery. Each point indicates group mean ± SEM; n = 10 animals per group, $p < 0.001$ ANOVA. Student t test: ***$p < 0.001$, N_2O/CCI rats versus N_2/CCI rats.

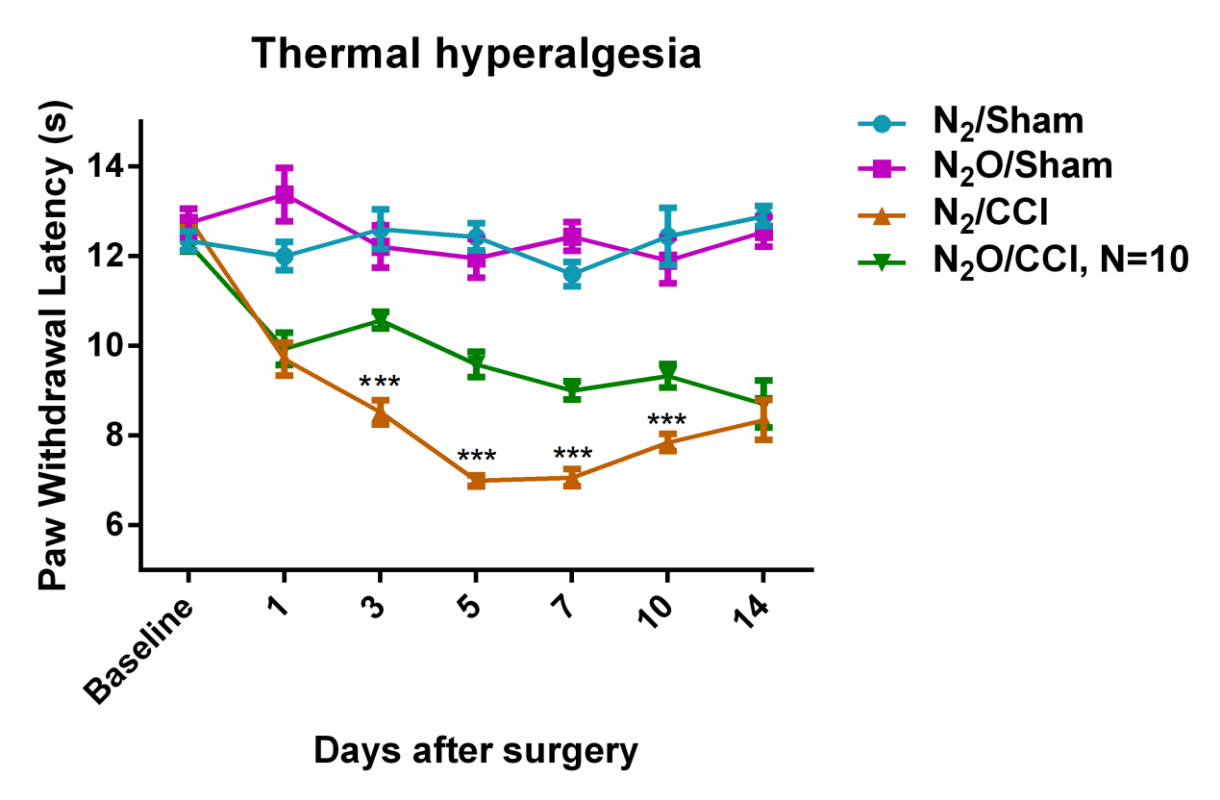

3.4 Discussions

In this experiment, we established CCI-induced chronic neuropathic pain model in rats. Compared with controls (sham surgery animals), mechanical allodynia and heat hyperalgesia were observed on day 3 after surgery and continued throughout the study. Nitrous oxide administration had no effect on mechanical allodynia or heat hyperalgesia in rats receiving sham surgery. However, nitrous oxide produced higher PWT and PWL after CCI surgery compared with controls (N_2/CCI), indicating a persistent antinociceptive effect with reduced mechanical allodynia and heat hyperalgesia, respectively. Our study confirmed the persistent antinociceptive effect of nitrous oxide and the rat model of chronic neuropathic pain for subsequent studies. The duration of the antinociceptive effect clearly outlasts the duration of simple ligand-receptor interactions. Therefore, further mechanisms of nitrous oxide-induced antinociceptive effect should be studied.

Limitations:

We only tested one model of chronic neuropathic pain in rats – CCI. This is a typical neuropathic pain model which places loose chromic ligatures on the sciatic nerve in rat to generate hypersensitive behavior that is analogous to neuropathic pain condition in humans. Nevertheless, there are other models to consider:

(1) Sciatic nerve ligation (as opposed to the loose constriction in CCI) can be used to produce abnormal sensory signs, i.e. nociception (Campbell et al., 2006; Malmberg et al., 1998). However, this model often results in limb weakness and may be difficult for mechanical allodynia;

(2) Chronic inflammatory pain can be produced by hind paw injection of prostaglandin E_2 (Kawabata et al., 2011) and complete Freund's adjuvant (Yu et

al., 2008). However, inflammatory models generally produced chronic pain of shorter duration (< 7 days). This may be derived from different pathways in neurotransmission and neuroendocrine functions of brain and spinal cord (Colpaert et al., 1987; Kong et al., 1999).

Conclusions:

This experiment established a chronic neuropathic pain model that lasted for more than 10 days. We also confirmed the persistent antinociceptive effect with nitrous oxide administration. Our subsequent experiments will focus on the mechanisms of nitrous oxide in development and maintenance of antinociceptive effects.

Chapter 4 Changes of Implicit Expression of NMDA Receptor in the Development of Chronic Neuropathic Pain

4.1 Introduction

The NMDA receptor contributes to excitatory synaptic transmission and is important in the regulation of neuropathological processes (Mori et al., 1995; Bursztajn et al., 2004). The NMDA receptor is a specific type of ionotropic glutamate receptor, which forms a heterotetramer between two NR1 and two NR2 subunits (Stephenson FA, 2006). NR1 subunit is widely expressed in the brain and spinal cord and is critical in controlling ion channel activity of the NMDA receptor (Cull-Candy et al., 2001). Continuously activated NMDA receptor may be involved in the development of persistent pain (Dickenson et al., 1997). A clinical study of thirty patients with neuropathic pain who received NMDA receptor antagonist ketamine showed that ketamine produced immediate (< 2 h) and long-lasting analgesic effect. These findings implied the involvement of NMDA receptor in the development and maintenance of neuropathic pain. Interestingly, the expression of NMDA receptor subunits NR2A and NR2B are reduced in a study investigating the pre-emptive effect of a NMDA receptor antagonist (Chang et al., 2011).

Previous works have demonstrated that nitrous oxide reduced NMDA-induced acute apoptosis in the brain (Jevtovic-Todorovic et al., 1998). The phosphorylated NR1, a critical subunit of spinal NMDA receptors, was induced by peripheral nerve injury and lasted for months in the chronic neuropathic pain model (Gao et al., 2005; Ultenius et al., 2006). Considering all these findings, we hypothesized that nitrous oxide produced long-term antinociceptive effect by persistent interaction with NMDA receptor. Therefore, continued expression of NMDA receptors may contribute to the persistent

analgesia of nitrous oxide. In this experiment on rats with CCI to the sciatic nerve, we evaluated the expression of NMDA receptors and NMDA-related genes.

4.2 Materials and Methods

4.2.1 Quantitative RT-PCR

The primer pairs for quantitative RT-PCR were designed with primer express software (Life Technologies, Carlsbad, CA). Power SYBR Green PCR master mix kit (Life Technologies, Carlsbad, CA) was used for detection. The reaction was performed in a final volume of 10 µL according to manufacturer's protocol. The following solution was added to the 384-well real-time PCR plate: 5 µL of 2X master mix solution, 0.75 µL of the primer pair (a mixture of forward and reverse primers, 10 µM each), 1 µL of DNase-free water and 2.5 µL of diluted cDNA solution (10-fold dilution from original cDNA solution). After incubation at 50°C for 5 min, the reaction mixture was denaturated at 95°C for 10 minutes, followed by 45 PCR cycles (denaturation at 95°C, 15 seconds, primer annealing and extension at 60 °C, 1 minute). The comparative cycle threshold (Ct) method was used for quantification of gene transcription. The relative transcription level of a specific gene in each group was normalized to the housekeeping gene β-actin and is expressed as 2-ΔΔCt method. The Ct value was read according to the number of cycles.

4.2.2 Western blot assay

The ipsilateral lumbar spinal cord (L4-6) was lysed in radio-immunoprecipitation assay (RIPA) buffer [50 mM Tris-HCl, 150 mM NaCl, 1 mM EDTA, 1% (v/v) NP40, pH 7.6] containing 10 mM sodium fluoride and complete protease inhibitor cocktail (Roche, Mannheim, Germany). The homogenate was then sonicated on ice with three

10-second bursts at high intensity and a 10-second cooling interval, and centrifuged at 12,000×g for 10 minutes at 4ºC. We determined protein concentration using protein assay kit (Bio-Rad, Hercules, CA). Samples were then mixed with 4× protein loading buffer [5mM Tris-HCl, pH 6.8, 2% (w/v) SDS, 10% (v/v) glycerol, 1% (v/v) β-mercaptoethanol, 12.5 mM EDTA, 0.02% (w/v) bromophenol blue] and heated at 99°C for 10 min. Samples were then loaded (25 µg of protein/lane) onto a 10% SDS-polyacrylamide gel and the separated protein was then blotted onto a hybridization nitrocellulose membrane (0.45 µm) (Miliipore, Bilierica, MA). The blots were incubated overnight at 4°C on a rocker with mouse monoclonal anti-NR1 (Cell Signaling #5704, 1:1000), and mouse monoclonal anti-β-tubulin (Cell Signaling # 2146, 1: 2000) antibodies. After washing three times with Tris-Buffered Saline with Tween-20 (TBST), membranes were incubated with a 1: 2,000 dilution in incubation solution of horseradish peroxidase-conjugate goat anti-rabbit IgG (Cell Signaling #7074, 1: 2,000) or goat anti-mouse IgG (Cell Signaling #7076, 1:2,000) antibodies for 1 hour at room temperature. Enhanced chemiluminescence detection system used to visualize the peroxidase-coated bands. Densitometric analysis of protein bands was performed using the J analysis software (Research Services Branch, National Institute of Mental Health, Bethesda, Maryland). The targeted protein levels were normalized to the corresponding β-tubulin levels.

4.3 Results

4.3.1 Implicit expression change in NMDA receptors and NMDA activity related genes

There was no transcriptional change in NMDA receptors in the spinal cord of rats receiving nitrous oxide or not during CCI or sham surgery (Figure 4.1). However, a

high level of NR1 (Grin1) expression was noted. Similarly, we observed no change in NMDA receptor-related genes, such as synaptosomal-associated proteins (Ptk2b, Nrxn1, Dlgap3 Shank1, and Shank3), as well as other functional or structural interaction proteins, Reln, Nlgn1, Htr1a and Eps8 (Figure 4.2). Western blot assays for NR1 was performed and confirmed the RNA profiling results (Figure 4.3).

Figure 4. 1 Expression of NMDA receptor genes

Relative expression levels of these subunit genes of N-methyl-D-aspartate receptors analyzed by RNA-seq. The averaged FPKM (fragments per kb of exon per million fragments mapped) value of three replicates were calculated in each group using RNA profiles. Data are mean ± SEM; $n = 3$ replicates per group. Error bars indicate SEM *$p < 0.05$.

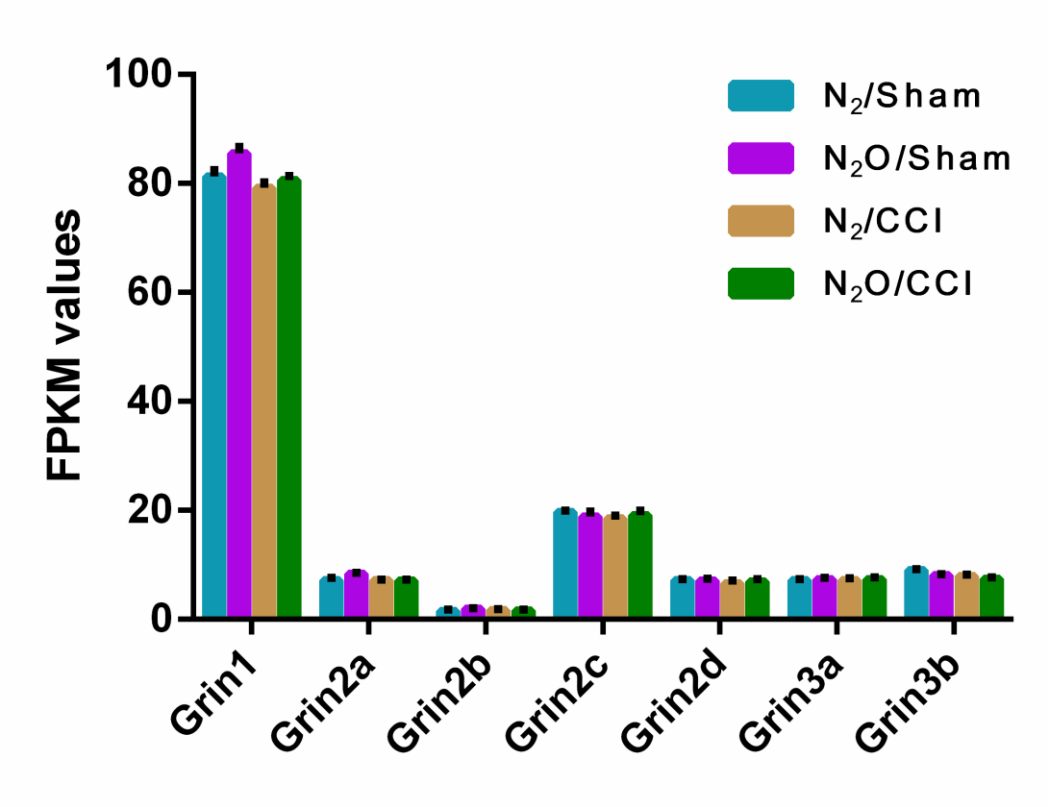

Figure 4. 2 The expression values of NMDA related genes

RNA sequencing of four groups (n=3 mice per group) showing relative expression levels among the 9 NMDA receptor function-associateed genes. The expression levels were calculated in terms of fragments per kilobase of exon model per million mapped reads (FPKM). Data are mean ± SEM; *n* = 3 replicates per group.

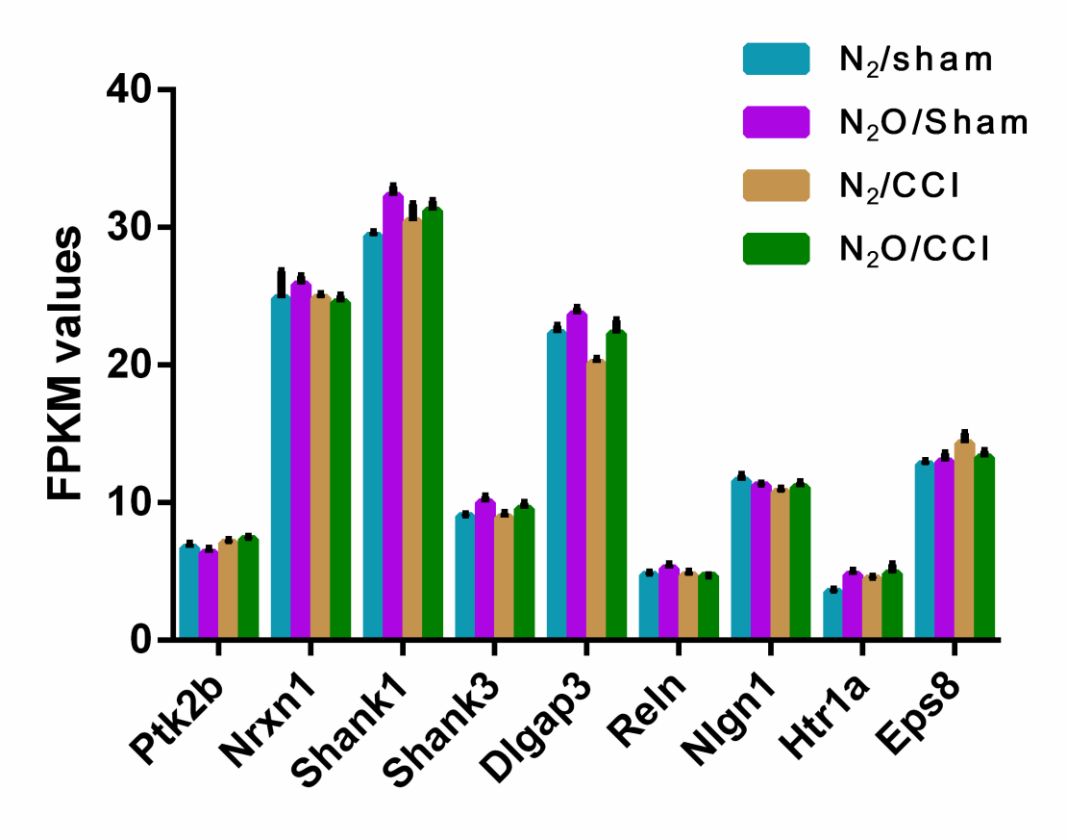

Figure 4. 3 Western blot assays of NR1 in NMDA receptor

Protein expression of NR1 subunit of NMDA receptor in ipsilateral spinal dorsal horn 3 days after surgeries. Representative Western blot results (two biological replicates for each group) (A) and quantitation of relative density (B) showed as below. The results revealed that there was a slight increase in CCI-induced chronic pain groups but no statistical difference when treated with nitrous oxide. The quantitation results are shown as group mean ± SEM. *$p < 0.05$, compared with the sham control group; $n = 4$ mice for each group.

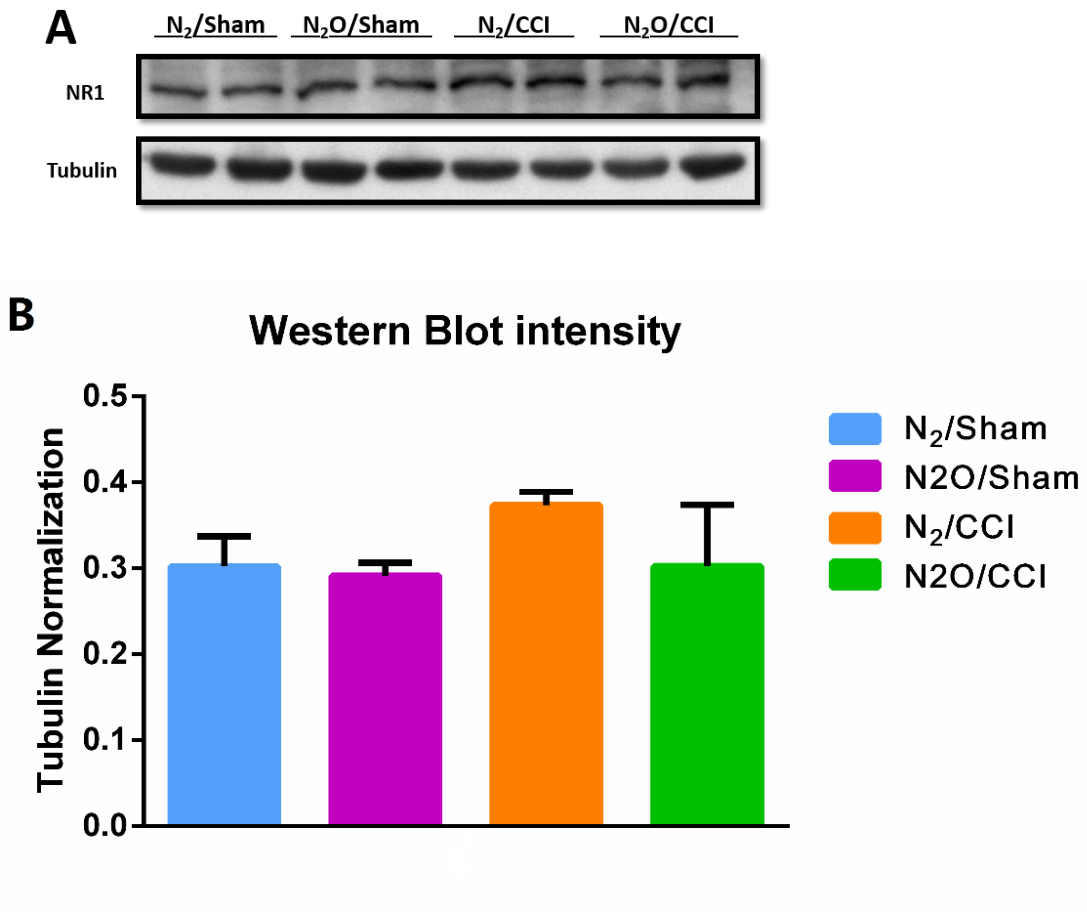

4.4 Discussions

Nitrous oxide has been considered as a NMDA receptor antagonist for neuroprotection (Jevtovic-Todorovic et al., 1998). Furthermore, it has been shown that spinal NMDA activation and increased phosphorylation of subunit NR1 is critical in the development of pathological and persistent pain (Dickenson et al., 1997; Ultenius et al., 2006; Gao et al., 2005). Using the $NR1^{+/-}$ knockdown mice, some data have demonstrated the dynamic interaction between NMDA receptor function and spinal chemokine and glial production in neuropathic pain states (Bursztajn et al., 2004). All these findings indicated that NMDA receptor signaling is involved in the nerve injury-induced pain process.

In our study, we aimed to evaluate the activity of NMDA receptor signaling in the prolonged anti-nociception in an aspect of the transcriptional change. Preliminarily, we found a slight increase in CCI group compared with sham control groups. However, we observed no significant expression change in NMDA receptor and other related genes after nitrous oxide administration.

Limitations:

In our study, we measured expression of NR1 and its total protein levels by Western blot assays. Previous studies have shown the phosphorylation of NR1 by quantification with immunostaining (Gao et al., 2005; Zhang et al., 2008). To further validate the role of NMDA receptor activity in our model of prolonged anti-nociception, more experiments will be required to confirm our results:

(1) Detection of NR1 phosphorylation in nitrous oxide-treated rats compared with no-nitrous oxide after CCI surgery;

(2) Comparing the antinociceptive effect of NMDA antagonist (MK801) with nitrous oxide.

If we fail to detect NR1 phosphorylation, this will suggest the lack of persistent activation of NMDA receptor after chronic pain development. Similarly, if MK801 fail to produce long-term antinociception compared with nitrous oxide, this will indicate that persistent antinociception of nitrous oxide is mediated through mechanisms other than the NMDA receptor interaction.

Conclusions:

In this experiment, we found that there were no significant changes in the expression of NMDA receptor or its related genes. The results suggested that nitrous oxide might not primarily act through NMDA receptor for long-term analgesia. Further investigation is required to define the role of NMDA receptor signaling in nitrous oxide-associated persistent antinociceptive effect.

Chapter 5 Transcriptome Signatures in the Development of Neuropathic Pain

5.1 Introduction

Nitrous oxide was thought to activate opioidergic and noradrenergic neurons in the periaqueductal gray matter and brainstem to enhance neurotransmission, resulting in the release of opioid and corticotropin-releasing factor (Sawamura et al., 2000; Fang et al., 1997). Both neurotransmitters contributed to the antagonism of NMDA receptor and inhibition of γ-Aminobutyric acid (GABA)-ergic interneurons, thereby activating the descending pathways in the spinal cord to produce nitrous oxide-induced antinociceptive effect (Sawamura et al., 2003; Ohashi et al., 2003; Orii et al., 2003). The descending inhibitory neurons in spinal cord were important for the analgesic action of nitrous oxide, since antagonism or genetic ablation of adrenoceptors may block the analgesic effect of nitrous oxide. In this respect, diminished antinociceptive effect were demonstrated in the spinal cord-transected rodents, as well as in animals that lack functional connectivity with the descending inhibitory neurons (Orii et al., 2002; Zhang et al., 1999; Ohashi et al., 2002).

Recently, it has been shown that interactions between extra-neuronal cells (i.e. immune cells) and the nervous system are important for the development of chronic pain (Scholz et al., 2007). Nerve injury induces activation of microglia through phosphorylation of p38 MAP kinase (Jin SX et al., 2003; Svensson et al., 2005) and other extracellular signal-related kinases (Zhuang et al., 2005). The activated spinal microglia is recruited to the dorsal horn. Similarly, toll-like receptor signaling has been shown to participate in these activation and recruitment (Kim et al., 2007; Tanga et al., 2005). Toll-like receptor signaling leads to activation of transcription factor NF- κB, upregulation of interferons and increased expression of proinflammatory cytokines

(Trinchieri et al., 2007) These findings highlight the potential molecular mechanism of nitrous oxide-induced antinociceptive effect.

In previous section, we have demonstrated the long-term antinociceptive effect of nitrous oxide in rats with CCI to the sciatic nerve. To further identify transcriptional alterations with nitrous oxide during the development of neuropathic pain, we performed transcriptome profiling by RNA sequencing of ipsilateral lumbar spinal cord. It is hoped that dynamic changes in transcriptome during the development of chronic pain may reveal signatures of pain-related gene expression. In this study, we hypothesized that nitrous oxide confers antinociception through transcriptional regulation of pain related genes and signaling pathways

5.2 Materials and methods

5.2.1 Sample collection and RNA extraction

Spinal cord tissues were collected 3 days after surgeries. The harvested ipsilateral lumbar spinal cord at L4-L6 were then homogenized in 1 ml of TRIzol LS reagent (Life Technologies, Carlsbad, CA). The homogenate was incubated for 5 minutes at room temperature after rigorous vortex to achieve complete dissociation. Chloroform (0.2 ml) was then added and the tube was shaken rigorously for 15 seconds. After 5 minutes of incubation at room temperature, the tubes were centrifuged at 12,000×g for 15 minutes at 4 °C. The upper aqueous phase was then transferred into a new RNase-free tube containing equal volume (about 0.5 ml) of 100% isopropanol. The mixture was then left at room temperature for 10 minutes, followed by centrifugation at 12,000×g for 10 minutes at 4 °C. Then the isopropanol was removed, followed by washing the pellet at the base of tube with 0.5 ml of 75% (v/v) ethanol in

diethylpyrocarbonate-treated water. The tube was tapped and inversed several times, then centrifuged at 7,400×g for 5 minutes at 4 °C. The excess ethanol was then removed and the pellets were dried in air. After resuspension with RNase free water, the RNA samples were quantified using NanoDrop spectrophotometer (Nanodrop, Wilmington, DE).

5.2.2 RNA sequencing

Total RNA was extracted using RNA/DNA/Protein Purification Plus Kit (Cat. 47700) (Norgen Biotek, Canada). RNA was quantified using a NanoDrop ND-1000 spectrophotometer (Nanodrop Technologies, Wilmington, NC, USA). RNA purity and integrity was determined using Agilent Bioanalyzer 2100. Only those samples having an RNA integrity number > 8.7 were used. A total of 12 samples consisting of 3 replicates in each of the four experimental groups (i.e. N_2/Sham group, N_2O/Sham group, N_2/CCI group, and N_2O/CCI group), were prepared. RNA library construction and sequencing were accomplished by Beijing Genome Institute (BGI) (Shenzhen, China). Reads were generated in a 100 bp paired-end for de novo assembly using an Illumina HiSeq 4000 platform.

5.2.3 Data processing and analysis

Principal component analysis (PCA) was conducted on all genes to assign the general variability in the data to a reduced set of variables. The resulting matrices were passed into a MATLAB PCA routine. Twelve variations of the PCA were completed, with the RNA-seq data, as described in (Yeung KY et al., 2001). RNA-seq analysis was performed as previously described. The differential expression was called by cuffdiff with a default FDR of 0.05. Downstream analyses were performed using the

Bioconductor EdgeR package and custom R scripts (Yu H et al., 2015). Hierarchical clustering was used to determine the relative distance of each sample using Pearson's correlation. Spearman correlation of gene expression profiles was used to define the similarity in gene expression profiles of the 12 samples.

5.3 Results

5.3.1 The features of RNA sequencing data

To explore the molecular mechanism beyond the nitrous oxide-induced persistent antinociception in transcriptional level, we performed the transcriptome RNA sequencing with the ipsilateral lumbar spinal cord on 3 days after the surgery when the hyperalgesia was significantly released. After removal of low-quality and contaminated reads, a total of 5.52×10^7 raw reads were acquired, containing on average 2.7 gigabases (Gb) of sequencing data per sample. The sequence reads were aligned to the R. norvegicus reference genome (rn5) with a concordant pair alignment rate of around 60%. Based on the sequencing depth in this study, it was expected that only differentially expressed genes (DEGs, genes whose expression levels were significantly different between two groups of experiments) of high expression levels could be identified.

To quantify transcriptomic variations among our samples, Cuff-links was used to assemble all reads. Subsequently, the expression levels for all transcripts were calculated in terms of fragments per kilobase of exon model per million mapped reads (FPKM). The read density was normalized to reflect the molar concentration of a transcript, which allowed comparisons within or between samples of different expression levels. After quantification and normalization, a total number of 26,254

unique transcripts were observed. Figures 5.1 and 5.2 showed the gene expression patterns in terms of FPKM of the 12 samples after normalization. There were about 48% of genes distributed between 1 and 100 FPKM (i.e. $\log_{10}$(FPKM): 0 - 2) and most of them exhibited with a FPKM < 10. These results suggested that the samples were comparable and suitable for subsequent transcriptomic variation analysis.

Figure 5. 1 Box plot of transcript expression levels (log_{10} (FPKM)) in RNA-seq samples before normalization

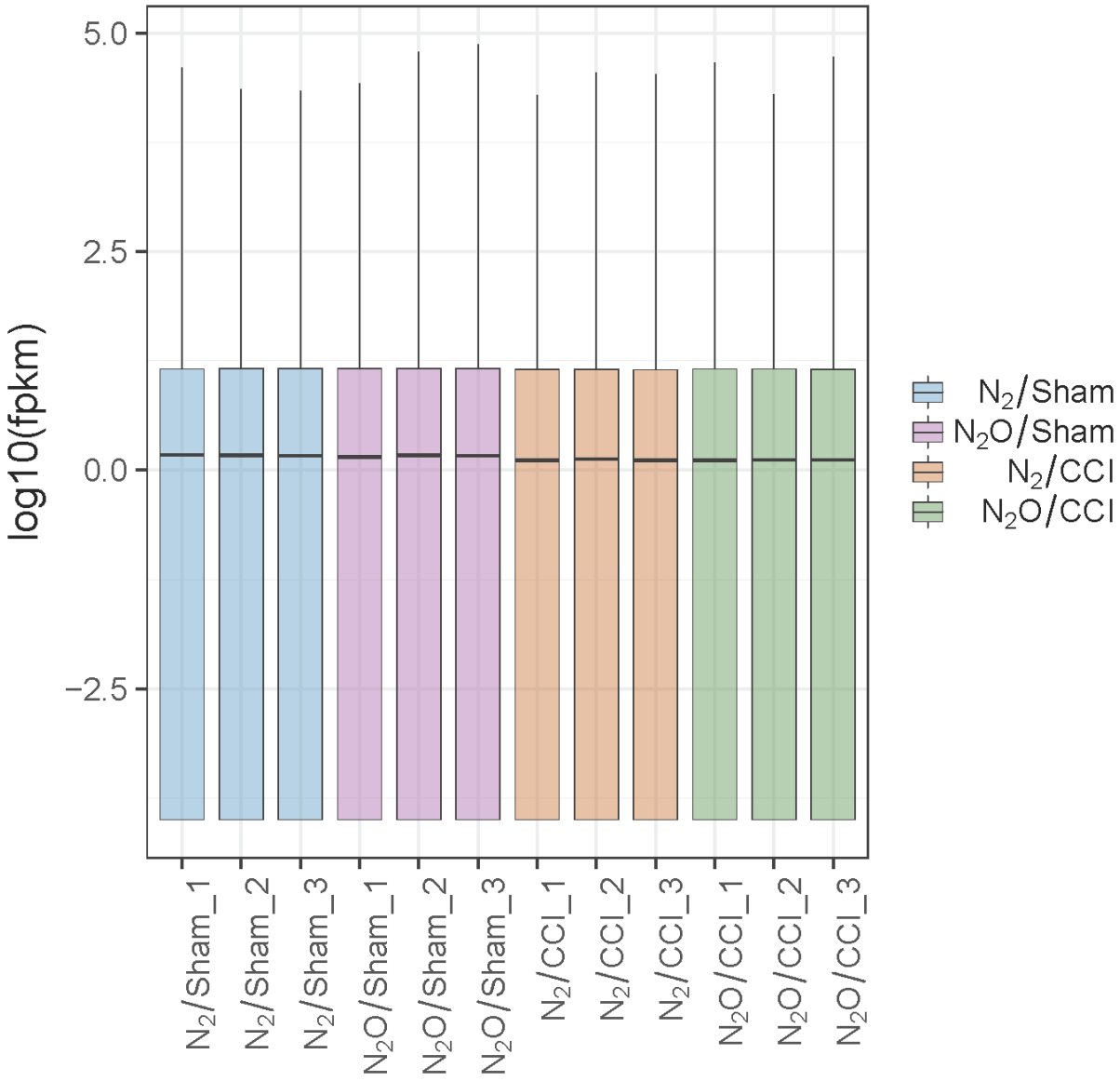

Figure 5. 2 Distributions of gene expression based on RNA-seq data after normalization

Kernel density estimates of FPKM distributions of RNA-seq data within 4 groups.

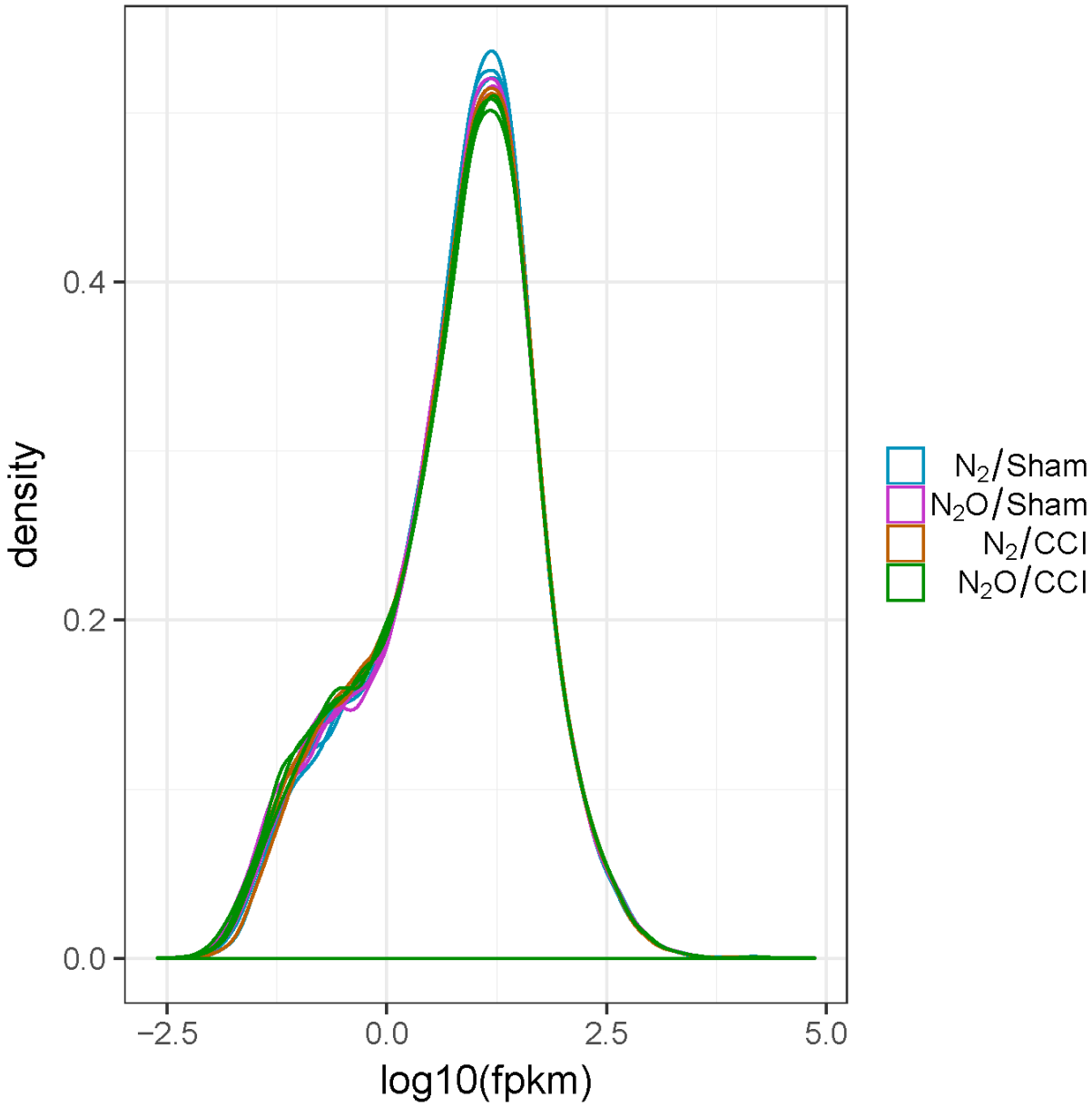

5.3.2 Nitrous oxide modified the CCI-induced transcriptome signatures

First, we conducted a preliminarily comparison to evaluate the effects of CCI and nitrous oxide administration on transcriptomes of ipsilateral spinal dorsal horn. Principal component analysis (PCA) was performed using correlation matrix calculated from $\log_{10}$-transfromed FPKM values and found that there was a large difference between CCI groups and sham controls (Figure 5.3). Furthermore, the transcriptomes of the nitrous oxide and controls in the CCI surgery groups differed in PC2 (y-axis), whereas the profiles between nitrous oxide and controls were similar in sham-operated groups. These findings reflected that CCI induced a profound transcriptional change regardless of nitrous oxide administration. The overall transcriptome similarities were also assessed using multidimensional scaling (MDS). Figure 5.4 shows the MDS plots. In this figure, CCI significantly affected the transcriptome profiles of the samples along M1 (x-axis), indicating substantial changes caused by CCI. Interestingly, despite the variations along M2 (the y-axis), the nitrous oxide-treated CCI groups were more closely grouped together than the sham-operated group along M1 (x-axis).

Apart from PCA and MDS, Spearman's correlation analysis of hierarchical clustering was conducted based on the transcriptome data of 12 samples (Figure 5.5). The transcriptomes of the two CCI groups were clearly distinct from those of two sham-operated groups, indicative of a dominant effect of CCI on gene expression. This finding was also in accordance with PCA and MDS results. Nitrous oxide samples were separated from controls in the CCI groups, indicating that intraoperative administration of nitrous oxide modified the transcriptome.

In order to identify the genes responsible for CCI or nitrous oxide-specific transcriptome signature, Volcano plot analysis was used (Figure 5.6) to define differentially expressed genes (DEGs) with adjusted p values ≤ 0.05. Both up- and down-regulated DEGs were represented by red dots. As compared with the N_2/Sham group, there were substantially more DEGs, predominately upregulated, in both N_2/CCI and N_2O/CCI groups. Notably, the number of DEGs in N_2/CCI group was more than that in N_2O/CCI group, confirming that chronic constrictive injury to sciatic nerve produced a dominant effect on spinal gene expression. Our data also suggested that nitrous oxide modified the CCI-induced transcriptional activity.

Taken together, we found that CCI-induced transcriptomic changes in the initiation of neuropathic pain. These changes potentially evoke the regulation of pain-related signal pathways. Importantly, administration of nitrous oxide modified CCI-induced transcriptomic changes, implying that regulation of gene expression might take part in persistent antinociceptive effect.

Figure 5. 3 Principal component analysis (PCA) of individual samples

PCA was performed on all genes to determine expressional differences among samples from nitrous oxide/chronic constrictive injury (N_2O/CCI) group (orange), no-nitrous oxide (N_2)/CCI (N_2/CCI, blue), N_2O/Sham (purple) and N_2/Sham (green).

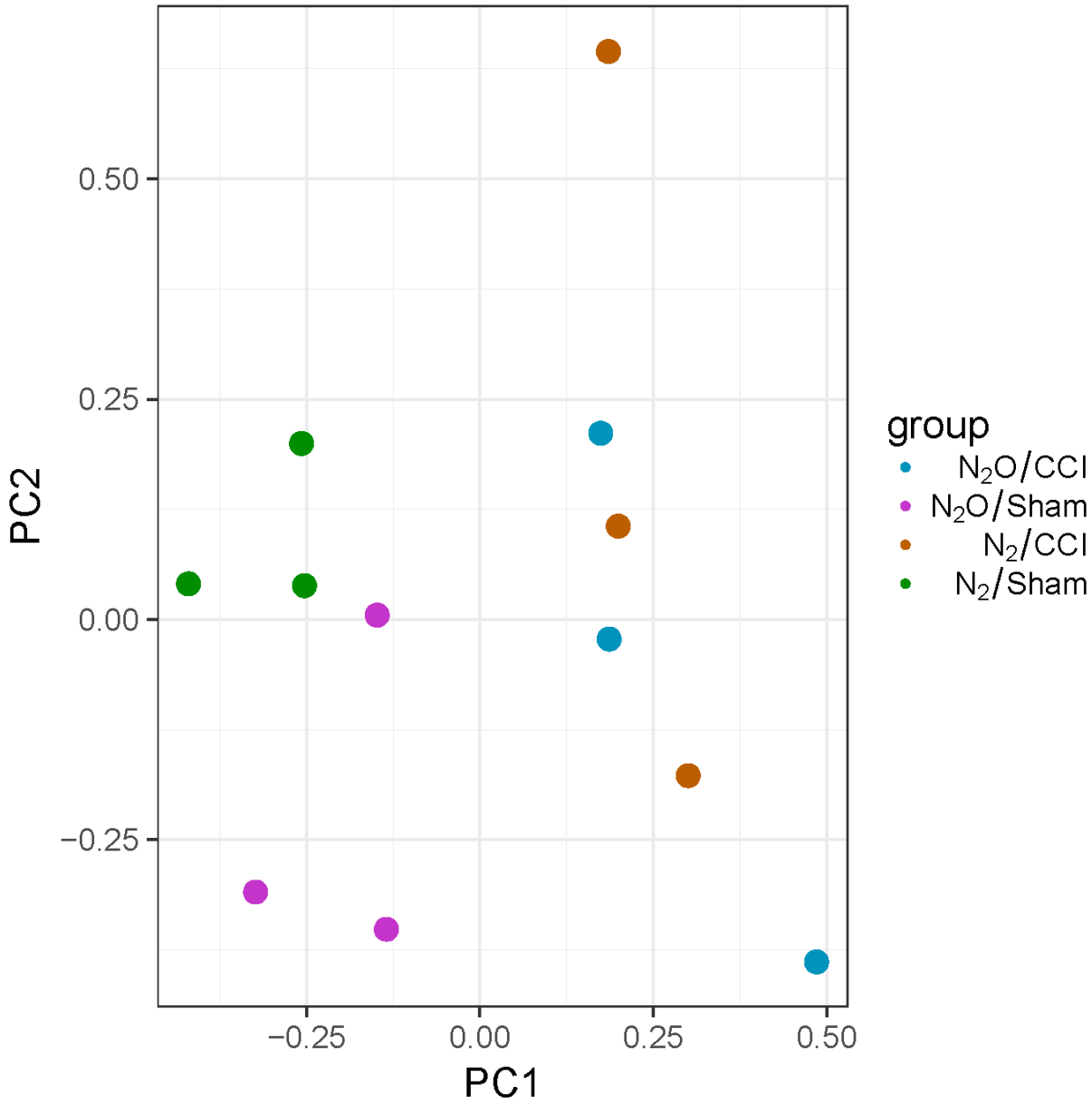

Figure 5. 4 Multidimensional scaling (MDS) plots of log_{10}-normalized FPKM of the 12 RNA-seq samples

MDS plots of the 12 samples suggested that CCI produced a prominent effect on transcriptomes as compared with sham control. The subtle differences could also be discerned between nitrous oxide/chronic constrictive injury, N_2O/CCI and no-nitrous oxide (N_2)/CCI, N_2/CCI groups.

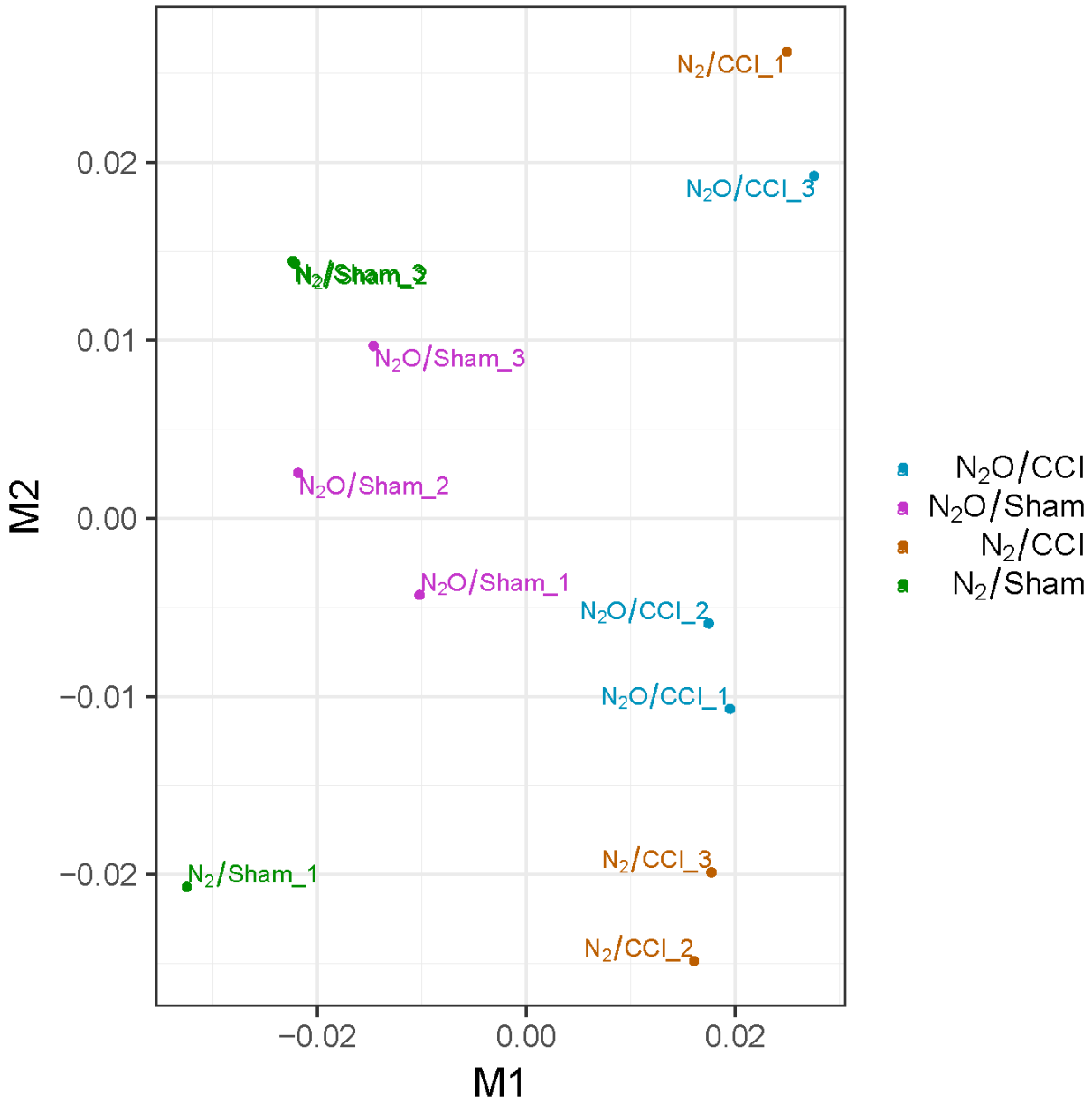

Figure 5. 5 Hierarchical clustering on pairwise correlation coefficients for transcriptome data from the 12 samples

Correlations coefficients were calculated based on Spearman's correlation. The hierarchical cluster analysis shows the distinct expression signature induced by chronic constrictive injury (CCI) or sham surgery and nitrous oxide (N_2O) or no-nitrous oxide (N_2).

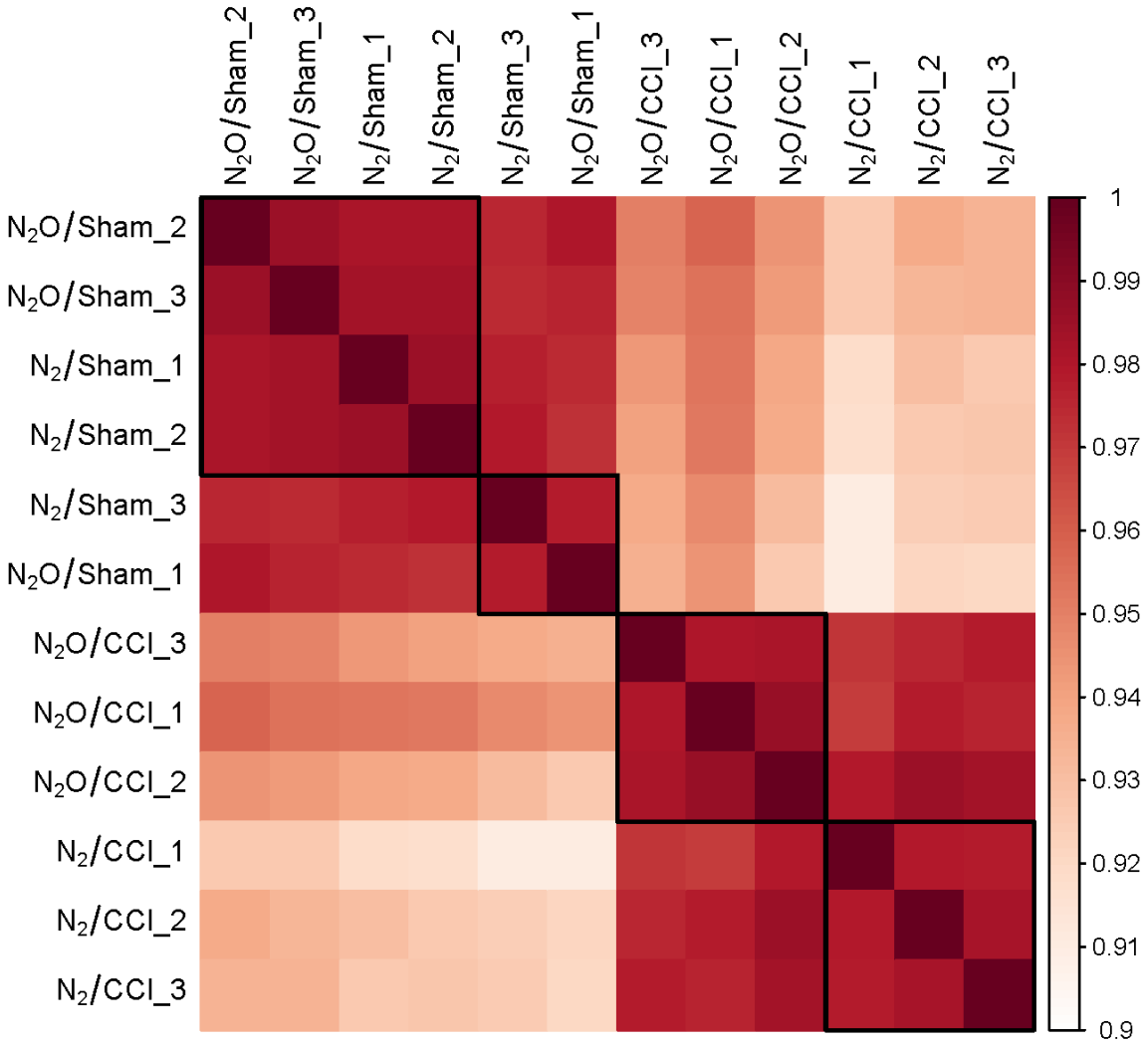

Figure 5. 6 Volcano plots for identification of DEGs based on RNA-sequencing gene expression analysis

The x-axes on the volcano plots are the log_2fold-change of the differences in gene expression in rats having chronic constrictive injury (CCI) or sham surgery with nitrous oxide (N_2O) or no-nitrous oxide (N_2), i.e. N_2/CCI, N_2O/CCI and N_2O/Sham as compared with the N_2/Sham group. The y-axes show the negative of the log_{10} corrected *p*-values of the comparison between the two groups. The differentially expressed genes (DEGs) with adjusted *p* values ≤ 0.05 are represented by red dots.

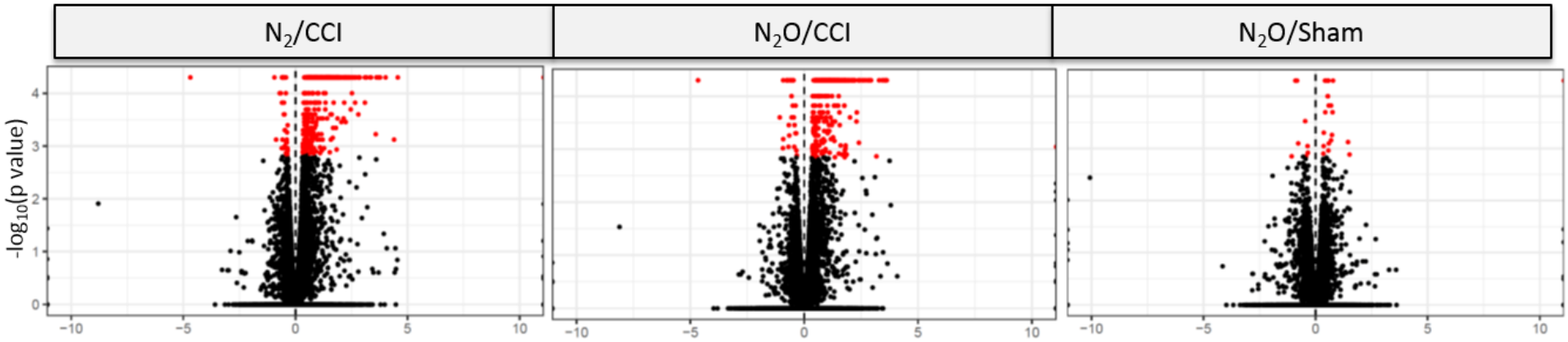

5.3.3 Nitrous oxide globally attenuated CCI-induced transcriptional changes

In order to analyze gene expression changes induced by CCI in the presence or absence of nitrous oxide administration, a Venn diagram of DEGs with adjusted p values ≤ 0.05 was constructed. Figure 5.7 shows the CCI-induced 630 DEGs compared with sham-operated controls but the number was reduced to 468 in the presence of nitrous oxide. Notably, among DEGs in the rats receiving CCI to sciatic nerve with nitrous oxide (N_2O/CCI group), 88% were overlapped with those in CCI but no-nitrous oxide (N_2/CCI) group. Several genes were co-deregulated in all three groups, but less DEGs were observed in the N_2O/Sham group.

The heatmap generated with expression values for all DGEs among four groups revealed that the samples of CCI and sham-operated groups clearly self-segregated into clusters (Figure 5.8). Notably, nitrous oxide-treated CCI groups were obviously closer to the sham control than the untreated CCI group.

Based on the Venn diagram, DEGs were divided into six modules. Figure 5.9 shows the expression pattern of genes in six modules. In general, the expression of genes in Module 1 was substantially altered by CCI but restored to the sham-control level by intraoperative administration of nitrous oxide. Genes in Module 2 exhibited similar expression changes upon CCI regardless of nitrous oxide administration. Modules 3 and 6 included genes whose expression showed remarkable changes only in rats with CCI or sham surgery and nitrous oxide: N_2O/CCI, N_2O/Sham groups, respectively. Genes in Modules 4 and 5 showed more dynamic expression changes in different groups.

Based on the aforementioned analyses, it was discerned that the expression of almost all genes deregulated by CCI could be restored to a relatively normal level upon nitrous oxide administration. In particular, most of the genes in Module 2 were markedly dysregulated by chronic never injury but amenable to rectification by nitrous oxide. These genes could be regarded as nitrous oxide-responsive neuropathic pain-related genes.

Figure 5. 7 Venn diagrams of DEGs

Venn diagram shows the total number of DEGs with $p < 0.05$ in transcriptomes of samples from N_2/CCI (blue circle), N_2O/CCI (yellow circle) and N_2O/Sham (pink circle) groups as compared with N_2/CCI.

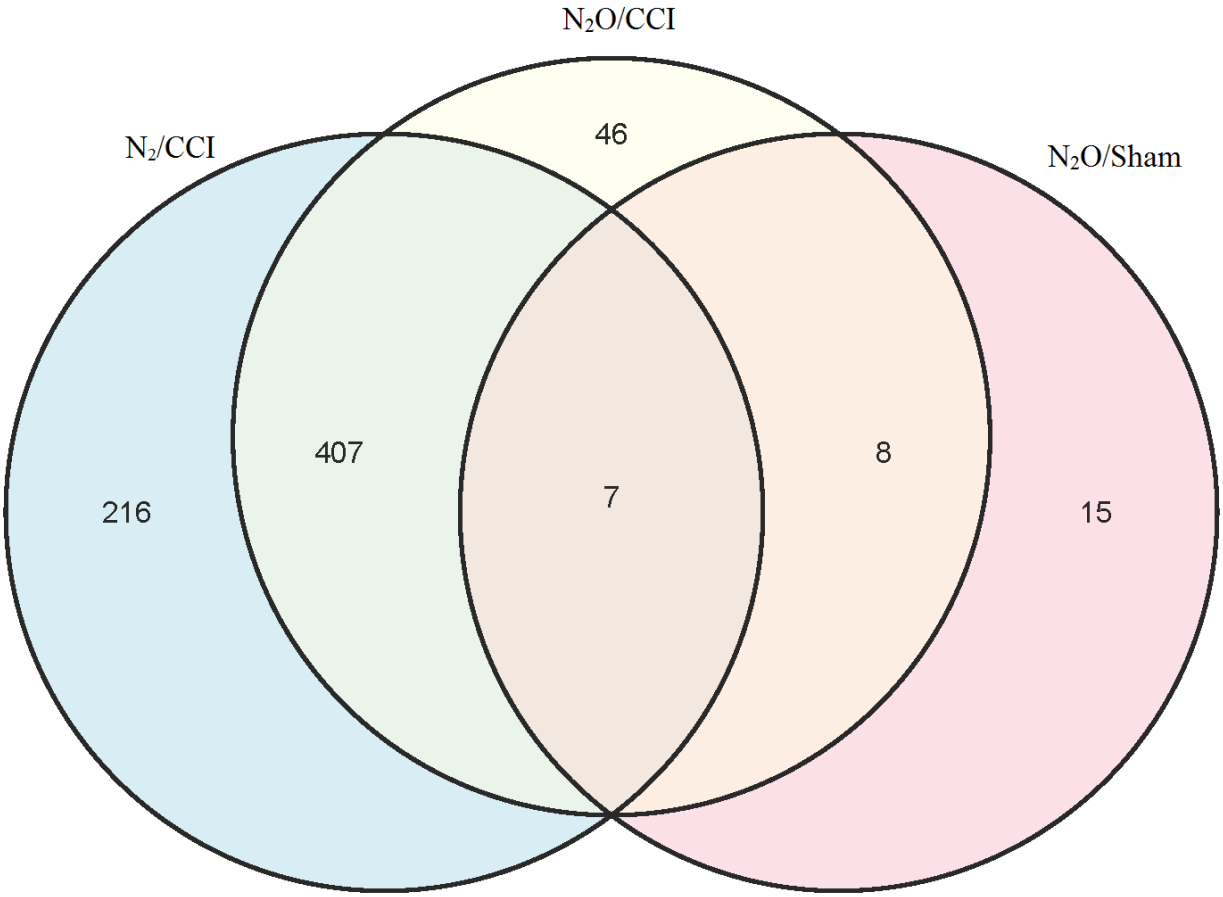

Figure 5. 8 Heatmap of expression levels of differential gene expressions in the four experimental groups

Expression levels of differentially expressed genes (DEG) identified in N_2/CCI, N_2O/CCI and N_2O/Sham groups as compared with the N_2/Sham group were hierarchically clustered and shown in the heatmap. Each row represents a single gene and each column represented one sample. A red-blue color scale as shown in the upper right corner was used to indicate the expression level.

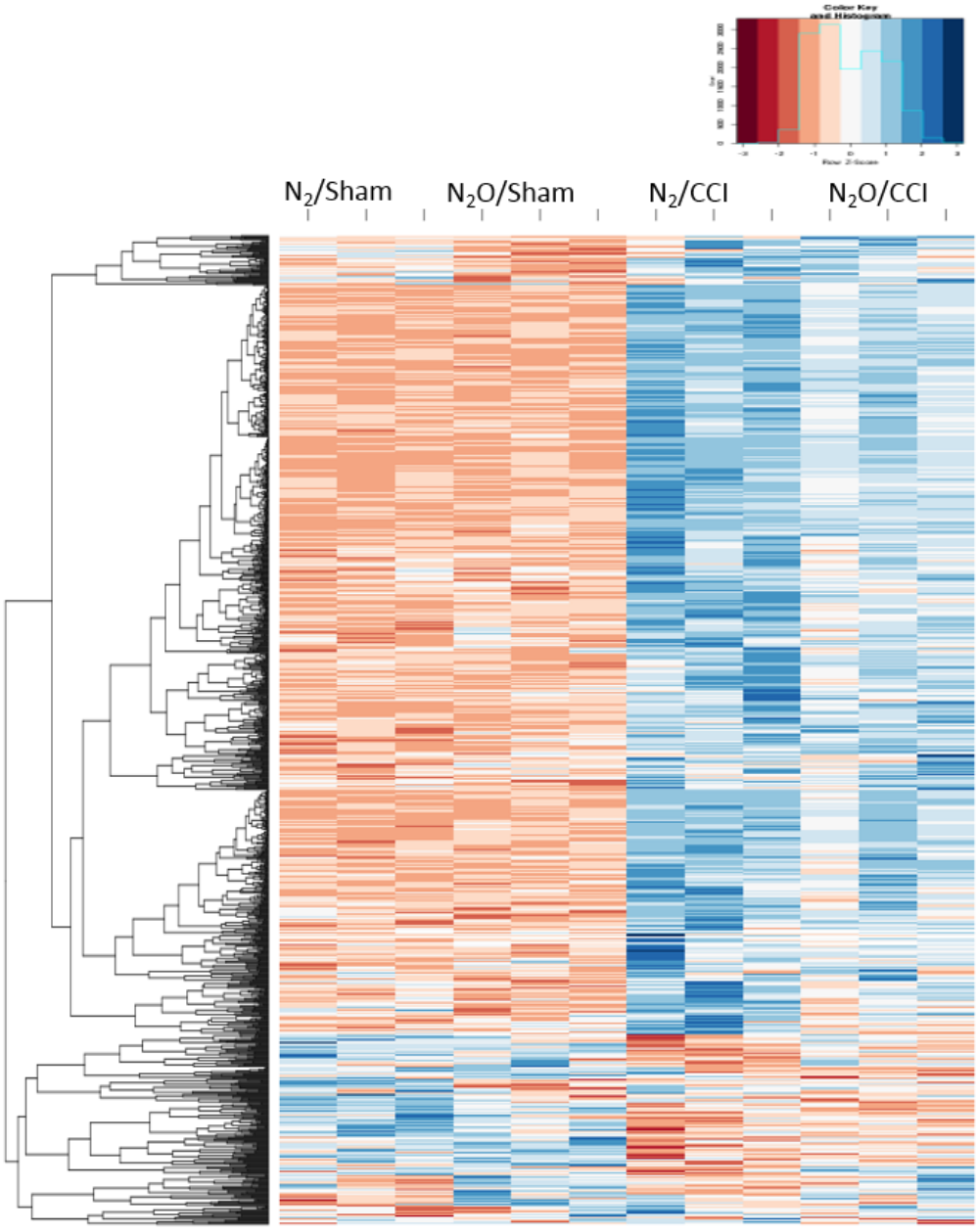

Figure 5. 9 Scattered line plots representing the expression changes of six modules based on the Venn diagram

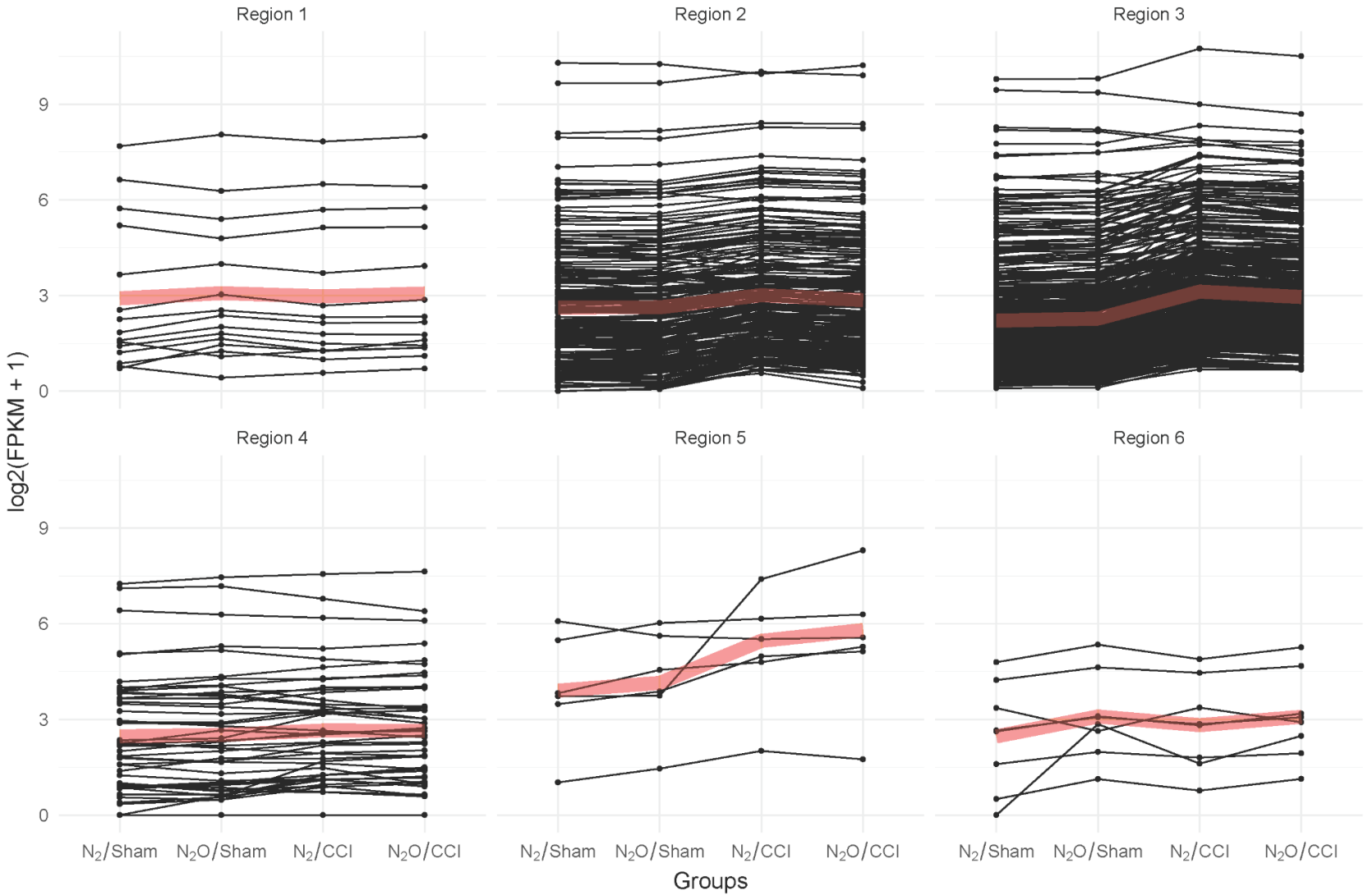

5.3.4 Nitrous oxide-dependently dysregulated genes functioned in neuron activity

There were 8 nitrous oxide-regulated targets (genes in Module 5) co-deregulated in both N_2O/CCI and N_2O/Sham groups (Figure 5.10). Three of them have been reported to perform neuronal activity-related functions, including Pex11a for peroxisome maintenance and proliferation regulator, Hpcal4 for neuronal calcium ions sensing, as well as Tac3, which encodes the neuropeptide Tachykinin 3.

Besides, genes in N_2O/Sham group which exhibited N_2O-denpendently dysregulation showed a great relationship with neuron development and neuroendocrine, including Calca for systemic inflammatory response, Ebf3 involved in the development of dopaminergic neurons, as well as Sst, which encodes somatostatin, marketable expressed in neuroendocrine tumors.

The identification of these DEGs involved in neuronal activity provides a valuable resource for further investigation of specific neuronal processes or pathways that are involved in the prolonged analgesic effect of nitrous oxide.

Figure 5. 10 The normalized expression values of neuronal activity-related genes in RNA-seq

The expression levels (FKPM values) of 6 overlapped DEGs between nitrous oxide/chronic constrictive injury (N_2O/CCI) and N_2O/Sham groups.

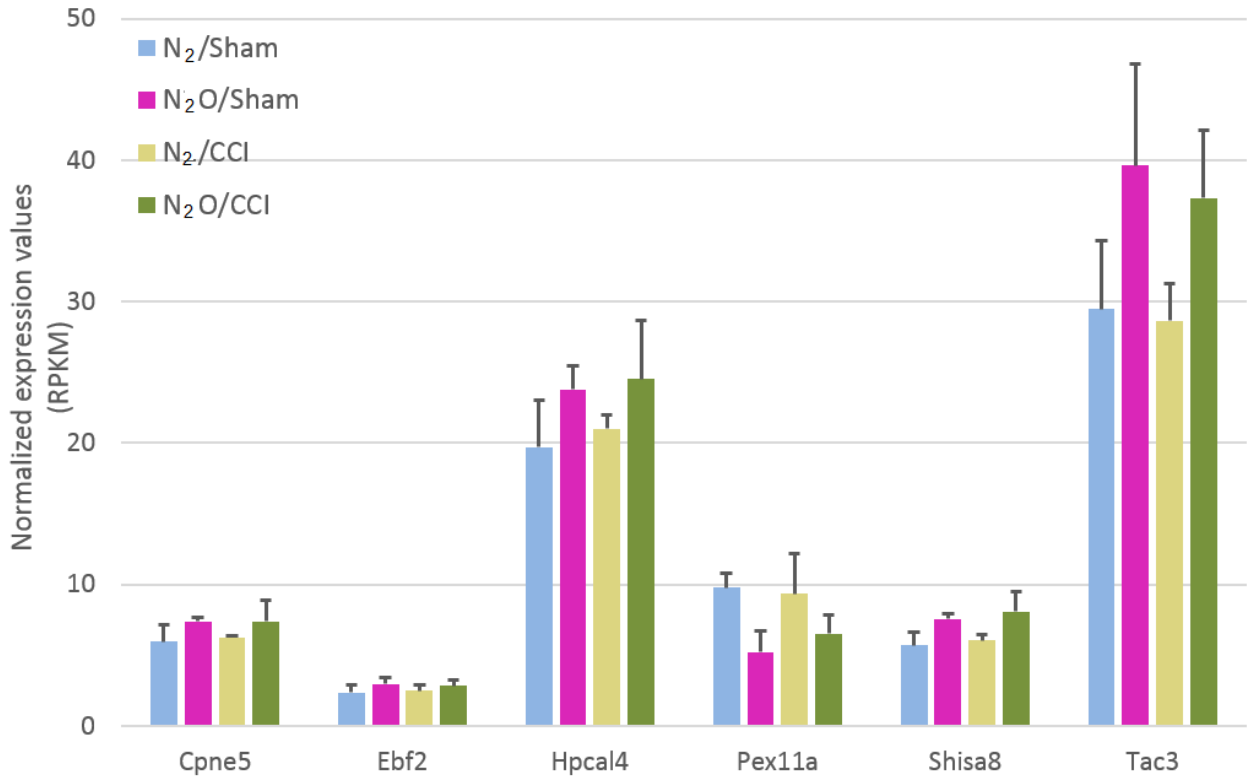

5.4 Discussions

We identified a total of 630 DEGs as neuropathic pain-related genes. Among these genes, expression changes of 216 genes (Module 1) showed a significant difference between CCI and sham surgery but became insignificant with addition of nitrous oxide. In particular, some of them play a role on the neuroprotection (Xu et al., 2015; Berger et al., 2016) and neuroendocrine regulation of reproduction (Rance et al., 2010; Valdes-Socin,H. 2014), which are expected to be key mediators of the prolonged antinociceptive effect of nitrous oxide. Besides, some DEGs like Pex11a, as well as Tac3 exhibited nitrous oxide-dependent expression change.

Limitations:

We conducted transcriptome analysis and found the altered expression pattern by perioperative administration of nitrous oxide. However, there were individual variances within group, especially in CCI groups. Further analysis need to consider the exact expression of each gene in individual level.

Conclusions:

Pain is known to activate neuron transmission activity preferentially in brain and spinal cord. Peripheral nerve injury provokes the reactivation of interacting among immune

cells, glial cells and neurons. The transcriptome analysis showed the CCI-induced transcriptional change while administration of nitrous oxide *per se* had a small effect on gene expression. Despite this small change, a large number of CCI-deregulated genes were restored to a relatively normal level by nitrous oxide. This observation implies that the long-term antinociceptive effect of nitrous oxide might be mediated through transcriptional regulation of neuropathic pain-related genes.

Chapter 6 Functional Enrichment Analysis of Differentially Expressed Genes

6.1 Introduction

In the previous chapter, we performed expression pattern analysis and identified that nitrous oxide attenuated the transcriptional changes induced by neuropathic pain. We divided the DEGs into different modules based on the Venn diagram and identified different expression patterns among the four experimental groups (i.e. N_2O/CCI, N_2O/Sham, N_2/CCI, N_2/Sham). A further evaluation at DEGs suggested that nitrous oxide might produce prolonged antinociceptive effects through transcriptional regulation.

Although most studies supported that the acute antinociceptive effect of nitrous oxide was mediated by the descending inhibitory neurons, factors that are involved in nitrous oxide-induced prolonged antinociception remain unclear. During the development of chronic pain, cytokines derived from immune cells and glial cells activated nociceptive neurons in the central nervous system (Bliss et al., 1993; Sandkuhler et al., 2009). These mediators include interleukins, TNFα and nitric oxide. Systematic investigation of signaling pathways that are involved in the secretion and production of these mediators will provide a new insight into the mechanism underlying the nitrous oxide-induced long-term antinociception.

In this study, Gene Ontology (GO) enrichment analysis, Kyoto Encyclopedia of Genes and Genomes (KEGG) pathway analysis, and motif-enriched transcription factor (TF) identification were performed to delineate the distinct functional features of the long-term effect of nitrous oxide on the protection against chronic neuropathic pain.

6.2 Materials and Methods

6.2.1 Gene ontology functional annotation

GO terms are created to represent a series of biological processes or molecular functions that include sets of genes known to be correlated to the descriptor. The GO analysis ranks the GO terms by significance via a false discovery rate (FDR)-adjusted *p*-value obtained from a Fisher's exact test. In this study, GO enrichment analysis was performed with DEGs identified in the 3 experimental groups (i.e. N_2/CCI, N_2O/CCI and N_2O/Sham). Categories with $p < 0.001$ and more than 5 involved genes were considered significant and ranked according to their corrected p values.

6.2.2 Kyoto Encyclopedia of Genes and Genomes pathway data and analysis

Pathway analysis was utilized to identify significant pathways of the DEGs according to KEGG. We used Fisher's exact test to select the significant pathways, and the threshold of significance was defined by p-value and FDR.

6.3 Results

6.3.1 Differences in gene ontology categories of two neuropathic pain groups

In order to characterize and provide an overview of the biological functions of genes involved in the transcriptional regulation by nitrous oxide in the protection against neuropathic pain, functional annotation and GO analysis of these genes were performed. Overall, a total of 90.8%, 91.2%, and 86.2% transcripts were assigned with a putative function in N_2/CCI, N_2O/CCI and N_2O/Sham groups, respectively. As shown in the GO map (Figure 6.1), the identified DEGs were mainly involved in cell cycle regulation, inflammatory response, regulation of signal transduction, and immune cell activity.

Remarkable differences were observed in the enriched GO categories between the N_2/CCI and N_2O/CCI groups. For instance, categories such as regulation of extracellular signal–regulated kinases (ERK)-1 and ERK2 cascade (GO:0070374, 16 genes), the apoptotic process (GO:0006915, 25 genes), response to hydrogen peroxide (GO:0042542, 10 genes), other early responses to never injury (including GO:0034341-response to interferon-gamma, GO:0051591-response to cAMP, and GO:0071347-cellular response to interleukin-1), and the recruitment and activation of spinal microglia and astrocytes (GO:0042113-B cell activation, GO:0002639-positive

regulation of immunoglobulin production) were only enriched in the N_2/CCI group but not in the N_2O/CCI group. All these functional categories have been reported to participate in the development of neuropathic pain (Zhuang et al., 2005; Song et al., 2005; Sawada et al., 2008; Malmberg et al., 1997). Other categories, such as positive regulation of interleukin-6 production (GO:0032755), positive regulation of IL1β secretion (GO:0050718), positive regulation of phagocytosis (GO:0050766) and mast cell activation (GO:0045576), were enriched in both N_2/CCI and N_2O/CCI groups.

Besides, in the N_2O/sham group, 30 DEGs were significantly clustered to the neuropeptide signaling pathway (GO:0007218, 5 genes), suggesting that nitrous oxide might directly regulate pain sensitivity by increasing the expression of opioid peptides and members in the tachykinin peptide hormone family.

Figure 6. 1 Gene ontology enrichment analysis of differentially expressed genes

Fisher exact test, filtering *p*-values for multiple testing using false discovery rate.

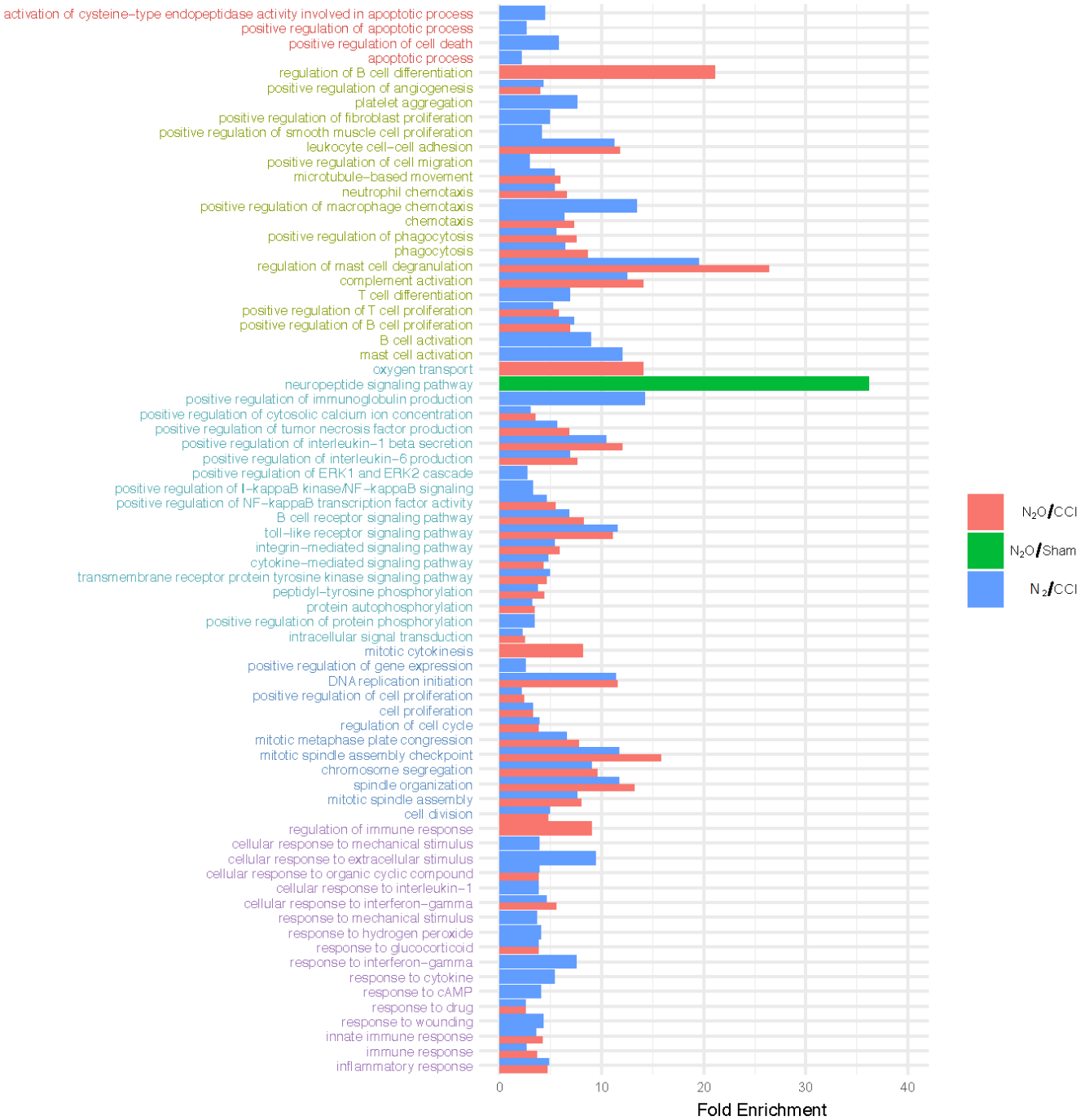

6.3.2 Preferences of multiple pain-related signaling pathways in neuropathic pain groups

Apart from GO analysis, we performed enrichment analysis of KEGG annotations with the 630 and 468 DEGs from the N_2/CCI and the N_2O/CCI groups, respectively. A total of 26 KEGG terms were identified, which were significantly over-represented in both groups (Figure 6.2). As expected, the enriched KEGG terms were implicated in signaling pathways that regulate the recruitment of resident spinal microglia and circulating monocytes to the dorsal horn, such as toll-like receptor signaling, Jak-STAT signaling, and nuclear factor (NF)-κB signaling pathways. These signaling pathways were shared by the two groups.

Notably, some novel pathways such as Fc gamma R−mediated phagocytosis, Fc epsilon RI signaling pathway, as well as osteoclast differentiation, exclusively enriched in the N_2/CCI group. It has been reported that ephrinB1-Fc contributes to the PI3K-mediated spinal nociceptive modulation (Yu et al., 2012). Other three highly enriched pathways implicated in neuropathic pain development were cell cycle, osteoclast differentiation and natural killer cell-mediated cytotoxicity (Scholz et al., 2007; Honore et al., 2000).

Furthermore, expression levels of genes involved in multiple signaling pathways were significantly different between N_2/CCI and N_2O/CCI groups, demonstrating that nitrous oxide treatment preferentially altered these signaling pathways (Figure 6.3). Among them, expression of three over-represented components of the enriched Jak-STAT signaling pathway, namely (1) receptors (IL4r and Csf2rb); (2) transducer (Stat3) and (3) feedback suppressors (Socs3) were all increased by CCI. The induction of these components was attenuated by intraoperative nitrous oxide administration.

Collectively, GO and KEGG analyses indicated that CCI provoked changes in multiple molecular circuitries, which could be attenuated by nitrous oxide administration. These counteracted effects of nitrous oxide might play an important role in the modulation of neuropathic pain.

Figure 6. 2 Kyoto Encyclopedia of Genes and Genomes enrichment analysis of differentially expressed genes identified from chronic constrictive injury rats with and without nitrous oxide

Significantly enriched KEGG pathways ($p < 0.05$) are presented. For each KEGG pathway, the y-axis and x-axis indicate pathway name and fold enrichment respectively. The size of circles and dots represents the number of involved genes.

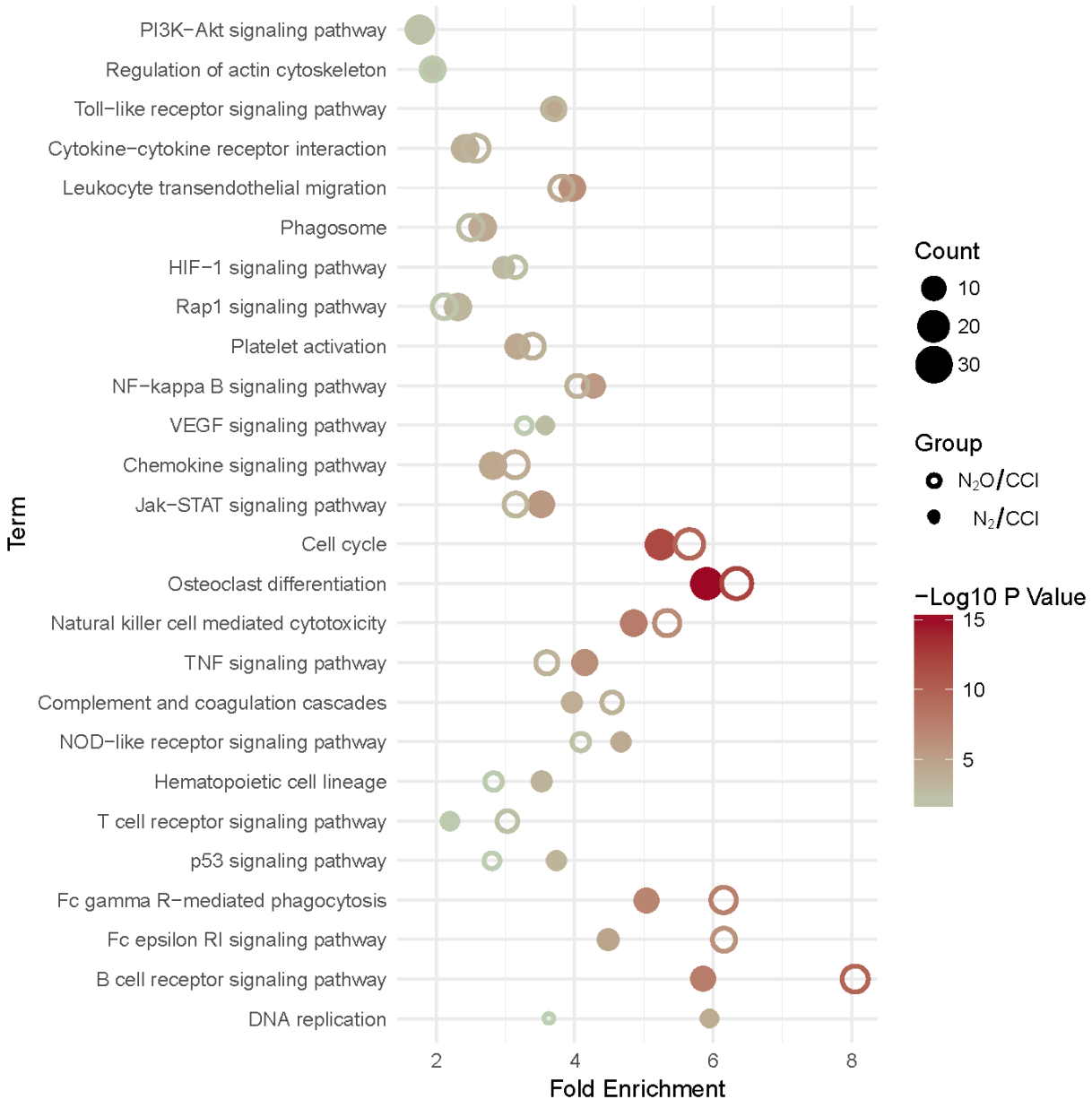

Figure 6. 3 The normalized expression values in selected signaling pathways

The expression levels were calculated in terms of fragments per kilobase of exon model per million mapped reads (FPKM). *n* = 3 replicates per group.

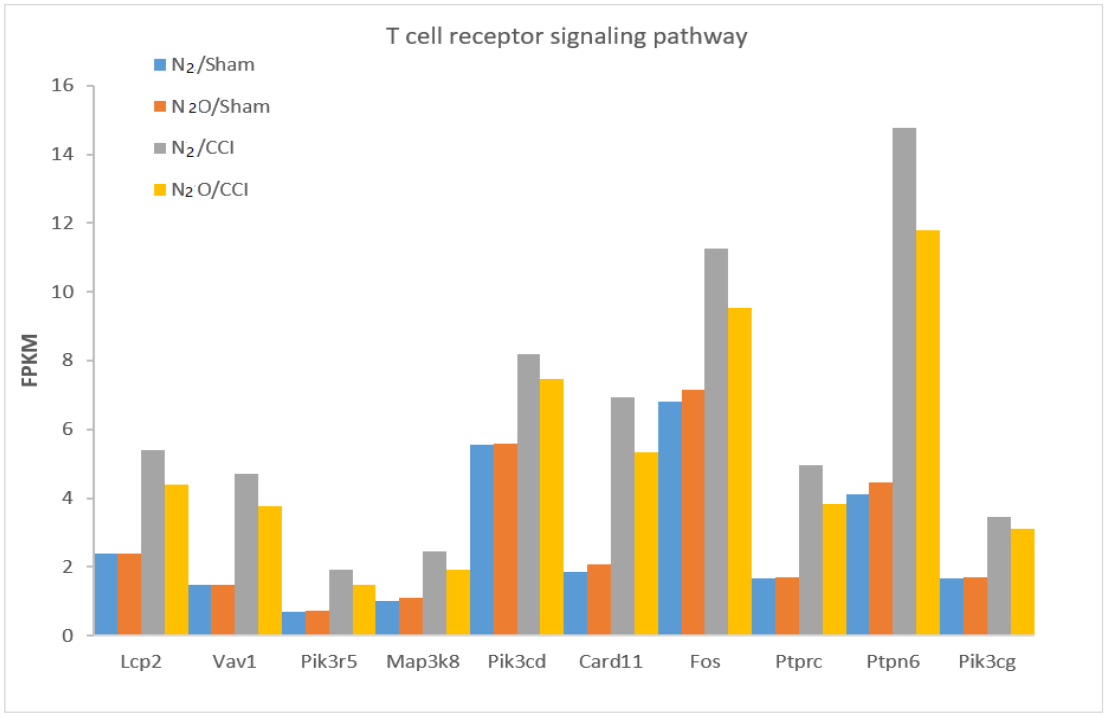

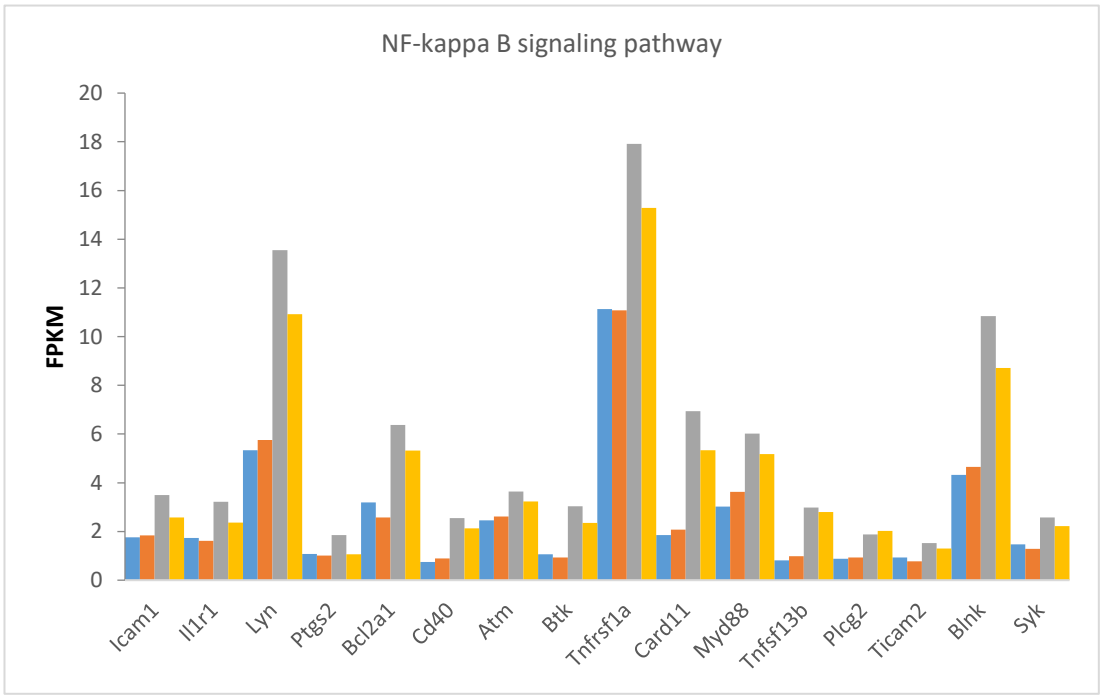

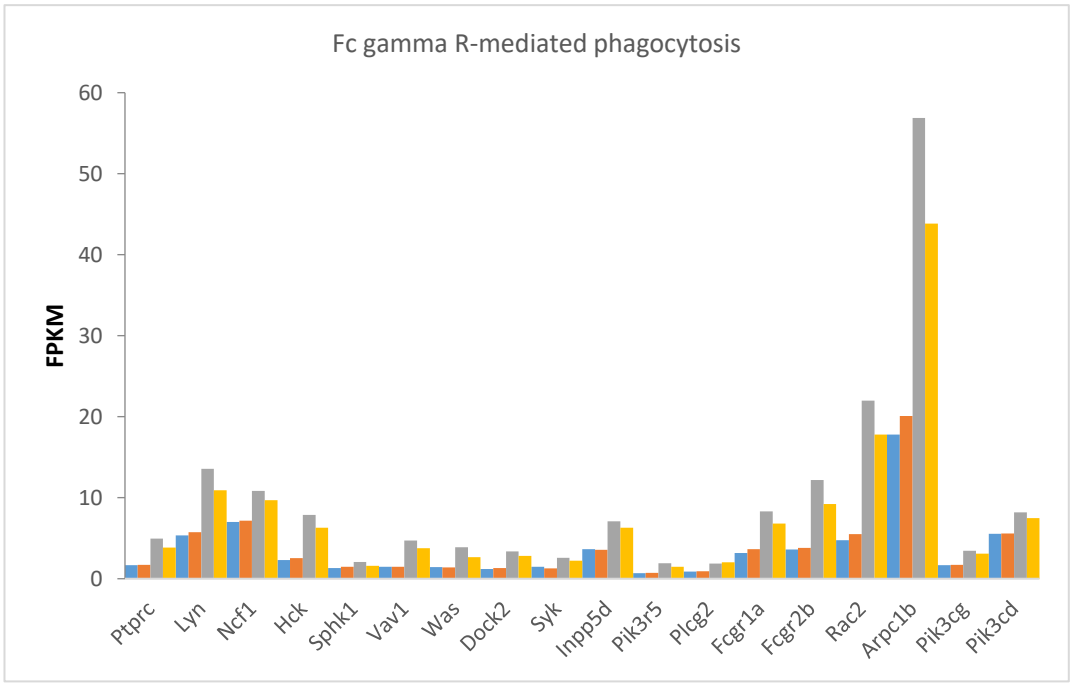

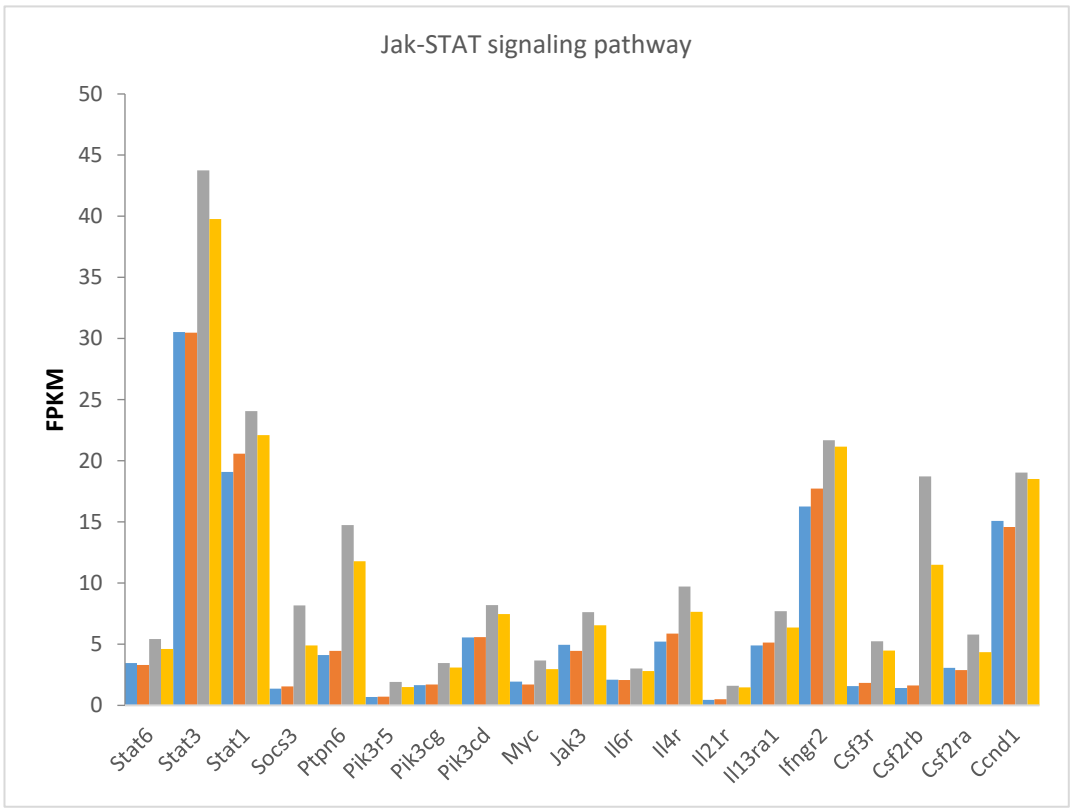

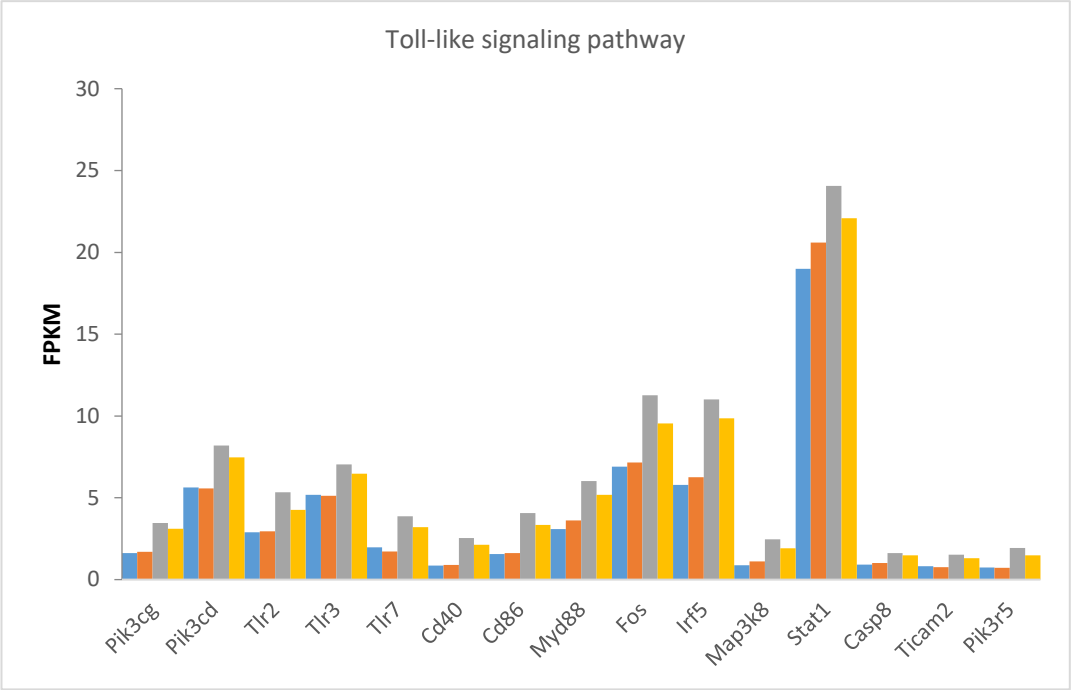

6.3.3 Transcription factor-binding site enrichment in differentially expressed genes of neuropathic pain

To further uncover the potential regulatory network contributing to the development of neuropathic pain, TF-binding site (TFBS) enrichment analysis was performed with the total dysregulated genes in Modules 2 and 4. About 140 TFs were identified to be significantly enriched among these nitrous oxide-sensitive neuropathic pain-related genes ($p < 0.05$) (shown as Appendix 1). According to the GO annotations, 10 TFs showed the association with the nervous system development. Remarkably, 5 TFs showed a strong relationship with glial cell differentiation and proliferation while 9 were related to neural crest cell migration or neural precursor proliferation. The interaction network of these enriched TFs was shown in Figure 6.4. Moreover, many of these enriched TFs have been implicated in the regulation of inflammatory response (such as TGF-beta signaling and MAPK signaling), which is important to the development of neuropathic pain.

Importantly, based on our RNA-sequencing data, 12 TFs were induced in the CCI model compared with the sham surgery group, while the upregulation was attenuated under nitrous oxide administration. These TFs showed their *p*-value of motif enrichment with the percentage of putatively targeted DEGs, as in Figure 6.5. Notably,

we found that over half of the DEGs were enriched for Stat3-, Stat1-, Spi1-, Irf8-, Irf5-, Ikzf1-, Foxm1-, Fli1-, Elk3-, and Egr1-binding sites. Besides, according to GO functional annotation, 10 of them played a role in the regulation of cell differentiation. Among these 10 DEGs, Ikzf1, Spi1, Egr1, Stat1, and Stat3 were involved in the immune and glial cell differentiation. Aberrant activation of non-neuronal cells has been reported to contribute to the development and persistence of neuropathic pain after never injury (Scholz et al., 2007). Therefore, the attenuated expression of these enriched TFs by nitrous oxide may be responsible for the long-term analgesic effect via transcriptional regulation in the development of neuropathic pain.

Figure 6. 4 The predicted protein-protein interaction network with significantly enriched transcription factors from common differentially expressed genes in neuropathic pain

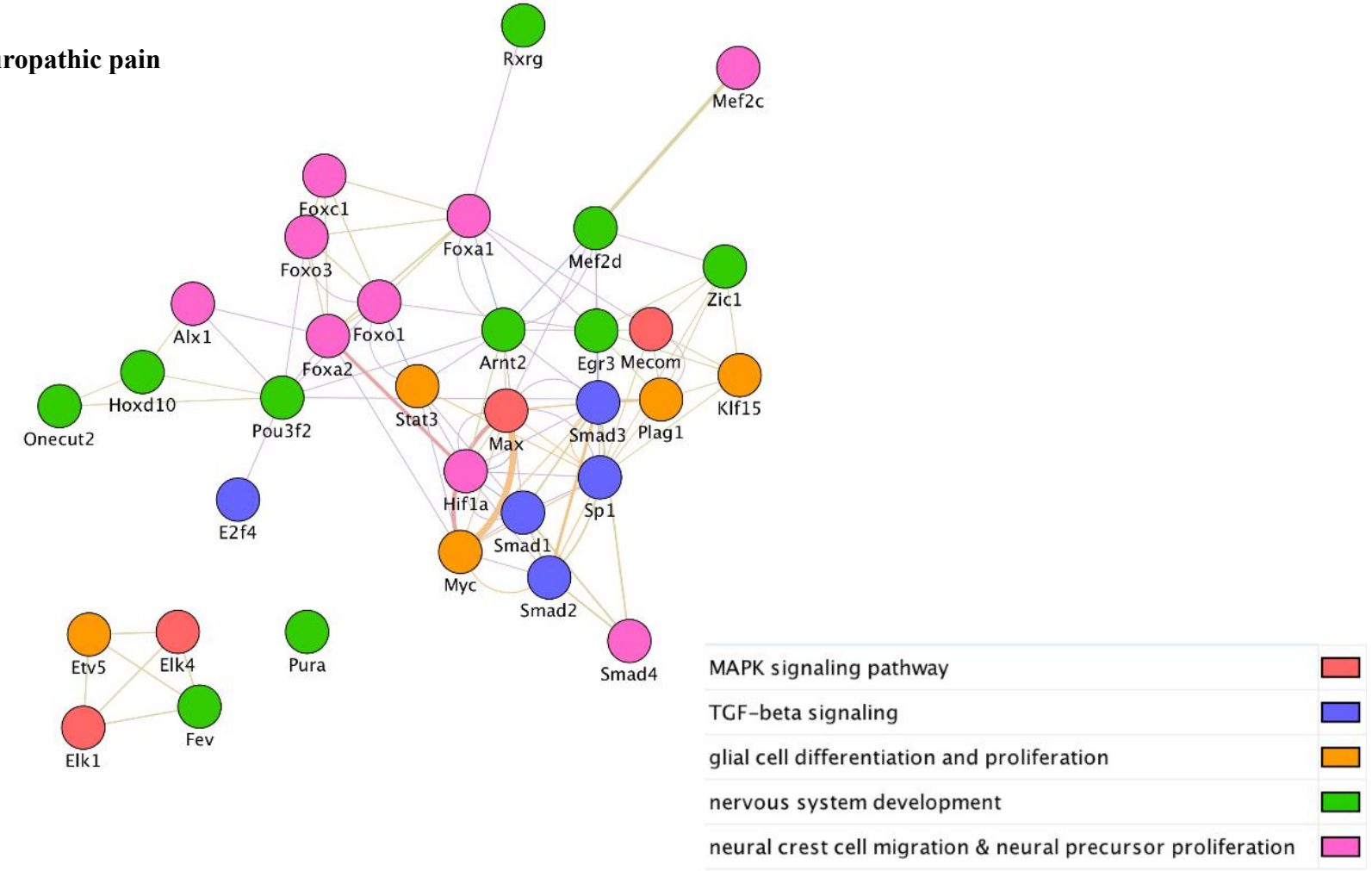

Figure 6. 5 Transcription factor binding motif enrichment analysis

TF-binding site (TFBS) enrichment analysis was performed with previously common dysregulated genes in two CCI groups. About 140 TFs were significantly enriched among these nitrous oxide-sensitive neuropathic pain-related genes. Among them, 12 enriched TFs were upregulated in the CCI model, and attenuated upon nitrous oxide administration. The results showed their enriched *p*-value and the percentage of putatively targeted DEGs.

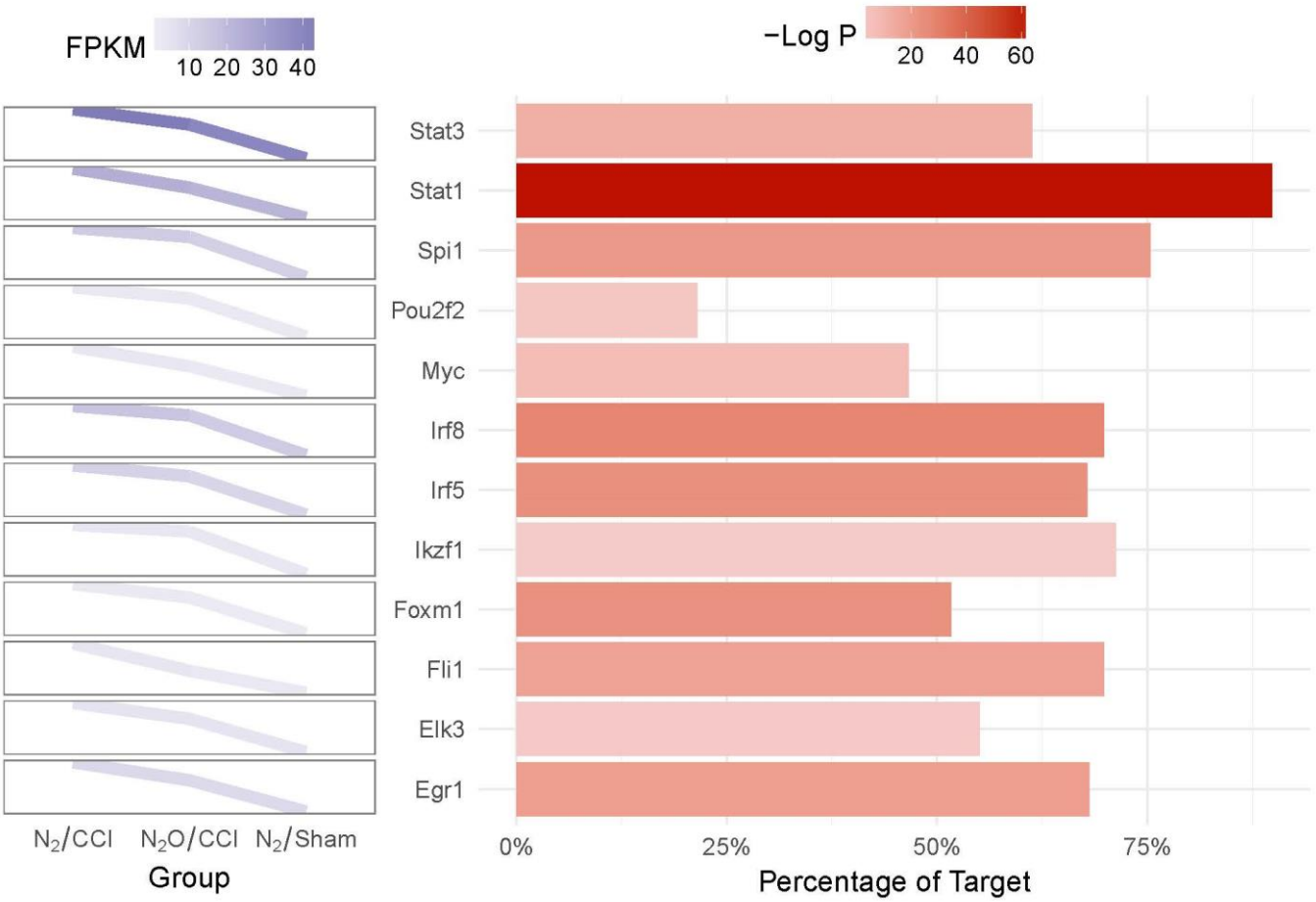

6.3.4 Distinctly dysregulated differentially expressed genes with or without nitrous oxide in chronic constrictive injury rats

The expression of dysregulated genes following neuropathic pain development were globally attenuated by nitrous oxide. These genes were involved in numerous cellular processes, such as activation of astrocytes, recruitment of microglial and neuronal cell responses. The differences in the DEGs between N_2/CCI and N_2O/CCI groups should be account for the long-term alleviation of CCI-induced neuropathic pain by nitrous oxide. To gain more insight into the subtle differences induced by nitrous oxide, we compared the RNA profiles of N_2O/CCI and N_2/CCI samples. Total 85 distinctly dysregulated genes (adjusted $p < 0.05$) between the two CCI groups were identified. Sixteen of them were upregulated whereas the remaining 69 were down-regulated in the N_2O/CCI group.

GO analysis of these DEGs was performed to define the most relevant signals induced by N_2O under neuropathic pain. Figure 6.6 illustrated the functionally grouped annotation network. Statistical significances were found in categories of oxygen transport (GO:0015671, Bonferroni-adjusted $p < 0.05$), positive regulation of B cell proliferation (GO:0030890, adjusted $p < 0.05$) and response to cytokine (GO:0034097, adjusted $p < 0.05$). GO analysis result was presented in Appendix 2. Notably,

consistent with the previous analysis, Stat1, Irf5, Fomx1, Fli1, Egr1, and Spi1 came out as the significantly enriched TFs during TFBS motif enrichment analysis (data not shown).

Figure 6. 6 Networks of significantly enriched gene ontology terms

Enrichment for gene ontology (GO) of differentially expressed genes between N_2/CCI and N_2O/CCI groups was done using the ClueGO plugin and Cytoscape software. Nodes are coloured according to grouping of related functions by statistically significant association of related GO terms Functional clustering. Node size corresponds to the significance of each GO term in the network and edges indicate statistically significant associations between GO terms.

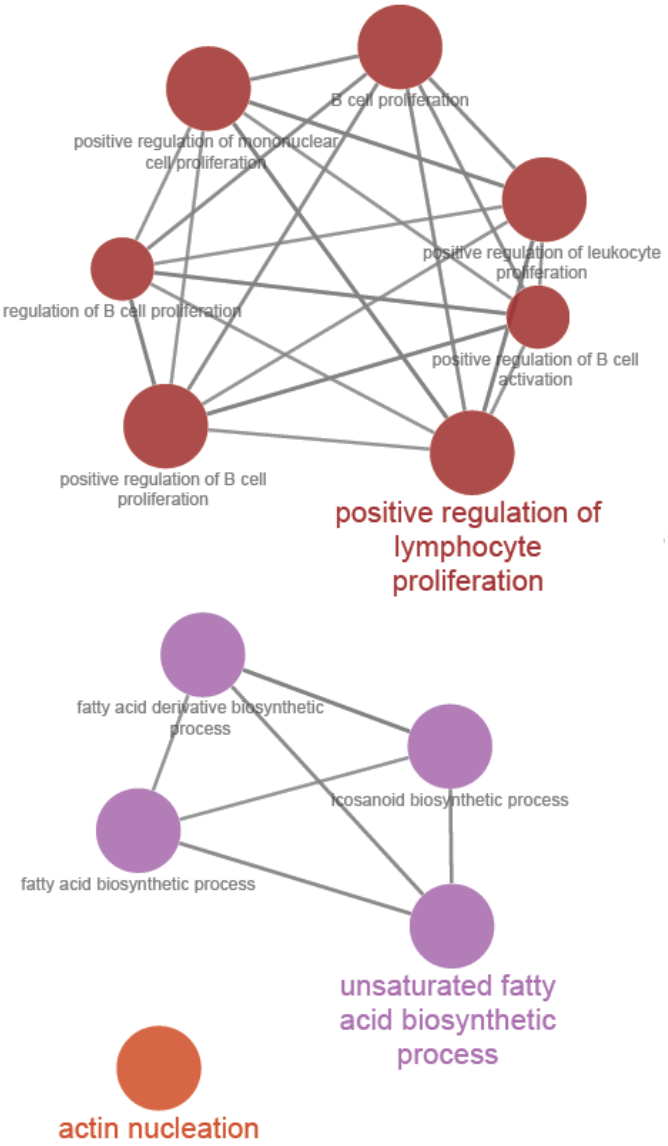

6.3.5 Atf3 was a potential target for nitrous oxide-mediated antinociception

In order to explore the molecular mechanism of nitrous oxide mediated analgesia, we first classified the differentially expressed genes by the following criteria: (1) the mRNA must be up-regulated by CCI surgery but reversed by intraoperative treatment with nitrous oxide, and (2) the expression of gene must be in a good mean-variance relationship across different groups. Atf3 was identified as most represented candidate gene (Figure 6.7). The expression level of Atf3 was further quantified by qPCR analysis (n = 4 per group). In common with RNA sequencing study, CCI surgery induced a dramatic increase of Atf3 mRNA, whereas intraoperative treatment with nitrous oxide significantly reversed nerve injury induced Atf3 upregulation on day 3 (Figure 6.8).

In the current study, Atf3 was identified as the most prominent differentially expressed transcription factors (DETFs) across 4 groups. Moreover, by motif enrichment analysis, we identified that the binding sites of Atf3 were overrepresented in the promoter region of DEGs (shown in Appendix 4). We hypothesized that Atf3-mediated transcriptional regulation contributs to the development of neuropathic pain and nitrous oxide prevents persistent pain through repressing Atf3 signaling.

Figure 6. 7 Mean-variance relationship of differentially expressed genes

Differentially expressed genes in $\log_{10}$ (fold changes) in x-axis represented for the expression variances, and the average expression values with FKPM values in the y-axis. Atf3 was indicated in red circle.

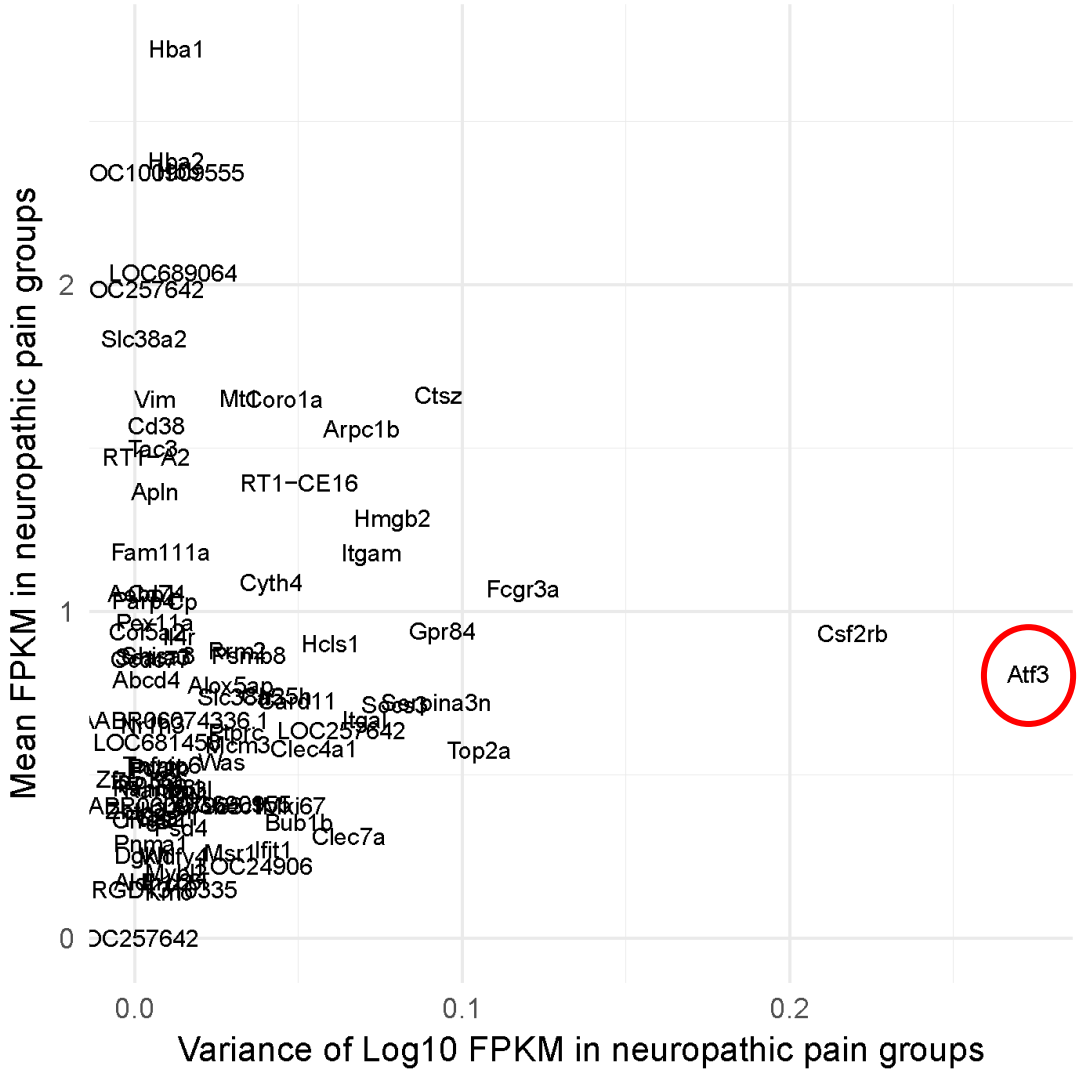

Figure 6. 8 Nitrous oxide partially reversed nerve injury induced Atf3 elevation in ipsilateral lumbar spinal

The tissues were collected 3 days after surgery. The expression levels were calculated in terms of fragments per kilobase of exon model per million mapped reads. Error bars are SEM; $n = 3$ replicates per group, one-way ANOVA, $^{**}p < 0.01$ compared to N_2/CCI.

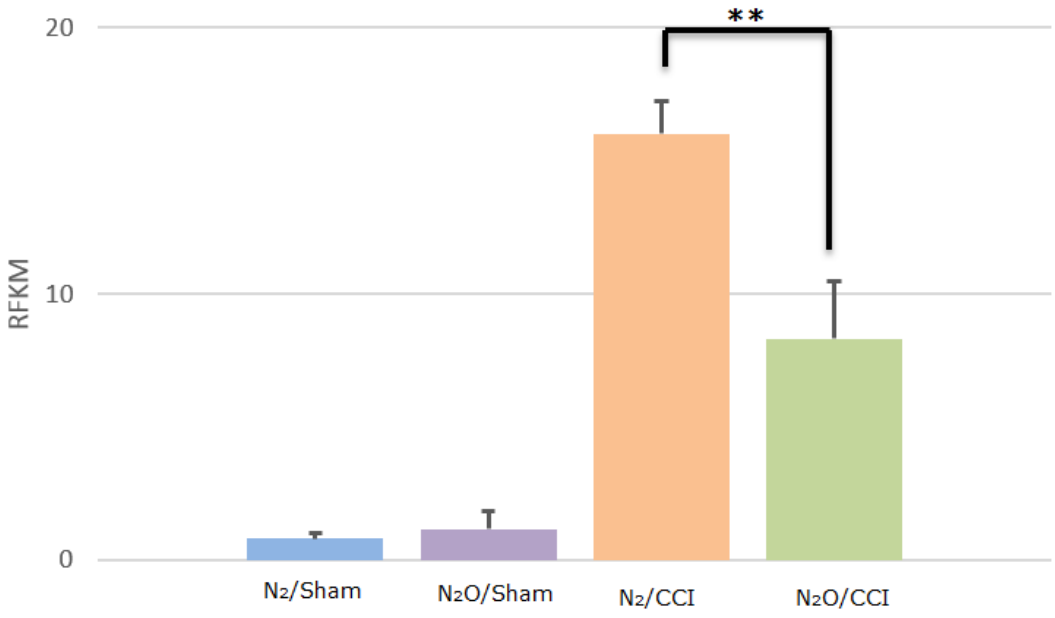

6.3.6 Atf3-centered regulation network controlled the development of neuropathic pain

In order to explore the relationship of ATF3 and DEGs, we identified the components of the Atf3-centered regulatory complex. Computation based approach was adopted to discover the protein-protein interaction network from the list of differentially expressed transcription factors (DETFs) (shown in Appendix 1). Atf3-interacting TFs were identified based on STRING database. As shown in Figure 6.9, 10 DETFs were regarded as the first-order neighbors of Atf3 and another 8 were the second-order TFs. Notably, several "nodes" in the interaction map are representative transcription factors involved in neuropathic pain, including STAT (stat1, stat3, and stat6) and AP1 (Junb, Fos, and Fosb). For instance, enhanced activity of signal transducer and activator of transcription 3 (Stat3) has been described to promote the expression of pro-nociceptive cytokines/chemokines and gliosis (Dominguez et al., 2008; Wang et al., 2014; Liu et al., 2015). Similarly, expression of c-Fos was widely used as a marker of neuronal excitation, including the pain projection neurons in spinal dorsal horn.

Further analysis on the regulatory network (red line) and protein-protein interaction network (gray line) of all DEGs (including DETFs) showed that Atf3-centered transcriptional complex connected with almost all DEGs between N_2/CCI and

N_2O/CCI groups (Figure 6.10). The in-silicon analysis suggested that ATF3 acted as a transcriptional "hub" to modulate the development of neuropathic pain.

Taken together, functional enrichment analysis indicated that nitrous oxide induced transcriptional regulation on different molecular circuitries for the protection against neuropathic pain development. Further differentially expressed gene analysis and protein-protein interaction analysis identified Atf3 as the most representative nitrous oxide-susceptible DEGs. It suggested that Atf3-centered transcriptional regulatory network is a potential mechanism for the persistent antinociceptive effect of nitrous oxide in neuropathic pain.

Figure 6. 9 Protein and protein interaction network of differentially expressed transcription factors

Nodes are individual transcription factors (TF). Edges represent the predicted interaction between two TF. Edges connecting to Atf3 are highlighted in pink. Nodes are color-coded based on neighborhood relationship to Atf3. Orange represents the first-order neighborhood. Green stands for the second-order neighborhood. The left nodes are presented as blue. Node size represents 'closeness centrality', which is calculated as the sum of the length of the shortest paths between the node and all other nodes in the graph. Node transparency level represents average expression level in all samples.

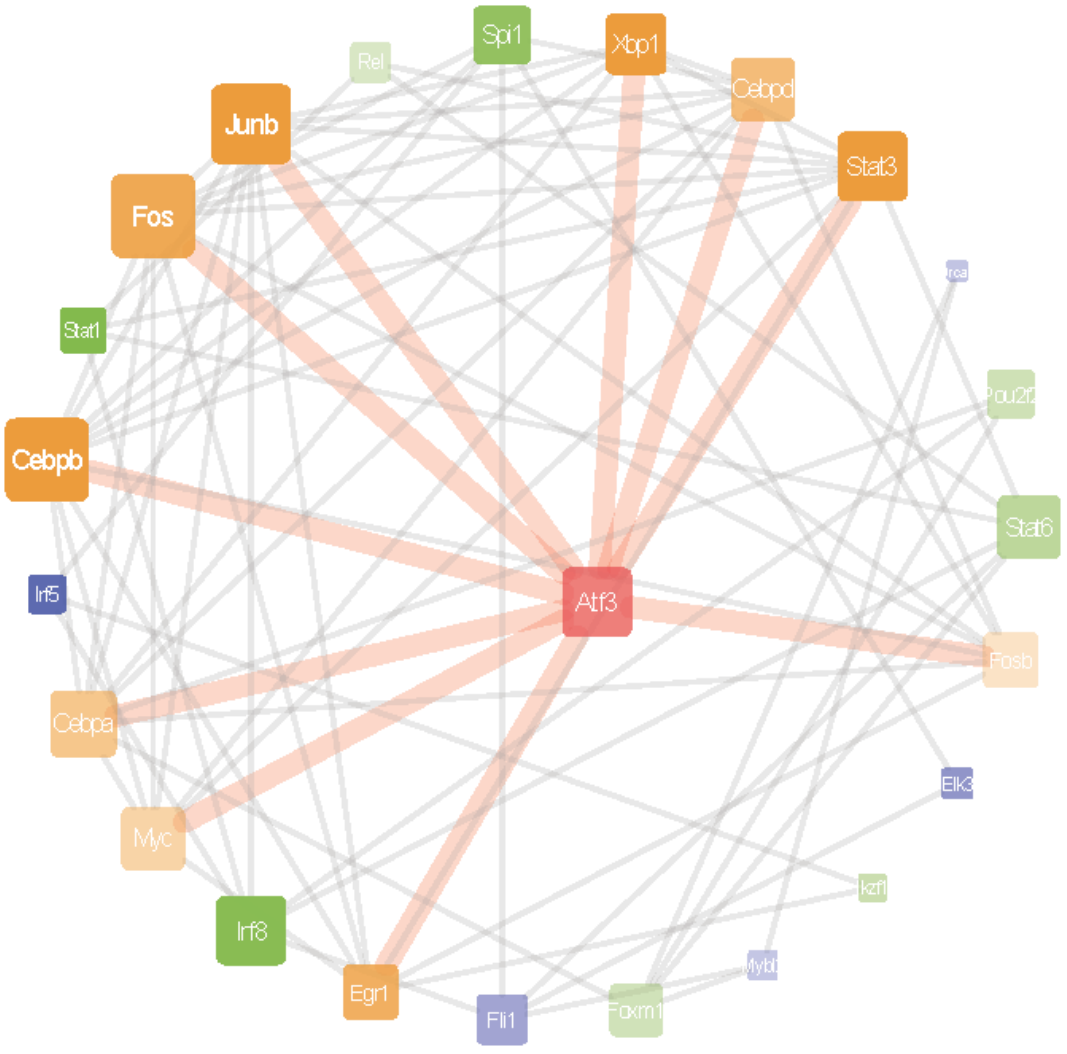

Figure 6. 10 Protein and protein interaction and regulatory network between differentially expressed transcription factors and expressed genes

The average expression level (FPKM) of genes in all group were represented using node transparency; variance of FPKM in all group was represented using node size. Square shape stands for transcription factor (TF) genes and round shape stands for differentially expressed genes (DEGs). DEGs of N_2/CCI vs N_2O/CCI were highlighted using yellow borders. Besides, the red line between a TF and the DEG means the corresponding motif in the promoter region of that DEGs.

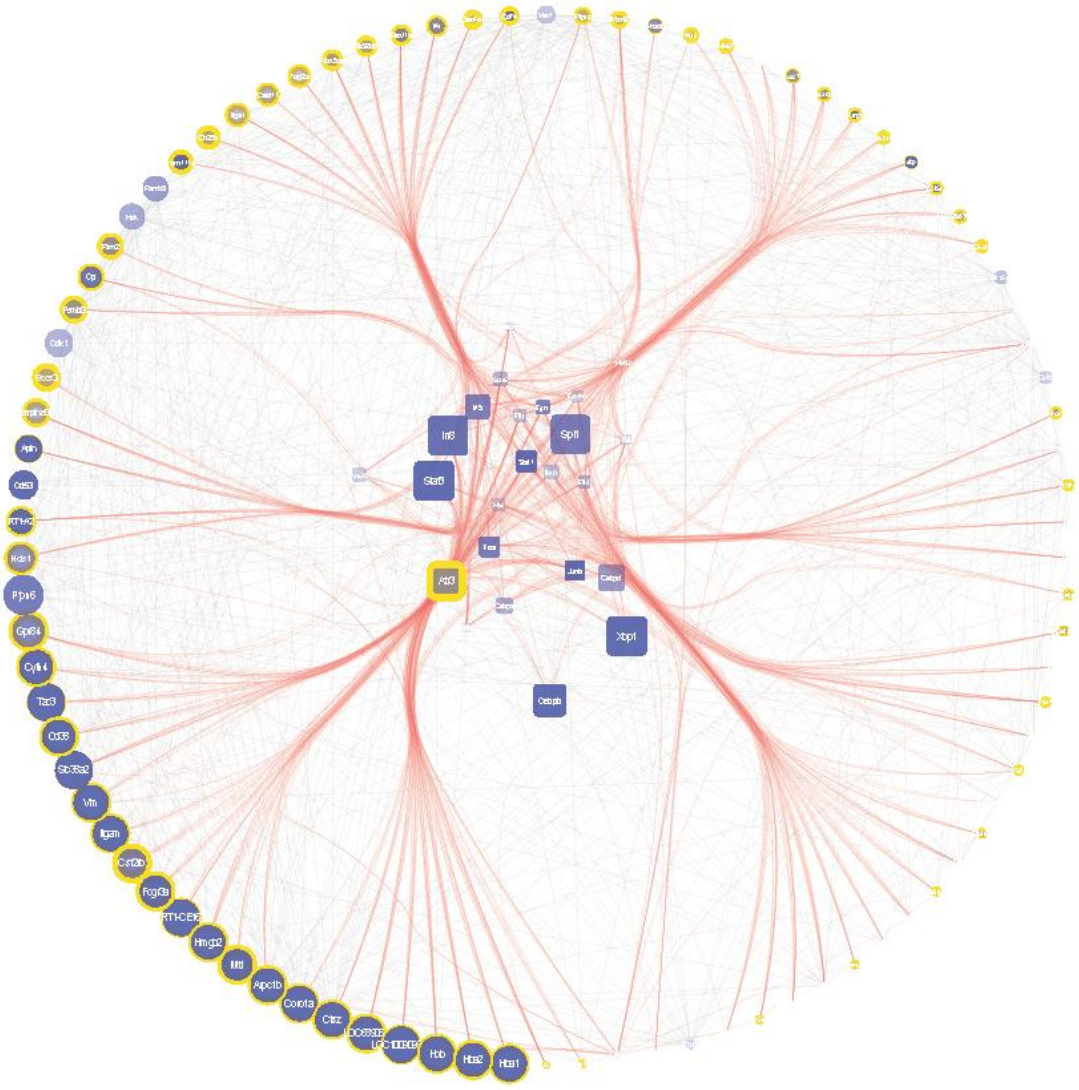

6.4 Discussions

In this part, GO functional enrichment analysis, KEGG pathway analysis, as well as TFBS-motif enrichment analysis were applied to identify the differentially regulated molecular circuitries between rats CCI models with or without intraoperative N_2O administration. Previous studies have reported that the signaling network altered in the spinal cord in neuropathic pain models included ion channel regulation, activation of the immune response and cell migration (Galbavy et al., 2017; Vallejo et al., 2016). Our GO and KEGG analyses showed that additional categories, including inflammatory response and immune cell activation-related signaling transduction, were significantly enriched, suggesting that the recruitment and activation of immune cell and microglia in the dorsal horn are crucial to the initiation of neuropathic pain (Scholz et al., 2007). Furthermore, nitrous oxide administration seemed to attenuate several inflammation-related pathways, such as IL1, cAMP and interferon gamma, in ipsilateral spinal dorsal horn as compared to the untreated CCI group.

Limitations:

In spite of the differences in enriched terms between N_2/CCI and N_2O/CCI, it does not make any biological sense. Further analysis of the average expression variance in each enriched KEGG pathways can be done to distinguish the most susceptive ones

to nitrous oxide.

Conclusions:

These analyses revealed that nitrous oxide alleviates neuropathic pain by modulating multiple molecular circuitries. Furthermore, Atf3 is a potential target for nitrous oxide-mediated antinociception. Functional study for this novel molecular target of nitrous oxide is discussed in chapter 8.

Chapter 7 Methylome Features of Neuropathic Pain

7.1 Introduction

Epigenetics processes, including histone modification and DNA methylation, have been associated with many neuronal functions including synaptic plasticity (Feng et al., 2007), learning and memory (Bird et al., 2002; Colciago et al., 2016; Karpova et al., 2017) and chronic pain (Denk et al., 2012). DNA methylation is the process by which methyl groups are added to the DNA molecule. It changes the activity of a DNA segment and leads to stable and heritable changes in gene function without any concomitant DNA sequence changes (Suzuki et al., 2008).

Since DNA methyltransferases prefer to targeting on the nucleosome-bound DNA (Feng et al., 2010; Chodavarapu et al., 2010; Gelfman et al., 2013), as well as the intragenic regions (Lokk et al., 2014; Jones et al., 2012; Maunakea et al., 2013), the various enrichment patterns of DMRs in these regions will suggest a functional role in transcriptional regulation.

In chronic pain, three main areas of epigenetic control can be identified based on previous studies: (1) epigenetic regulation of peripheral inflammation, (2) epigenetic gene regulation in pain processing, and (3) epigenetic involvement in plasticity and

cortical pain processing (Crow et al., 2013; Bai et al., 2015). It has been reported that methylation of lysine 4 of histone 3 (H3K4) helped to recruit NF-κB to proinflammatory genes, which were involved in the action of both glial and neuronal NF-κB under chronic inflammatory pain states (Li et al., 2008; Fu et al., 2010). Interestingly, the methyl CpG binding protein (MeCP2), that has been shown to promote abnormal upregulation of a group of genes in inflammatory pain, was further demonstrated to alter pain thresholds (Samaco et al., 2008).

A recent report also found that the increased DNA methylation in SPARC gene promoter was associated with the chronic pain in both mice and humans (Tajerian et al., 2011). Re-expression of the gene encoding ET (B) receptor (EDNRB), has been shown to attenuate cancer pain (Viet et al., 2011). This finding demonstrated that the methylation of EDNRB acted through a novel regulatory mechanism in cancer pain. Another nociceptive gene, CBS was significantly upregulated at both protein and mRNA level in peripheral inflammation induced by intraplantar injection in rat dorsal root ganglia (DRG). Epigenetic regulation of CBS expression may contribute to the inflammatory hyperalgesia (Qi et al., 2013). In specific gene region, the methylation changes in intergenic CpG-riched regions also affected the hippocampal neuronal activity (Guo et al., 2011).

Taken together, a surge of research suggests that DNA methylation may be an important contributor to chronic pain (Votta-Velis et al., 2013; Bell,J. et al., 2014; Ciampi et al., 2017). Examination of the genome-wide methylome signature in chronic pain model will be useful to explore the epigenetic process and provide new basics for future drug development.

7.2 Materials and Methods

7.2.1 DNA dot blot

Genomic DNA (gDNA) was isolated by phenol- chloroform extraction. Samples were diluted in 0.1 M sodium hydroxide, heated to 95°C, spotted onto a positively charged nylon membrane, dried and cross-linked with ultraviolet (UV) light for 4 min. The membrane was blocked in PBS-Tween 20 buffer with 10% non-fatty milk, and then was incubated with anti-5-methylcytosine (5mC) mouse antibody (1: 5,000 dilution, GeneTex, Inc) overnight at 4°C. The secondary anti-mouse IgG antibody, conjugated with horseradish peroxidase (Cell Signaling Technology), was applied for 45 min at room temperature. Chemiluminescent signals were then visualized with an ImageQuant™ LAS 4000 biomolecular imager (GE Healthcare).

7.2.2 Genome-wide methylation sequencing by MeDIP

Genomic DNA (gDNA) was isolated from the same tissues as RNA extraction did and extracted with DNeasy Blood & Tissue Kits (QIAquick Cat No./ID: 69504). The genomic DNA was fragmented into an average fragment size of 200–300 bp. Immunoprecipitation of methylated DNA and subsequent library construction and sequencing were performed by Genome, Inc. (Beijing, China). Reads were generated in a 50 bp paired-end using an illumina HiSseq 2500 platform.

7.2.3 Identification of differentially methylated regions (DMRs)

For screening of DMRs, we determined the frequency of methylated cytosines (mCs) in each bin size of 100 bp throughout the genome. For each bin, the methylation level at each cytosine site was calculated for each sample. The bins containing at least three mCs and a minimum difference of 20% methylation level with the *p*-value less than 0.05 were identified as DMRs.

7.3 Results

7.3.1 Characterization of the methylation features in spinal-neuropathic pain model

To examine the involvement of methylation changes in neuropathic pain, we collected the ipsilateral lumbar spinal horn on day 3 after CCI or sham surgery, with or without

nitrous oxide treatment (i.e. N_2/Sham, N_2O/Sham, N_2/CCI and N_2O/CCI group) for methylated DNA immunoprecipitation (MeDIP) sequencing. After removal of low-quality and contaminated reads, a total 1.19×10^8 raw reads were acquired from 12 samples. The sequence reads were mapped to the rat reference genome with a concordant pair alignment rate of around 95.2 - 96.2% (shown as Appendix 3).

Spearman's correlation analysis of hierarchical clustering was conducted based on the MeDIP sequencing data of 12 samples (Figure 7.1). The data showed that the methylation signatures of CCI groups was clearly distinct from sham-operated groups.

The heatmap generated with the methylation signals in the four experimental groups revealed that the samples of CCI and sham-operated groups clearly self-segregated into clusters. As shown in Figure 7.2, the DNA methylation pattern had a subtle change under different surgical conditions.

In order to further delineate the methylation alterations, the average methylation density among four groups was performed (Figure 7.3) and found that the methylation density became much higher with the increased methylation values, both in nitrous oxide-administrated sham group and CCI surgery groups. Nevertheless, higher

methylation density was found in sham group within the low methylated signal region.

In order to evaluate the distribution of methylation signals, we calculated methylation peaks within the methylated regions (FKPM > 10) through CpG island-based (CpG islands, CpG shores, CpG shelves, and CpG inter-regions), and gene-based (the promoter, upstream, exon, intron, as well as intergenic regions) annotations. Regarding the CpG island-based annotations, only 6% of the methylation signals was located in CpG islands, while over 80% of signals were distributed in CGI inter-regions (Figure 7.4A).

Subsequently, methylation signals were counted and compared across specific gene regions. Almost a half number of DNA methylation peaks was located in the gene body regions (15.3-19.4% in exon regions and 27-28.5% in intron regions), while only about 2.5% of the DNA methylation peaks was distributed in the promoter and upstream regions (Figure 7.4B). What more, a similar pattern was observed among different groups. When compared to N_2/Sham rats, DNA methylation was increased in exons, introns and intergenic regions after CCI surgery. Interestingly, intraoperative nitrous oxide-inhalation completely reversed nerve injury-induced methylation in exon and intron regions (Figure 7.4B). These results suggested that nitrous oxide may prevent

neuropathic pain through modulating methylation level, especially in the gene body regions.

We then compared the DNA methylation levels under different surgery conditions. Dot blot assay was performed to compare the global methylation level. As shown in Figure 7.5, the global DNA methylation in neuropathic pain group was significantly increased when compared to sham group, whereas perioperative administration of nitrous oxide reversed the nerve injury-mediated increase.

Based on the aforementioned analyses, it was discerned that the alterations on genome-wide DNA methylation occurred upon nitrous oxide administration and this may contribute to the prolonged antinociceptive effect in the development of neuropathic pain.

Figure 7. 1 Spearman correlation of relative methylation score

Unsupervised hierarchical clustering analysis based on the Spearman correlations of CpG methylation levels among samples from four groups having a chronic constrictive injury (CCI) or sham surgery with and without nitrous oxide (N_2O/CCI, N_2/CCI, N_2O/Sham and N_2/Sham). Points in dark blue clusters are those have a similar methylation score, and points in light blue are those with diverse methylation of their CpGs.

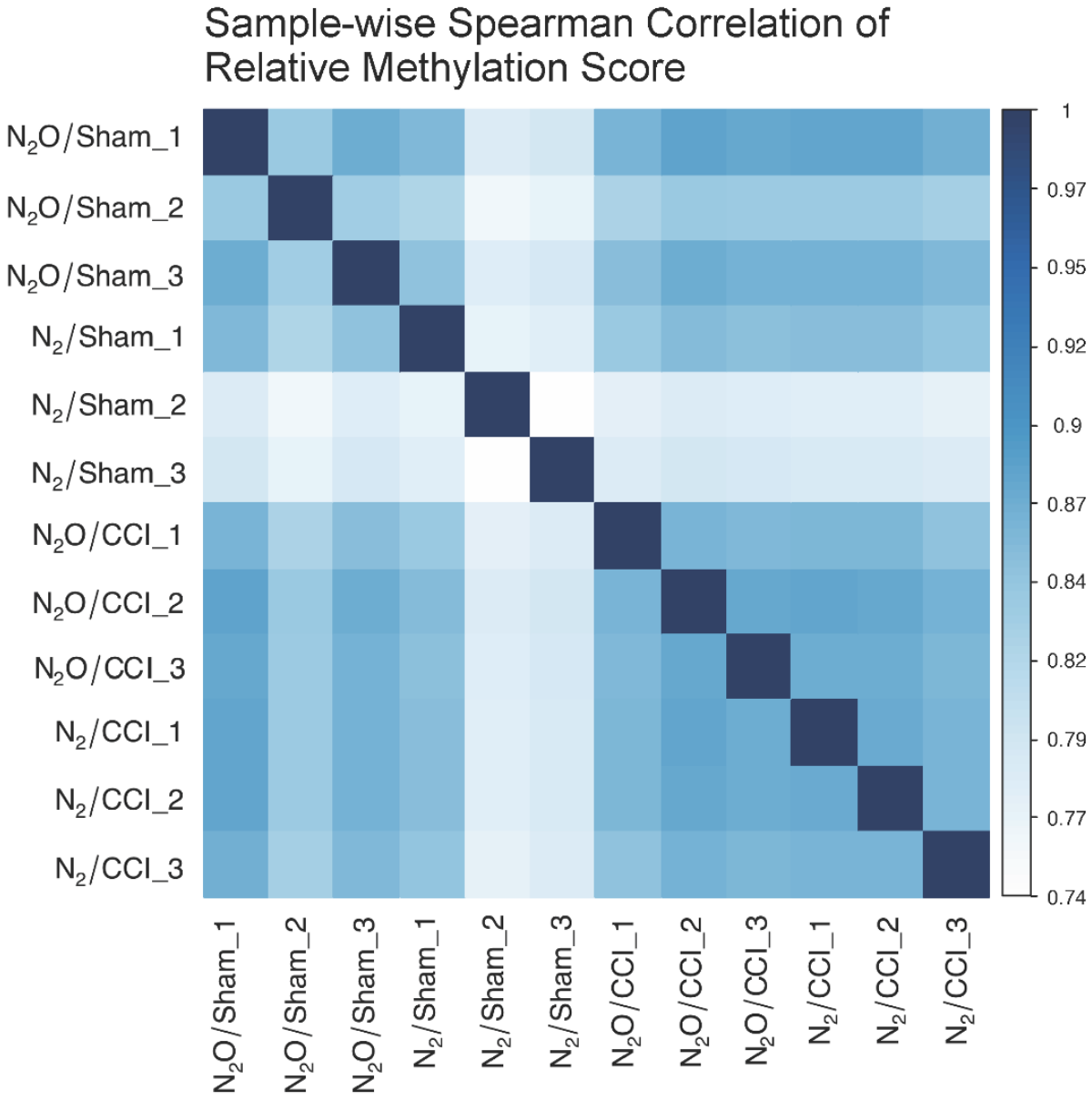

Figure 7. 2 Heatmap of expression of all methylation signals in four experimental groups

Expression levels of methylation identified in rats receiving chronic constriction injury (CCI) or sham surgery with and without nitrous oxide (N_2/CCI, N_2O/CCI and N_2O/Sham groups) compared with the N_2/Sham group were hierarchically clustered and shown in the heat-map. Each row represents a single gene and each column represents one sample. A red-blue color scale as shown in the upper left corner was used to indicate the expression level.

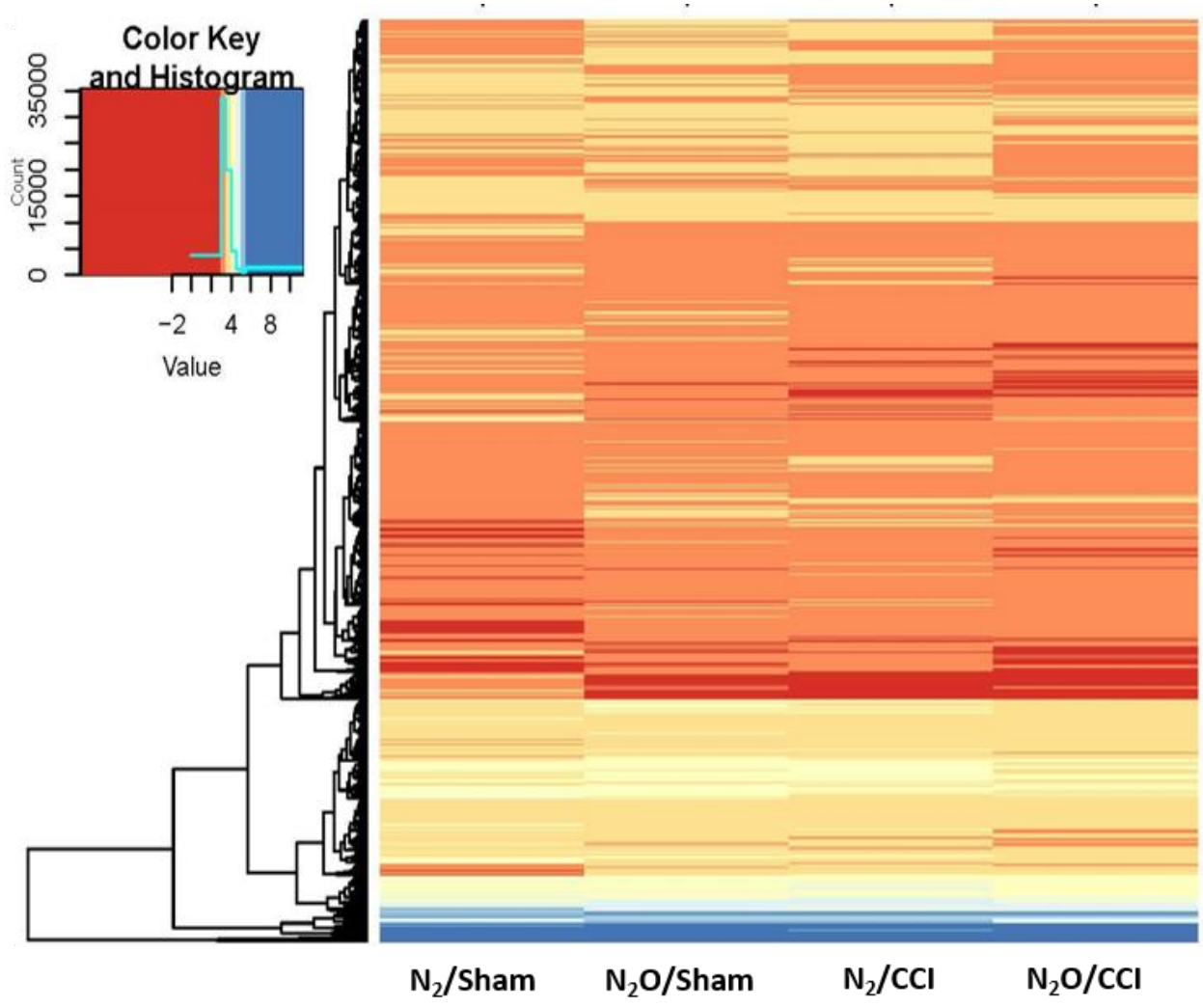

Figure 7. 3 Density plot of relative DNA methylation levels in the four experimental groups

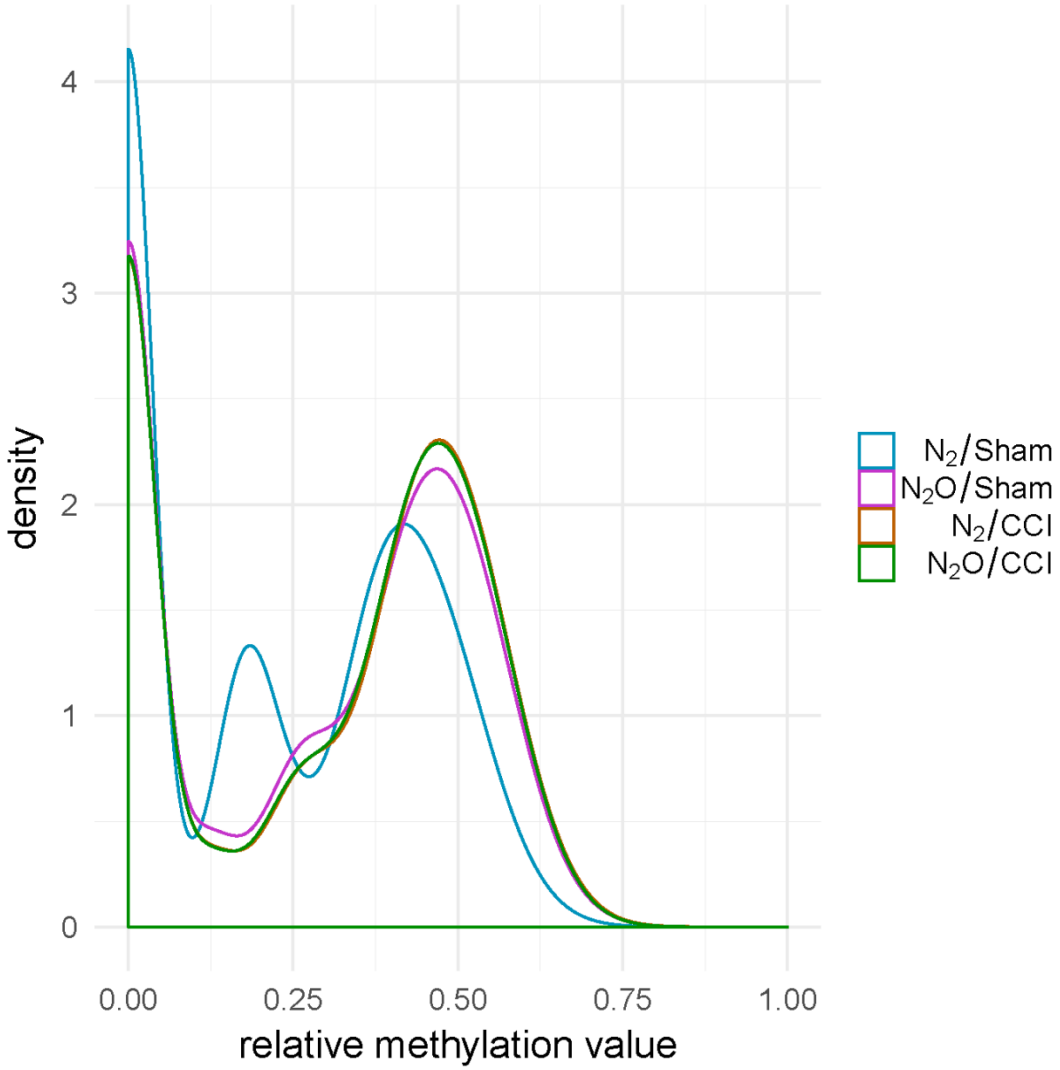

Figure 7. 4 Methylation peaks in ipsilateral lumbar spinal cord of sham or chronic constrictive injury models with or without nitrous oxide administration

Percentages of methylated peak in CpG island based distributions (A), Numbers of the methylated peak based on their localized genomic features (B).

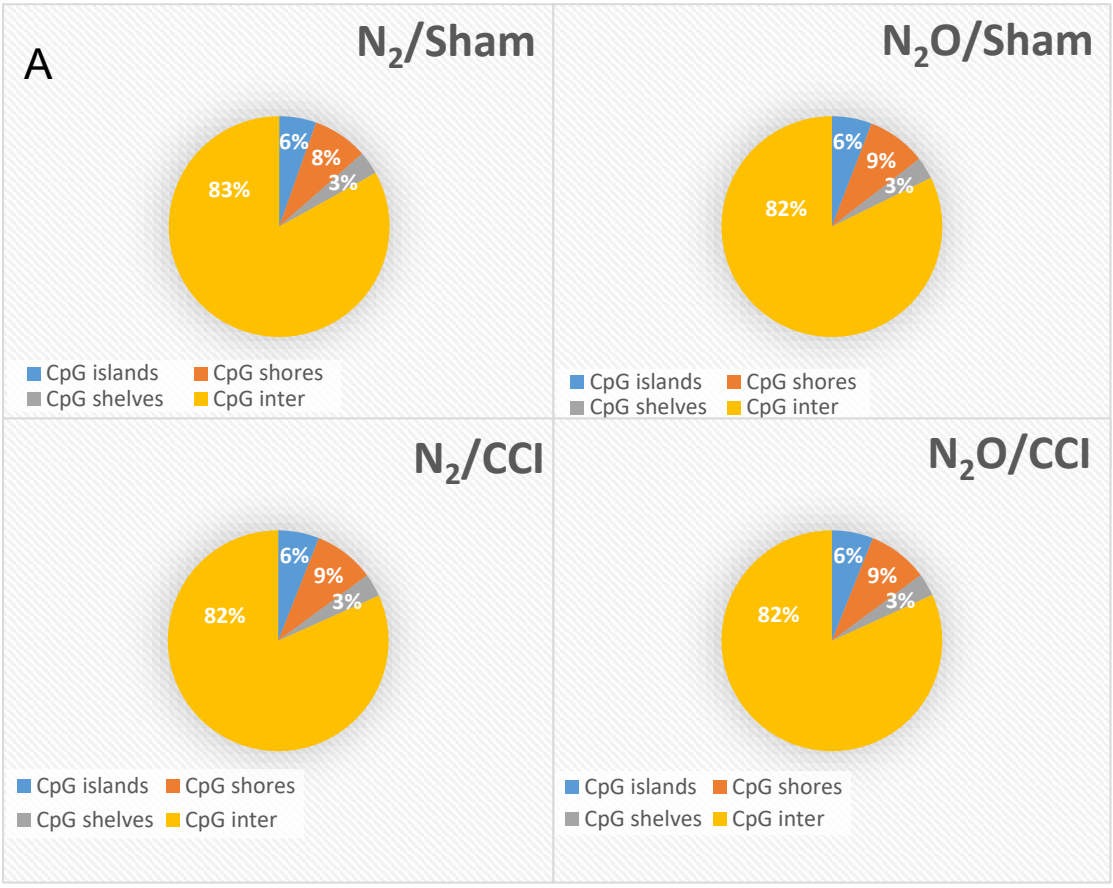

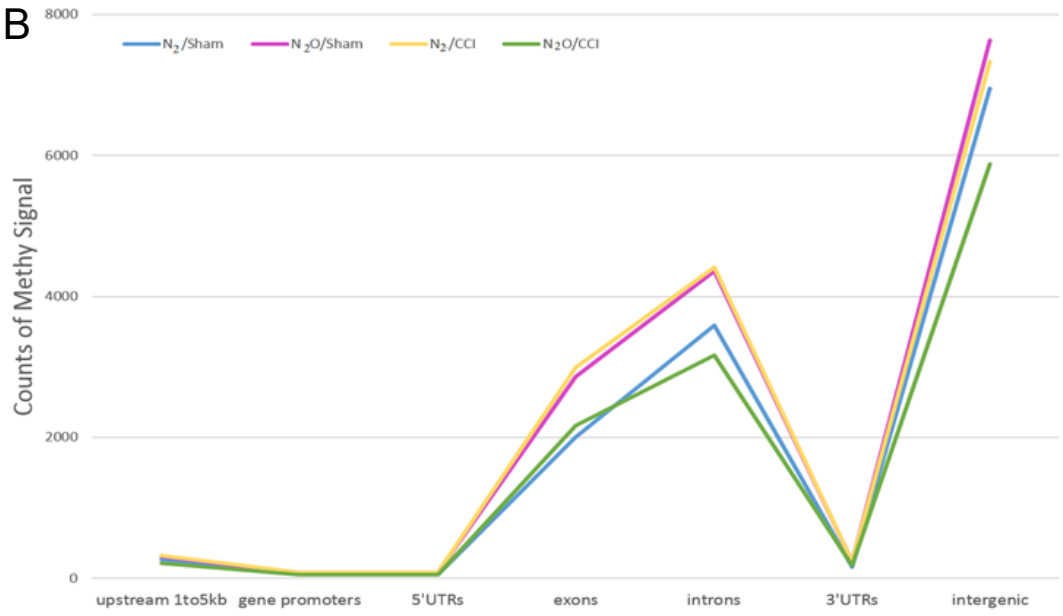

Figure 7. 5 Dot-blot assay for measuring genomic 5mC levels in the four experimental groups

The genomic 5mC content of different groups (N_2/Sham, N_2O/Sham, N_2/CCI and N_2O/CCI groups) were measured. Aggregates were detected using the 5mC-specific antibodies. The bar graph shows the relatively integrated density bases of each sample (mean ± S.E.M.). N_2/Sham and N_2O/CCI group led to significantly elevated genomic 5mC levels as compared to N_2/CCI group (*p <0.05, **p <0.01). Calculations were based on three independent datasets.

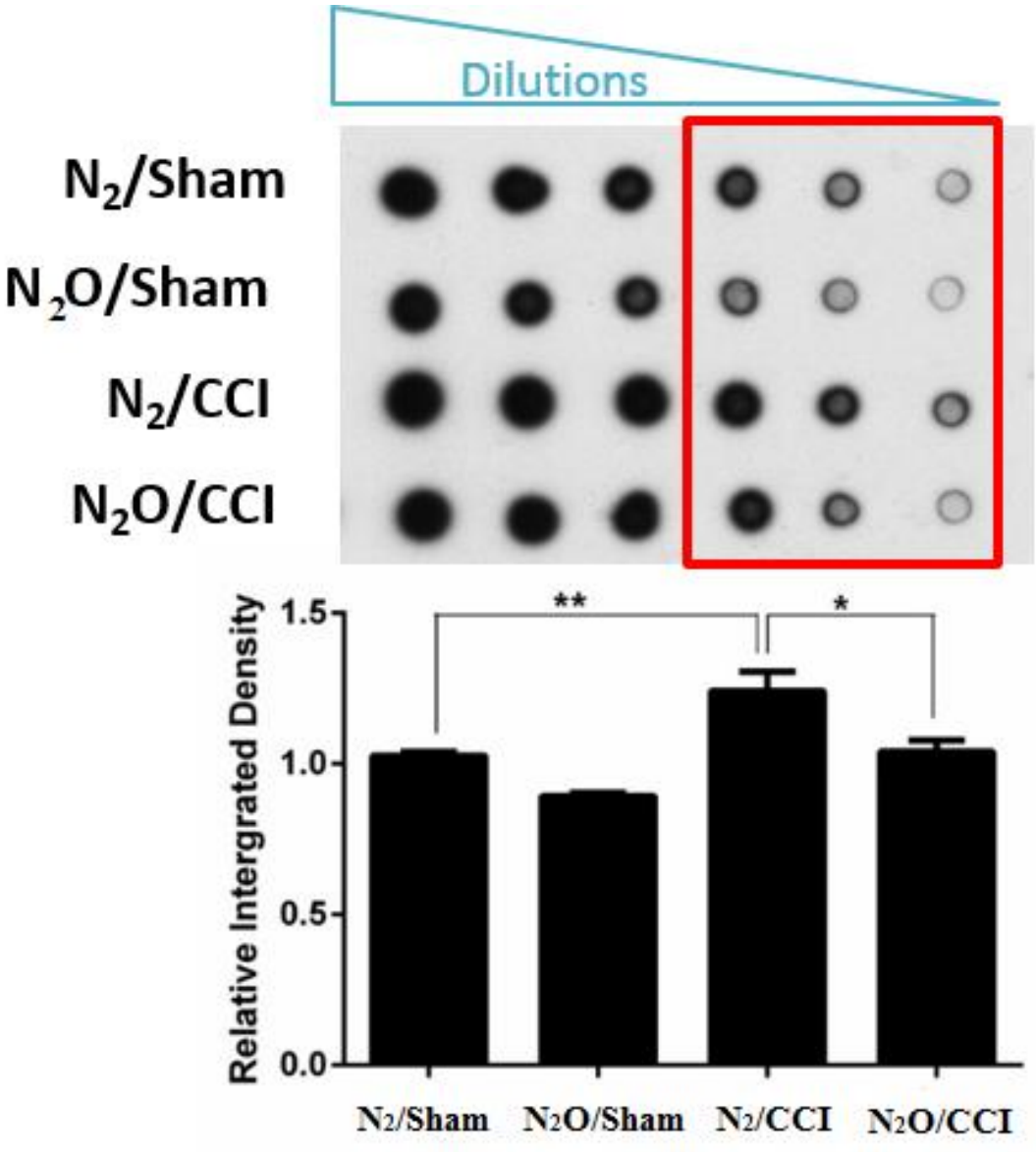

7.3.2 Identification of CCI-specific and nitrous oxide-susceptible differentially methylated regions (DMRs)

In order to investigate the DNA methylation signature associated with CCI and nitrous oxide treatment, we first plotted the distribution of hypo- and hyper-DMRs. Figure 7.6 showed that 842 DMRs, including 799 hypo- and 43 hyper-DMRs, were identified in normal neuropathic pain group (N_2/CCI) relative to normal sham control. Comparably, 197 hypo- and 6 hyper-DMRs were identified in nitrous oxide-exposed neuropathic pain group with total 203 DMRs. Notably, 125 CCI-specific DMRs were found. Besides, there were total 359 DMRs identified (341 hypo- and 18 hyper-DMRs) in somatic chromosome upon nitrous oxide exposure. However, there were just 5 hypo- and 3 hyper-DMRs in N_2O/CCI group compared with N_2/CCI group.

Principal component analysis (PCA) was performed using correlation matrix calculated from $\log_{10}$-transformed FRKM values and found that the DMRs were large differences among the four experimental groups (Figure 7.7)

Figure 7. 6 Overall representation of methylation

Distribution of hypo/hyper-differentially methylated regions (DMR) in four groups of rats having a chronic constriction injury (CCI) or sham surgery with and without nitrous oxide (N_2O) - N_2O/Sham, N_2/CCI and N_2O/CCI compared with N_2/Sham control group. This illustration shows that a higher proportion of hypo-DMRs (compared to hyper-DMRs) are consistent in three groups.

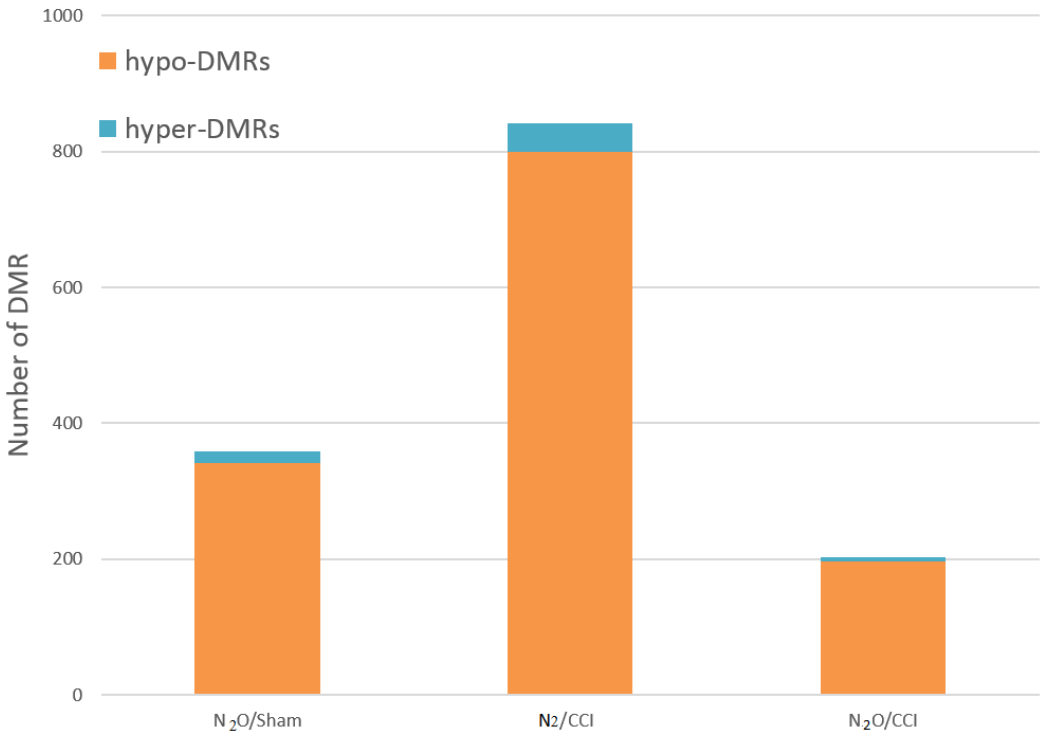

Figure 7. 7 Principal component analysis (PCA) of individual samples

PCA was performed on all DMRs to determine expressional difference among samples from four groups of rats having chronic constriction injury (CCI) or sham surgery with and without nitrous oxide (N_2O) - N_2O/CCI (orange), N_2/CCI (blue), N_2O/Sham (green) and N_2/Sham (purple) group.

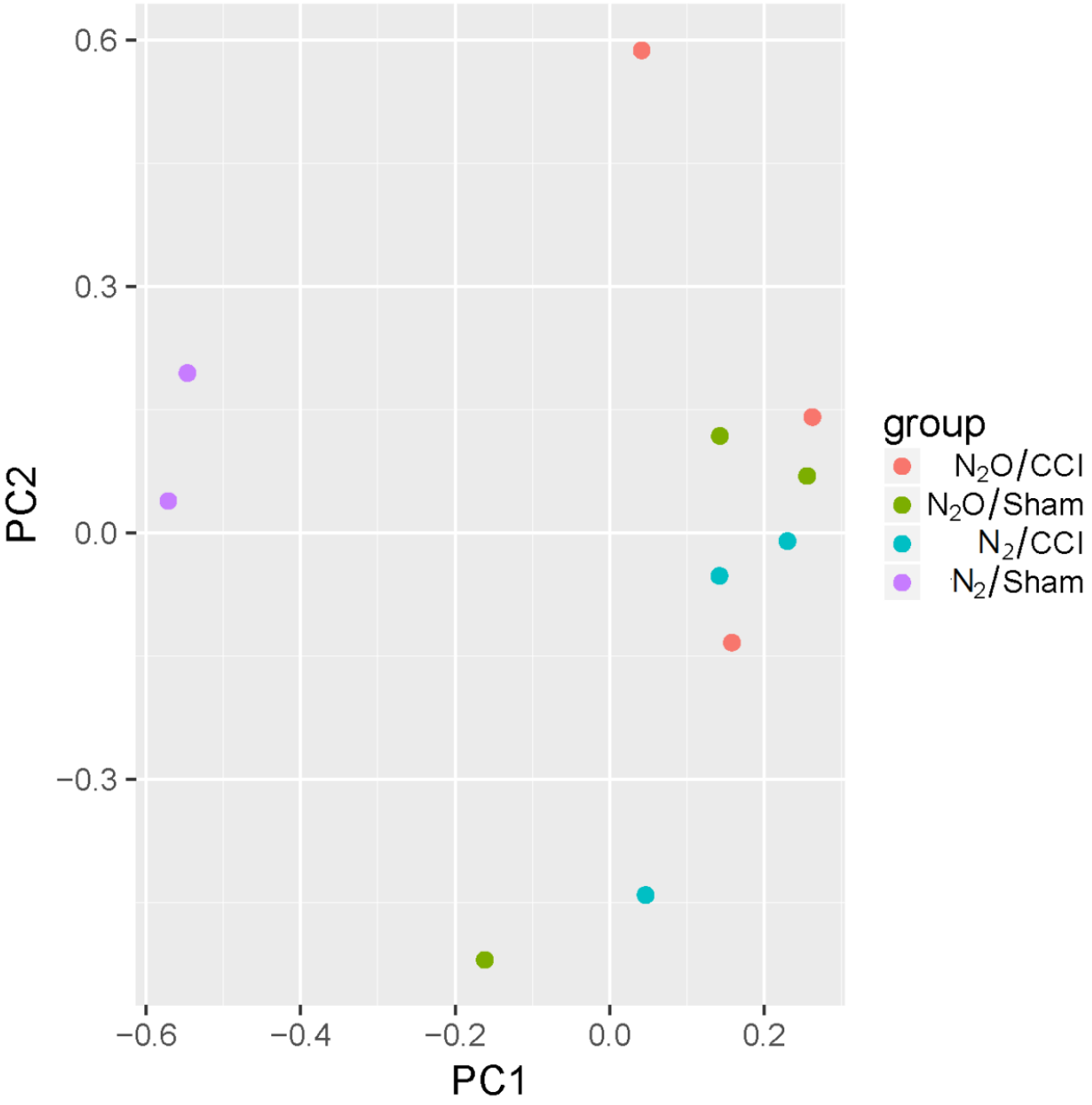

7.3.3 Genome-wide distribution of neuropathic pain-related DMRs

In order to study the genome-wide distribution of neuropathic pain-related DMRs, we analyzed the distributions of DMRs in different genomic elements, such as CpG islands, promoters, exon and intron. Compared with N_2/Sham group, we found that a high percent of DMRs mapped to the non-coding regions (intergenic regions and introns) with the predominate percentage of hypo-DMRs.

Twelve hypo-DMRs were identified within coding regions (CDS) in N_2O/CCI group. The number of hyper-DMRs was 2-fold higher than that of hypo-DMRs in N_2/CCI group. Moreover, two neuropathic pain groups exhibited enrichment of DMRs in exon-intron boundary regions, with 7 hypo-DMRs in N_2O/Sham and 14 hypo-DMRs in N_2/CCI, respectively (Figure 7.8. A). Our data demonstrated that hypo-DMRs were extremely enriched in intergenic as well as intron region (Figure7.8. B).

Taken together, similar enrichment patterns across different genomic elements were observed for hyper- and hypo-DMRs in the comparison of two neuropathic pain groups, suggesting the potential contributions of expression changes by the aberrant methylation modifications.

Figure 7. 8 Distribution of DMRs among genomic features

The hypo- and hyper- DMRs were calculated in different genomic regions, such as exon-intron boundaries, gene coding sequence (CDS), as well as intergenic regions, compared with N_2/Sham group.

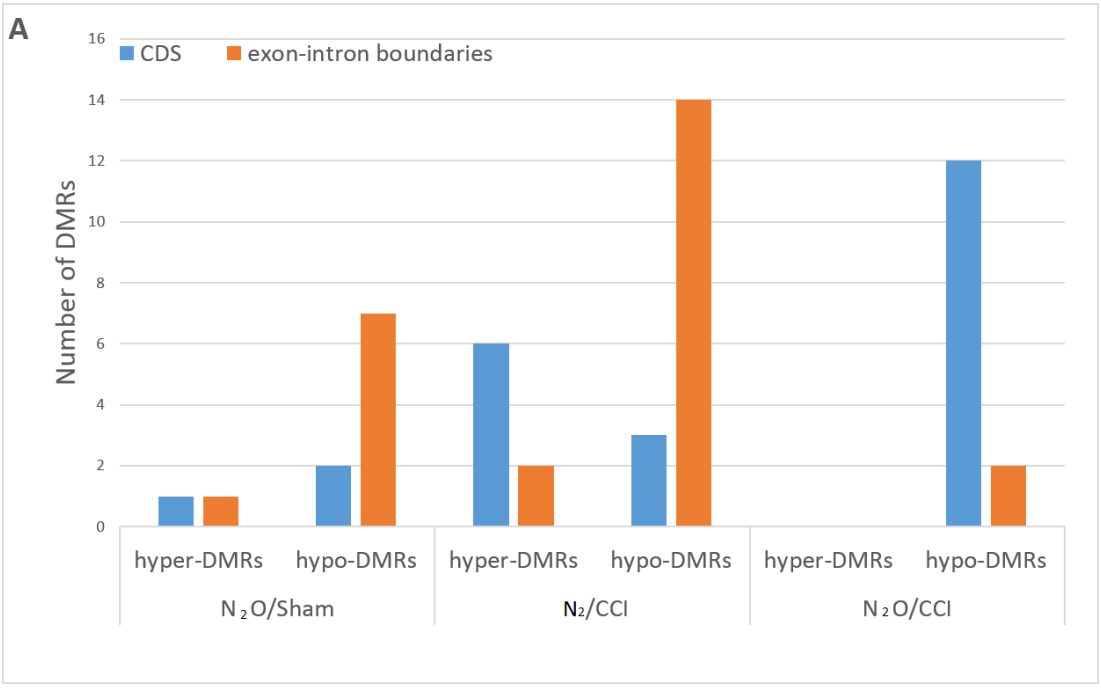

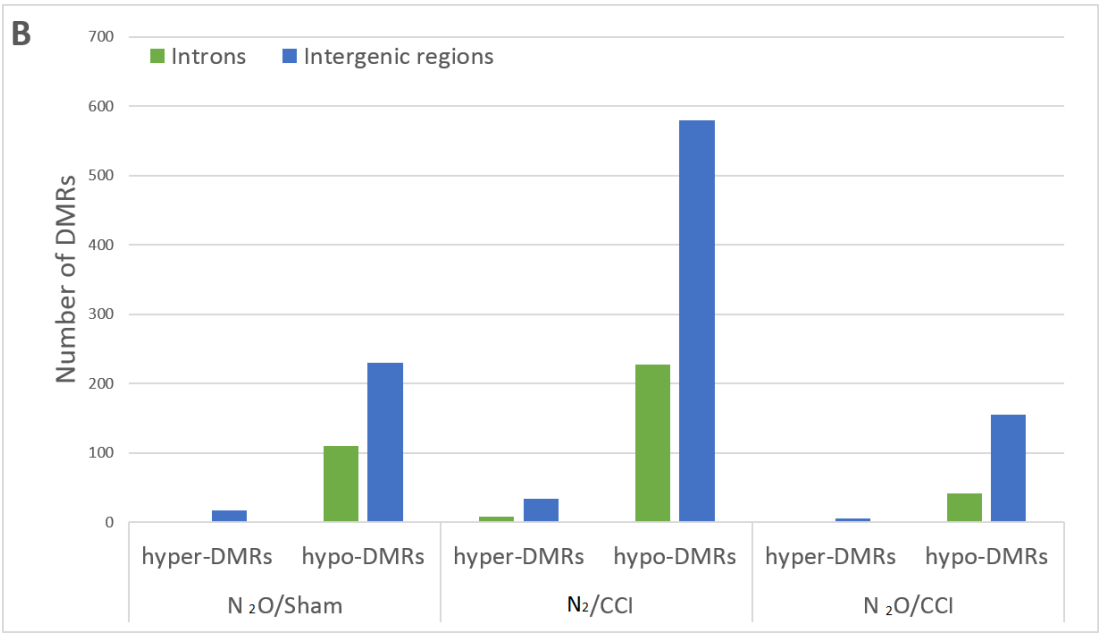

7.3.4 Correlation of Atf3 expression with distal DMR

In order to identify genes associated with CCI- or nitrous oxide-specific DMRs, Volcano plots were used to define DMR-associated genes. A total of 9 (30%), 541 (85.9%), and 93 (19.9%) DEGs were identified associated with DMRs in N_2O/CCI, N_2/CCI and N_2O/CCI groups compared with N_2/Sham group, respectively. Figure 9.9 showed significant hypomethylation changes of DEGs both in N_2/CCI and N_2O/CCI groups, demonstrating the hypomethylation-associated transcriptional regulation in chronic neuropathic pain.

We identified some nitrous oxide-susceptible differentially methylated regions (DMRs) in distal regions of Atf3. Further correlation analysis confirmed that nitrous oxide-induced DNA demethylation was a potential mechanism to control the transcriptional activity of Atf3 (Figure 7.10).

Figure 7. 9 Differentially methylated regions associated expressed genes in neuropathic pain

The left plot is the N_2/CCI group and the right one is the N_2O/CCI group. The x-axes on the scatter plot are the log_2-fold change of the differences in gene expression. The y-axes show the negative of the log_2 corrected p-values of the comparison between the two groups.

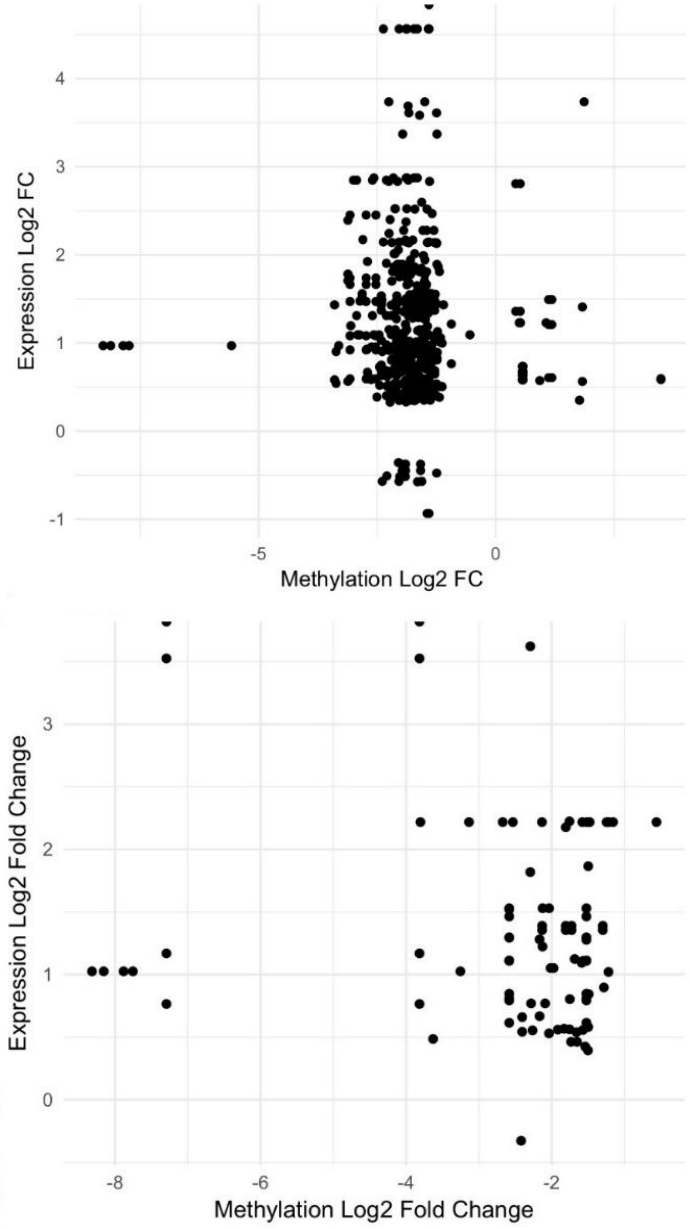

Figure 7. 10 Correlation of Atf3 expression and the methylation values with its predicted distal differentially methylated regions

The x-axes on the scatter plot are the gene expression values of Atf3 in four groups. The y-axes show the methylation values of corresponded distal DMRs

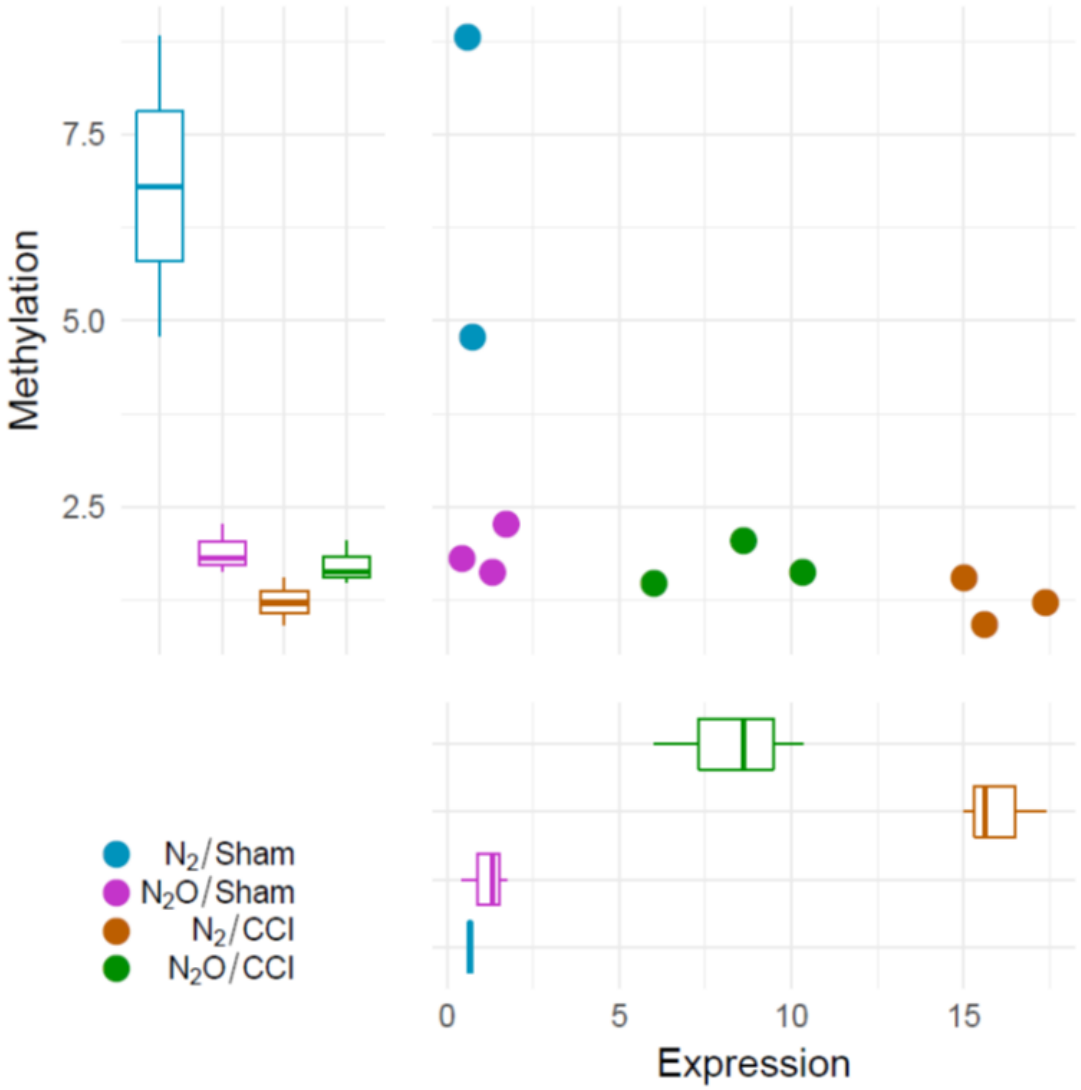

7.4 Discussions

Only blood samples are available in current genome-wide methylation studies to examine the complex neurological phenotypes in humans. In the present work, the animal model was used as a reference point. In our methylation data, we found a decrease of DNA methylation in ipsilateral lumbar spinal cord after nitrous oxide administration. Changes on methylome signatures help to identify differentially methylated regions (DMRs) that are susceptible to the antinociceptive effect of nitrous oxide.

Limitations:

We attempted to evaluate the correlation between DNA methylation and gene expression. Since the predominant DMRs were identified with the intergenic distribution, but not the promoter region, we suggested other strategies to explore the contribution of DNA demethylation-mediated analgesic effect, like chip sequencing.

Conclusions:

In this part, we identified the nitrous oxide-susceptible differentially methylated regions (DMRs) and found out the significant hypomethylation changes with DEGs in N_2/CCI and N_2O/CCI groups. Our data suggested that the DNA methylation-mediated

transcriptional regulation cannot completely explain the antinociceptive effects of nitrous oxide. Nevertheless, we identified nitrous oxide-susceptible DMRs located in distal regions of Atf3 which may be a potential mechanism to control the transcriptional activity of Atf3.

Chapter 8 Atf3 Down-regulation Attenuated Pain Hypersensitivity

8.1 Introduction

Activating transcription factor 3 (Atf3) binds to cAMP response element (CRE) which are located in the promoter region of many inflammatory cytokines and chemokines. The function of Atf3 on inflammatory genes expression, however, is controversial. Several studies indicated that Atf3 deficiency increased the expression of pro-inflammatory genes (such as Il-6 and Il-8) through increasing NF-κB signaling (Kwon et al., 2015; Wu et al., 2017; Gilchrist et al., 2006). Similarly, it demonstrated that knockdown of Atf3 resulted in an increase of Il-6 mRNA in human colonic cells (Calton et al., 2013).

In contrast, a recent study reported that Atf3 deletion decreased cytokine-induced IL6 transcription in chondrocytes by repressing NF-κB activity (Iezaki et al., 2016). In the endothelial cell, angiotensin II (Ang II) treatment increased Atf3 SUMOylation which may inhibit ATF3 degradation, and this in turn contributes to up-regulation of mRNA expression of TNF-α, IL-6 and IL-8 (Zhang et al., 2016). In a model of islet transplantation, the increased expression of immunomodulation genes, including Il-6, IL-1β and TNF, were blunted in Atf3-KO mice (Zmuda et al., 2010). Moreover, many reports showed a positively correlated expression of Atf3 and pro-inflammatory

cytokines (Table 3). All these findings indicate that ATF3 acts as an important transcriptional regulator of pro-inflammatory genes, although such modulation (activation or suppression) was context dependent.

Previous studies have shown that peripheral nerve injury increased expressions of Atf3 and several pro-inflammatory factors (e.g. IL6, IL1β and Tnfα) in the ipsilateral dorsal root ganglia (DRG) (Latremoliere et al., 2008; Mika et al., 2008; Galbavy et al., 2015; Sacerdote et al., 2008). Given that multiple putative Atf3 binding sites were found in the Il6 promoter, we hypothesized that Atf3 activity contributed to nerve injury-induced Il6 up-regulation, and by this way acted as a pro-nociception protein. Verification of such hypothesis may provide the potential molecular mechanism on the preventive role of nitrous oxide in chronic pain development.

Table 4. Previously reported coherent expression pattern of ATF3 with proinflammatory genes.

ATF3 EXPRESSION	Upregualted proinflammatory cytokines	Design/Treatment	Sample Source	Disease/Model	References
UP	IL1β, IL6	Tumors with high or low COX-2 expression	Human colon cancer tissue	Tumor	(Asting et al., 2011)
UP	IL6, IL1β, TNF	Bipolar patients with health controls	Human blood monocytes	Bipolar disorder	(Padmos et al., 2008)
UP	IL6, IL8	Omentectomy or not during RYGB surgery	Human skeletal muscle biopsies	Skeletal muscle inflammation	(Tamboli et al., 2011)
UP	IL6, IL8	Cristobalite silica treatment	Human bronchial epithelial cell	Cristobalite silica treatment	(Perkins et al., 2012)
UP	IL6	Melphalan treatment	Human melanoma	Isolated limb perfusion with	(Wouters et al., 2012)

				melphalan	
UP	IL6	Melanocortin 1/4 receptor agonist treatment	Rat liver samples	Hemorrhagic shock	(Lonati et al., 2012)
UP	IL6	Cyclic mechanical stretching	Rat retinal glial (Müller) cells	Retinal injury	(Wang et al., 2013)
UP	IL6, IL8	Treated with virus or house dust mite	Airway epithelial cells	Immune responses	(Golebski et al., 2014)
UP	IL1β, IL6, IL10, IL18	Treatment with LPS	Lung tissue from Atg4b-null mice	Endotoxemia	(Aguirre et al., 2014)
UP	IL6	Administration of MK-8825	Rat trigeminal ganglion and spinal trigeminal nucleus	CCI combined with nerve ligation	(Michot et al., 2015)
DOWN	high IL-6	Blood samples of patients with acute sepsis	Leukocytes from patient blood	Sepsis	(Hoetzenecker et al., 2011)

8.2 Materials and Methods

8.2.1 Selection of effective Atf3 shRNA

The pLVX-shRNA-puro lentiviral vectors containing Atf3 specific short hairpin RNAs (shRNA) and the scramble control shRNA were produced by GenePharma (Shanghai, China). The final titer of all virus is 1×10^8 TU/ml. For shRNA selection, 1 μL of the virus was added to PC12 cells and kept in the normal culture condition for 48 hours. This was followed by RNA isolation, cDNA synthesis and quantitative PCR (qPCR) analysis of Atf3 expression.

8.2.2 Intra-spinal injection of shRNA lentiviral vectors

Intra-spinal injections were performed as described previously (Chen et al., 2016). Briefly, hemi-laminectomy was performed at the 1st lumbar vertebra. One μL of Atf3-shLV or control-LV (1 × 108 TU/ml) viral particles was given in two ipsilateral sites with 0.8 mm apart and 0.5 mm deep for each rat. These injections were made 7 days before the CCI surgery.

8.2.3 *In vivo* validation of Atf3 knockdown

Spinal dorsal horn was harvested for RNA or protein extraction after spinal injection (7 days) and CCI surgery (additional 3 days). The knockdown efficiency was then

determined by qPCR and Western blotting.

8.2.4 Behavioral testing

Mechanical allodynia and heat hyperalgesia assessment were performed as described in chapter 3.

8.3 Results

8.3.1 Atf3 knockdown attenuated the CCI-induced thermal hyperalgesia

According to the analysis above, Atf3 appeared to be a potential target which was responsible for the nitrous oxide-induced antinociceptive effect. We then evaluated the effects of Atf3 knockdown on pain like responses. Lentivirus-based shRNA delivery was applied for Atf3 gene silencing. Two shRNA sequence targeting at different positions on Atf3 (shAtf3-1 and shAtf3-2), and scramble control shRNA (shControl) were designed and cloned into a pLVX-shRNA-puro lentiviral plasmid. The lentiviral particles were then produced and concentrated to a titer of 1×10^8 TU/ml. For effective shAtf3 selection, lentiviral particles were added to PC12 cells. Forty-eighty hours after transduction, total RNA was isolated for Atf3 analysis. As compared with shControl, shAtf3-1 and shAtf3-2 reduced 50% and 10% of Atf3 mRNA, respectively. Therefore, only shAtf3-1 was selected for further experiments (Figure 8.1).

Next, *in vivo* knockdown efficiency was evaluated through intra-spinal injection of shAtf3 or shControl viral particles. Since Atf3 was barely detected in spinal dorsal horn of sham-operated rats, CCI surgery was performed on rats with lentivirus treatment. To test whether Atf3-shRNA is feasible *in vivo*, we evaluated gene knockdown efficiency in spinal dorsal horn two weeks after intra-spinal injection by quantitative real-time RT-PCR. An averaged 50% reduction in Atf3 expression was detected compared with shControl-injected CCI group (Figure 8.2). Consistently, Western blotting further conformed the knockdown efficiency of shAtf3-1 (Figure 8.3). These data showed that shAtf3-1 was effectively silenced Atf3 mRNA expression *in vitro* and *in vivo*.

We subsequently evaluated the effects of impaired Atf3 on pain behaviors. As shown in Figure 8.4, impaired Atf3-expression significantly reduced the withdrawal latency (thermal hyperalgesia) on day5 after CCI surgery, and this effect lasted for at least two weeks as compared with control shRNA-treated CCI group. These results demonstrated that Atf3 attenuated CCI-induced thermal hyperalgesia.

Figure 8. 1 The qPCR validation of Atf3-shRNA in PC12 cell line

The detection was conducted after 2 days of infection. The transduction efficiency was shown 48 hours after infections. Sham group is normal PC12 cell line. Error bars are SEM; 3 replicates per group, One-way ANOVA, *$p < 0.05$ compared to shControl.

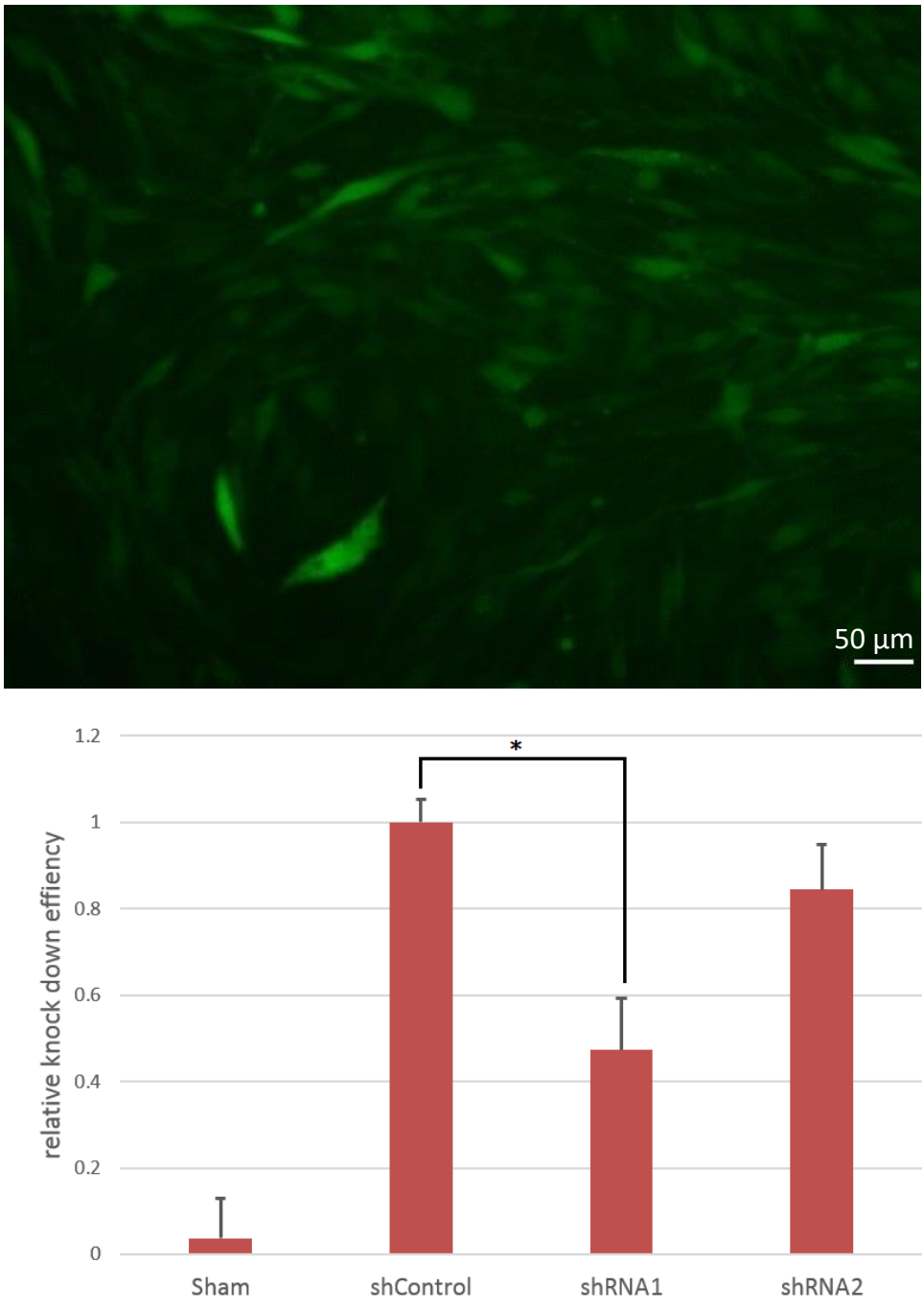

Figure 8. 2 The qPCR validation of in vivo Atf3 knockdown

One week before pain model development, the lentiviral vector was injected into the spinal cord. The detection was conducted on the day 3 after CCI surgery (about two weeks after intra-spinal injection) with about 40% decrease. Error bars are SEM; 3 animals per group, One-way ANOVA, *$p < 0.05$ compared to shControl/CCI.

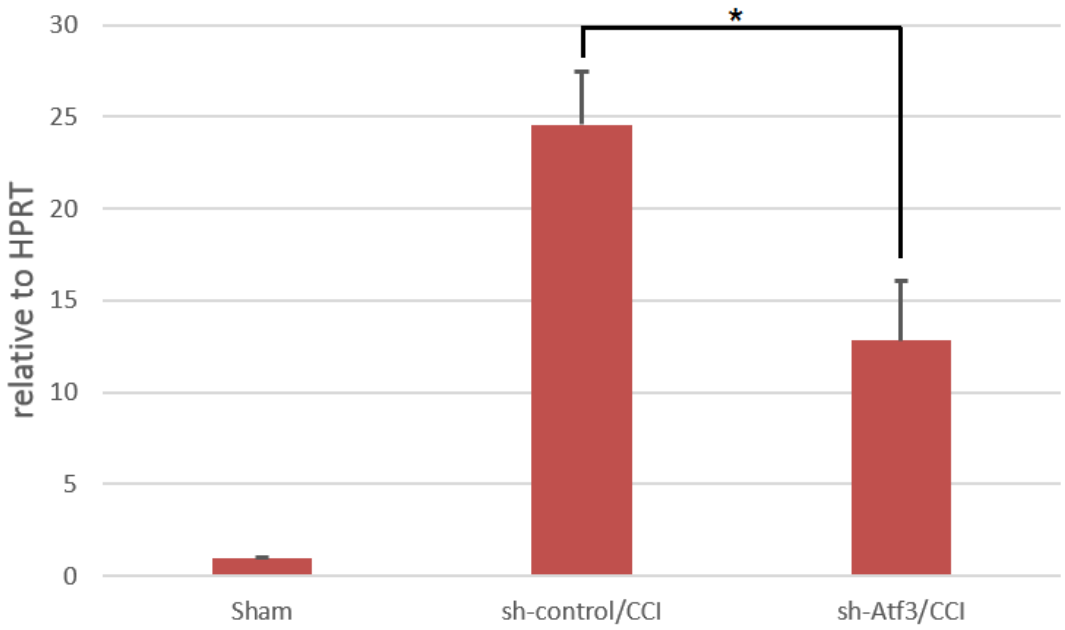

Figure 8. 3 Western blotting evaluation of in vivo Atf3 knockdown

Seven days in prior to CCI surgery, the lentiviral vector was injected into the spinal dorsal horn. The detection was conducted on the day 5 after CCI surgery. NS stands for shRNA control; KD groups stand for Atf3 knock down groups. The quantification analysis was compared with tubulin signals, shown as the group mean ± SEM. $^{**}p < 0.01$ compared with the control shRNA/CCI group; $n = 3$ rats for each group.

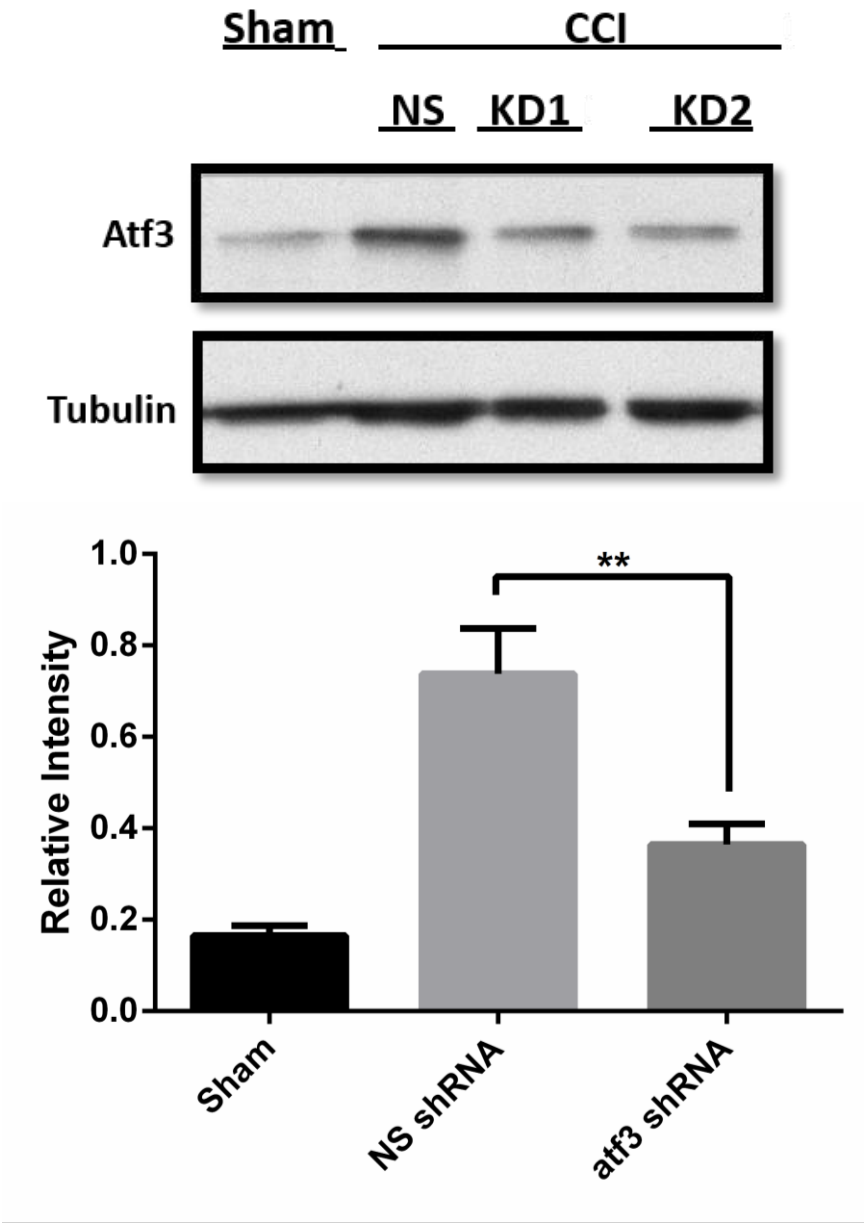

Figure 8. 4 Atf3 knockdown attenuated chronic constriction injury (CCI)-induced thermal hyperalgesia

CCI or sham surgery was performed on the day 7 after intrathecal injection of lentivirus vectors. Results are mean ± SEM of 7 animals per group. ***$p < 0.001$ compared with CCI group; Two-way ANOVA followed by the Bonferroni's *post hoc* test was used.

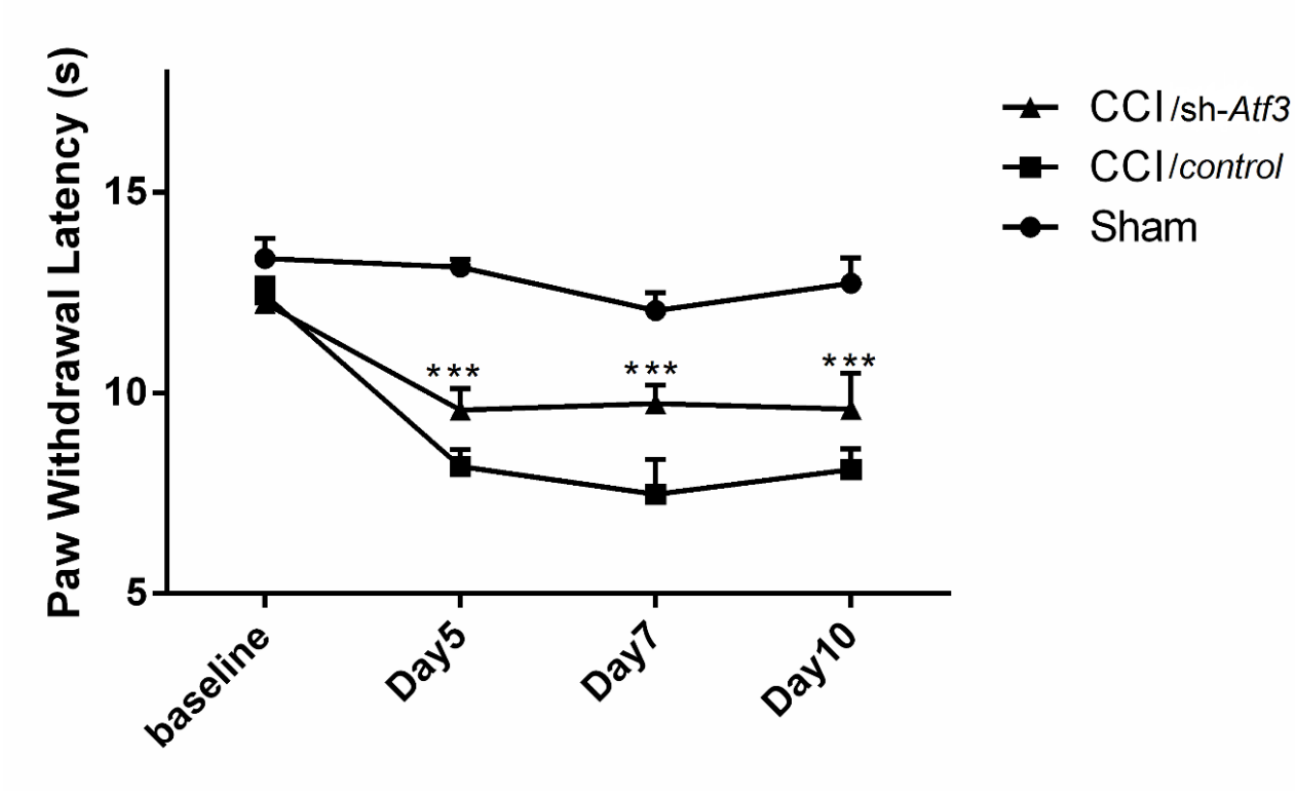

8.3.2 Il 6 reduction was coincided in Atf3 knockdown- and nitrous oxide-treated CCI group.

After behavior testing, ipsilateral lumbar spinal cord was harvested to detect the changes at the molecular level. As expected, shAtf3-1 injection reversed CCI-induced Atf3 induction as compared with shControl, indicating a long-term RNAi effect (Figure 8.5.A). Notably, a reduction of Il6 mRNA was also observed in shAtf3-1 treated rats (over 30%). By contrast, the Il-1β level was comparable between shAtf3-1 and shControl groups. Interestingly, the modulation of Il1β and Il6 mRNA was similar to that observed between the N_2/CCI and N_2O/CCI treated rats (Figure 8.5.B). These results suggested that Atf3 may function as a transcriptional activator of Il6 after peripheral nerve injury.

Figure 8. 5 The attenuation of spinal Il6 expression in Atf3 knockdown- and nitrous oxide-treated CCI models

(A) Spinal Il-6 expression was decreased following Atf3 knockdown. After behavioral testing, the spinal dorsal horn was harvested for qPCR analysis. The expression of Atf3 in CCI/shAtf3 group remained significantly lower than CCI/shControl group. Il-6, but not Il-1β was reduced by Atf3 knockdown. Error bars are SEM; 3 animals per group. (B) Same decrease was fond in RNA profiling data. n=3, t-test: *$p < 0.05$. **$p < 0.05$

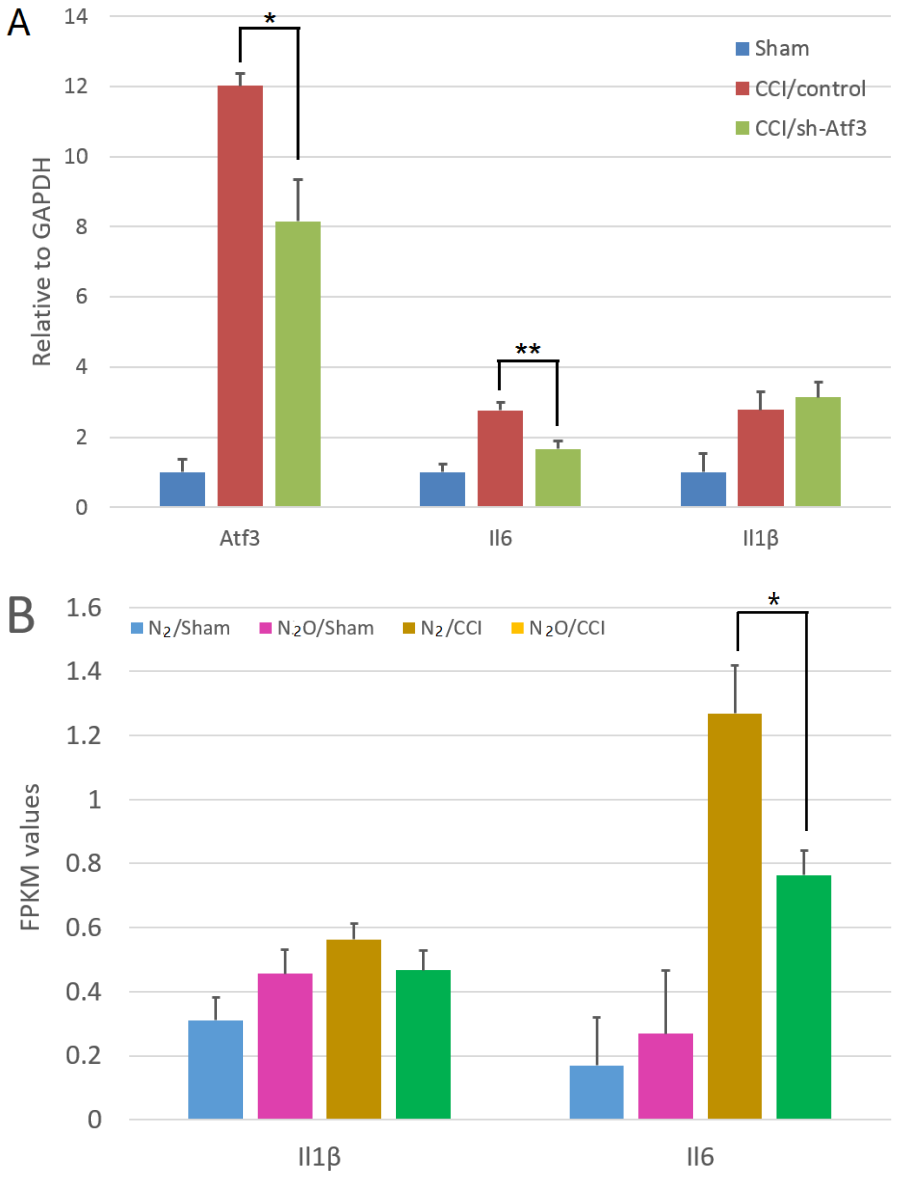

8.4 Discussions

In this experiment, we evaluated the role of upregulated Atf3 and indicated that a decrease in its expression alleviated the hyperalgesia in CCI model, just as nitrous oxide did. These immediately upregulated expression pattern have also been reported in other clinical disorders of the nerve system or inflammatory diseases (Padmos et al., 2008; 2008; Golebski et al., 2014). These findings suggest that Atf3 can be regarded as a pain target with potential clinical importance.

Besides, Atf3 gene variants have been reported to not only influence the risk of genetic disease, but also associate with C reactive protein, a serum inflammatory marker in a Taiwanese population (Ana Beleza-Meireles et al., 2008; SemonWu et al., 2011). Therefore, the SNPs in ATF3 gene may be regarded as predictive markers for chronic postsurgical pain, which still warrants further investigation.

Limitations:

As an early response gene, Atf3 upregulated rapidly in response to nerve injury (Tsujino et al., 2000; Malaspina et al., 2010). Here we just evaluated the analgesic effect in Atf3 knockdown model by intra-spinal injection of shRNA lentivirus. Nevertheless, Atf3 knock-out model should be taken into consideration. This knock-

out model has been used to study inflammatory responses (Zhao et al., 2017; Nguyen et al., 2014). Here we should conduct CCI with perioperative administration of nitrous oxide in Atf3 knock-out mice.

Conclusions:

In the current study, we found that Atf3 knockdown was associated with a reduction in the expression of IL6 in spinal dorsal horn. This result suggested Atf3 may function as a transcriptional activator of pro-inflammatory genes in spinal cord. Atf3 silencing, via nitrous oxide administration, seems to be an efficient approach for regulating inflammation control in the development of chronic pain.

PART III CONCLUSIONS AND FUTURE PERSPECTIVES

Chapter 9 Conclusions

We concluded that:

1. Administration of nitrous oxide produced a persistent antinociceptive effect that lasted for ten days in our neuropathic pain model of chronic constriction injury (CCI). Hyperalgesia was significantly attenuated on Day 3 after surgery.
2. Transcriptome analysis revealed that perioperative administration of nitrous oxide attenuated the global expression pattern of CCI-induced dysregulated genes during the initiation of neuropathic pain. Furthermore, functional clustering and transcription factor motif enrichment analysis suggested that the dysregulated transcription factors may explain for the preferential expression variances of multiple pain-related signaling pathways between nitrous oxide-treated CCI group and normal CCI group.
3. The nitrous oxide-susceptible DEG, Atf3-centered transcriptional regulatory network was a potentially considerable mechanism for the nitrous oxide-induced persistent analgesia in neuropathic pain.
4. A decrease in Atf3 expression alleviated the hyperalgesia in CCI model.
5. Nitrous oxide administration impaired the DNA methylation pattern in ipsilateral lumbar spinal cord. The attenuated increase of global DNA methylation in

neuropathic pain extremely changed the methylome signatures and generated the nitrous oxide-susceptible differential methylated regions.

Chapter 10 Future Perspectives

1. To clarify the activity of NMDA receptors in persistent analgesia, we plan to do more work to detect the phosphorylation of NMDA receptor subunits. Specifically, two experiments would be required:

   (1) The detection of phosphorylated NR1 by immune-staining calculation;

   (2) Receptor activity assays of NMDA receptors.

2. To identify the exact targeted gene/signaling under Atf3-mediated transcriptional regulation, we would verify the functional role of targeted gene. Our work suggested that Atf3 may function as a transcriptional activator of Il6 which is responsible for the persistently alleviated neuropathic pain. Given that Il6 promotes central sensitization in pain model, we speculate that suppression of Atf3/Il6 pathway may explain nitrous oxide-mediated antinociceptive effects.

   Two experiments have been proposed:

   (1) The co-localization of immune-staining with ATF3 and IL-6 in ipsilateral lumbar spinal cord;

   (2) The chip-sequencing on the distal regulatory region of Il6 gene

Figure 10. 1 The schematic diagram of experiment design

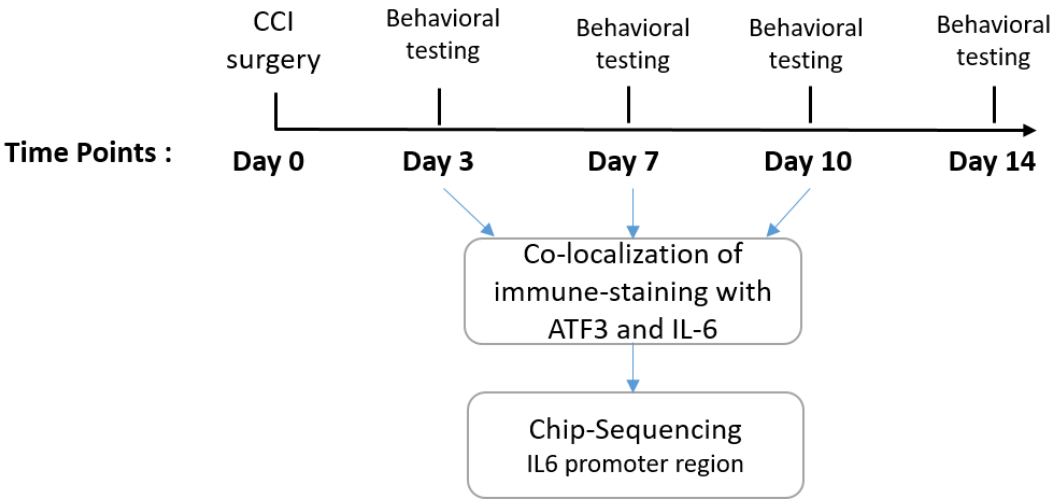

3. To explore the putatively involved epigenetic mechanism on regulation of Atf3 by nitrous oxide, we design a three-step experiment,

First, establish an *in vitro* transgenic cell model with a luciferase gene inserted into the downstream of Atf3 in genome.

Then, pre-treat the cell culture medium with N_2O/O_2 (20/30 mixture) or air (80%/20% mixture N_2/O_2) bubbling (using a gas diffusing stone) for 30 minutes in a closed glass container. .

Finally, immediate delivery of the medium added with 5 azacytidine (inhibitor of DNA methylation) to the transgenic cells for 30 minutes, in order to detect the luciferase activity at different culture durations.

PART IV REFERENCES

AGUIRRE, A., LOPEZ-ALONSO, I., GONZALEZ-LOPEZ, A., AMADO-RODRIGUEZ, L., BATALLA-SOLIS, E., ASTUDILLO, A., BLAZQUEZ-PRIETO, J., FERNANDEZ, A. F., GALVAN, J. A., DOS SANTOS, C. C. & ALBAICETA, G. M. 2014. Defective autophagy impairs ATF3 activity and worsens lung injury during endotoxemia. Journal of Molecular Medicine (Berlin, Germany), 92, 665.

ANTKOWIAK, B. & KIRSCHFELD, K. 2000. Neural mechanisms of anaesthesia. Anasthesiologie Intensivmedizin Notfallmedizin Schmerztherapie, 35, 731.

ARRUDA, J. L., COLBURN, R. W., RICKMAN, A. J., RUTKOWSKI, M. D. & DELEO, J. A. 1998. Increase of interleukin-6 mRNA in the spinal cord following peripheral nerve injury in the rat: potential role of IL-6 in neuropathic pain. Brain research.Molecular brain research, 62, 228.

ARRUDA, J. L., SWEITZER, S., RUTKOWSKI, M. D. & DELEO, J. A. 2000. Intrathecal anti-IL-6 antibody and IgG attenuates peripheral nerve injury-induced mechanical allodynia in the rat: possible immune modulation in neuropathic pain. Brain research, 879, 216.

ASTING, A. G., CAREN, H., ANDERSSON, M., LONNROTH, C., LAGERSTEDT,

K. & LUNDHOLM, K. 2011. COX-2 gene expression in colon cancer tissue related to regulating factors and promoter methylation status. BMC cancer, 11, 238.

AVRAMOV, M. N., SHINGU, K. & MORI, K. 1990. Progressive changes in electroencephalographic responses to nitrous oxide in humans: a possible acute drug tolerance. Anesthesia and Analgesia, 70, 369.

BAI, G., REN, K. & DUBNER, R. 2015. Epigenetic regulation of persistent pain. Translational research : the journal of laboratory and clinical medicine, 165, 177.

BARANAUSKAS, G. & NISTRI, A. 1998. Sensitization of pain pathways in the spinal cord: cellular mechanisms. Progress in neurobiology, 54, 349.

BATTI, L., SUNDUKOVA, M., MURANA, E., PIMPINELLA, S., DE CASTRO REIS, F., PAGANI, F., WANG, H., PELLEGRINO, E., PERLAS, E., DI ANGELANTONIO, S., RAGOZZINO, D. & HEPPENSTALL, P. A. 2016. TMEM16F Regulates Spinal Microglial Function in Neuropathic Pain States. Cell reports, 15, 2608.

BELL, J. T., LOOMIS, A. K., BUTCHER, L. M., GAO, F., ZHANG, B., HYDE, C. L., SUN, J., WU, H., WARD, K., HARRIS, J., SCOLLEN, S., DAVIES, M. N.,

SCHALKWYK, L. C., MILL, J., MU, T. C., WILLIAMS, F. M., LI, N., DELOUKAS, P., BECK, S., MCMAHON, S. B., WANG, J., JOHN, S. L. & SPECTOR, T. D. 2014. Differential methylation of the TRPA1 promoter in pain sensitivity. Nature communications, 5, 2978.

BELL, J. T., LOOMIS, A. K., BUTCHER, L. M., GAO, F., ZHANG, B., HYDE, C. L., SUN, J., WU, H., WARD, K., HARRIS, J., SCOLLEN, S., DAVIES, M. N., SCHALKWYK, L. C., MILL, J., MU, T. C., WILLIAMS, F. M., LI, N., DELOUKAS, P., BECK, S., MCMAHON, S. B., WANG, J., JOHN, S. L. & SPECTOR, T. D. 2014. Differential methylation of the TRPA1 promoter in pain sensitivity. Nature communications, 5, 2978.

BEN BOUJEMA, M., LABOUREYRAS, E., PYPE, J., BESSIERE, B. & SIMONNET, G. 2015. Nitrous oxide persistently alleviates pain hypersensitivity in neuropathic rats: A dose-dependent effect. Pain research & management, 20, 309.

BENRATH, J., KEMPF, C., GEORGIEFF, M. & SANDKUHLER, J. 2007. Xenon blocks the induction of synaptic long-term potentiation in pain pathways in the rat spinal cord in vivo. Anesthesia and Analgesia, 104, 106.

BERGER, J., DORNINGER, F., FORSS-PETTER, S. & KUNZE, M. 2016.

Peroxisomes in brain development and function. Biochimica et biophysica acta, 1863, 934.

BERKOWITZ, B. A., FINCK, A. D. & NGAI, S. H. 1977. Nitrous oxide analgesia: reversal by naloxone and development of tolerance. The Journal of pharmacology and experimental therapeutics, 203, 539.

BERKOWITZ, B. A., FINCK, A. D. & NGAI, S. H. 1977. Nitrous oxide analgesia: reversal by naloxone and development of tolerance. The Journal of pharmacology and experimental therapeutics, 203, 539.

BERKOWITZ, B. A., NGAI, S. H. & FINCK, A. D. 1976. Nitrous oxide "analgesia": resemblance to opiate action. Science (New York, N.Y.), 194, 967.

BESSIERE, B., LABOUREYRAS, E., BEN BOUJEMA, M., LAULIN, J. P. & SIMONNET, G. 2012. A high-dose of fentanyl induced delayed anxiety-like behavior in rats. Prevention by a NMDA receptor antagonist and nitrous oxide (N(2)O). Pharmacology, biochemistry, and behavior, 102, 562.

BESSIERE, B., LABOUREYRAS, E., CHATEAURAYNAUD, J., LAULIN, J. P. & SIMONNET, G. 2010. A single nitrous oxide (N2O) exposure leads to persistent alleviation of neuropathic pain in rats. The journal of pain : official journal of the American Pain Society, 11, 13.

BESSIERE, B., RICHEBE, P., LABOUREYRAS, E., LAULIN, J. P., CONTARINO, A. & SIMONNET, G. 2007. Nitrous oxide (N2O) prevents latent pain sensitization and long-term anxiety-like behavior in pain and opioid-experienced rats. Neuropharmacology, 53, 733.

BINSHTOK, A. M., WANG, H., ZIMMERMANN, K., AMAYA, F., VARDEH, D., SHI, L., BRENNER, G. J., JI, R. R., BEAN, B. P., WOOLF, C. J. & SAMAD, T. A. 2008. Nociceptors are interleukin-1beta sensors. The Journal of neuroscience : the official journal of the Society for Neuroscience, 28, 14062.

BIRD, A. 2002. DNA methylation patterns and epigenetic memory. Genes & development, 16, 6.

BIRD, A. 2002. DNA methylation patterns and epigenetic memory. Genes & development, 16, 6.

BLISS, T. V. & COLLINGRIDGE, G. L. 1993. A synaptic model of memory: long-term potentiation in the hippocampus. Nature, 361, 31.

BROTMAN, M. & CULLEN, S. C. 1949. Supplementation with demerol during nitrous oxide anesthesia. Anesthesiology, 10, 696.

BURSZTAJN, S., RUTKOWSKI, M. D. & DELEO, J. A. 2004. The role of the N-

methyl-D-aspartate receptor NR1 subunit in peripheral nerve injury-induced mechanical allodynia, glial activation and chemokine expression in the mouse. Neuroscience, 125, 269.

CALTON, C. M., WADE, L. K. & SO, M. 2013. Upregulation of ATF3 inhibits expression of the pro-inflammatory cytokine IL-6 during Neisseria gonorrhoeae infection. Cellular microbiology, 15, 1837.

CAMPBELL, J. N. & MEYER, R. A. 2006. Mechanisms of neuropathic pain. Neuron, 52, 77.

CHAN, M. T., PEYTON, P. J., MYLES, P. S., LESLIE, K., BUCKLEY, N., KASZA, J., PAECH, M. J., BEATTIE, W. S., SESSLER, D. I., FORBES, A., WALLACE, S., CHEN, Y., TIAN, Y., WU, W. K., AND THE, A. & NEW ZEALAND COLLEGE OF ANAESTHETISTS CLINICAL TRIALS NETWORK FOR THE, E.-I. I. I. 2016. Chronic postsurgical pain in the Evaluation of Nitrous Oxide in the Gas Mixture for Anaesthesia (ENIGMA)-II trial. British journal of anaesthesia, 117, 801.

CHAN, M. T., WAN, A. C., GIN, T., LESLIE, K. & MYLES, P. S. 2011. Chronic postsurgical pain after nitrous oxide anesthesia. Pain, 152, 2514.

CHANG, W. K., TAO, Y. X., CHUANG, C. C., CHEN, P. T., CHAN, K. H. & CHU,

Y. C. 2011. Lack of beneficial effect for preemptive analgesia in postoperative pain control: verifying the efficacy of preemptive analgesia with N-methyl-D-aspartate receptor antagonists in a modified animal model of postoperative pain. Anesthesia and Analgesia, 112, 710.

CHAPARRO, L. E., SMITH, S. A., MOORE, R. A., WIFFEN, P. J. & GILRON, I. 2013. Pharmacotherapy for the prevention of chronic pain after surgery in adults. Cochrane Database of Systematic Reviews.

CHAPARRO, L. E., SMITH, S. A., MOORE, R. A., WIFFEN, P. J. & GILRON, I. 2013. Pharmacotherapy for the prevention of chronic pain after surgery in adults. The Cochrane database of systematic reviews, (7):CD008307. doi, CD008307.

CHAPMAN, C. R. & BENEDETTI, C. 1979. Nitrous oxide effects on cerebral evoked potential to pain: partial reversal with a narcotic antagonist. Anesthesiology, 51, 135.

CHAPMAN, C. R. & BENEDETTI, C. 1979. Nitrous oxide effects on cerebral evoked potential to pain: partial reversal with a narcotic antagonist. Anesthesiology, 51, 135.

CHAPMAN, W. P., ARROWOOD, J. G. & BEECHER, H. K. 1943. The Analgetic

Effects of Low Concentrations of Nitrous Oxide Compared in Man with Morphine Sulphate. The Journal of clinical investigation, 22, 871.

CHEN, D. C. & QUOCK, R. M. 1990. A study of central opioid receptor involvement in nitrous oxide analgesia in mice. Anesthesia Progress, 37, 181.

CHEN, G., XIE, R. G., GAO, Y. J., XU, Z. Z., ZHAO, L. X., BANG, S., BERTA, T., PARK, C. K., LAY, M., CHEN, W. & JI, R. R. 2016. beta-arrestin-2 regulates NMDA receptor function in spinal lamina II neurons and duration of persistent pain. Nature communications, 7, 12531.

CHODAVARAPU, R. K., FENG, S., BERNATAVICHUTE, Y. V., CHEN, P. Y., STROUD, H., YU, Y., HETZEL, J. A., KUO, F., KIM, J., COKUS, S. J., CASERO, D., BERNAL, M., HUIJSER, P., CLARK, A. T., KRAMER, U., MERCHANT, S. S., ZHANG, X., JACOBSEN, S. E. & PELLEGRINI, M. 2010. Relationship between nucleosome positioning and DNA methylation. Nature, 466, 388.

CHUNG, E., BURKE, B., BIEBER, A. J., DOSS, J. C., OHGAMI, Y. & QUOCK, R. M. 2006. Dynorphin-mediated antinociceptive effects of L-arginine and SIN-1 (an NO donor) in mice. Brain Research Bulletin, 70, 245.

CIAMPI DE ANDRADE, D., MASCHIETTO, M., GALHARDONI, R., GOUVEIA,

G., CHILE, T., VICTORINO KREPISCHI, A. C., DALE, C. S., BRUNONI, A. R., PARRAVANO, D. C., CUEVA MOSCOSO, A. S., RAICHER, I., KAZIYAMA, H. H. S., TEIXEIRA, M. J. & BRENTANI, H. P. 2017. Epigenetics insights into chronic pain: DNA hypomethylation in fibromyalgia-a controlled pilot-study. Pain.

COLCIAGO, A. & MAGNAGHI, V. 2016. Neurosteroids Involvement in the Epigenetic Control of Memory Formation and Storage. Neural plasticity, 2016, 5985021.

COLPAERT, F. C. 1987. Evidence that adjuvant arthritis in the rat is associated with chronic pain. Pain, 28, 201.

COULL, J. A., BEGGS, S., BOUDREAU, D., BOIVIN, D., TSUDA, M., INOUE, K., GRAVEL, C., SALTER, M. W. & DE KONINCK, Y. 2005. BDNF from microglia causes the shift in neuronal anion gradient underlying neuropathic pain. Nature, 438, 1017.

COURTIERE, A. & HARDOUIN, J. 1997. Behavioural effects induced by nitrous oxide in rats performing a vigilance task. Behavioural Pharmacology, 8, 408.

CROMBIE IK, C. P. R. L. S. J. L. L. V. K. M. S. Chronic postsurgical pain, Epidemiology of pain: a report of the Task Force on Epidemiology of the

International Association for the Study of Pain. 1999. 125.

CROW, M., DENK, F. & MCMAHON, S. B. 2013. Genes and epigenetic processes as prospective pain targets. Genome medicine, 5, 12.

CULL-CANDY, S., BRICKLEY, S. & FARRANT, M. 2001. NMDA receptor subunits: diversity, development and disease. Current opinion in neurobiology, 11, 327.

CZECH, D. A. 1995. Nitrous-Oxide Induces Feeding in the Nondeprived Rat That Is Antagonized by Naltrexone. Physiology & Behavior, 58, 251.

DAWSON, C., MA, D. Q., CHOW, A. & MAZE, M. 2004. Dexmedetomidine enbances analgesic action of nitrous oxide - Mechanisms of action. Anesthesiology, 100, 894.

DE BEAUFORT, D. G., SESAY, M., STINUS, L., THIEBAUT, R., AURIACOMBE, M. & DOUSSET, V. 2012. Cerebral blood flow modulation by transcutaneous cranial electrical stimulation with Limoge's current. Journal of Neuroradiology, 39, 167.

DE SOUSA, S. L. M., DICKINSON, R., LIEB, W. R. & FRANKS, N. P. 2000. Contrasting synaptic actions of the inhalational general anesthetics isoflurane and xenon. Anesthesiology, 92, 1055.

DEACON, R., LUMB, M., PERRY, J., CHANARIN, I., MINTY, B., HALSEY, M. & NUNN, J. 1980. Inactivation of methionine synthase by nitrous oxide. European journal of biochemistry, 104, 419.

DEGERLI, S., ACAR, B., SAHAP, M., POLAT, A. & HORASANLI, E. 2013. Investigation of Middle Ear Pressure Changes During Prone Position Under General Anesthesia Without Using Nitrous Oxide. Journal of Craniofacial Surgery, 24, 1950.

DELEO, J. A., COLBURN, R. W., NICHOLS, M. & MALHOTRA, A. 1996. Interleukin-6-mediated hyperalgesia/allodynia and increased spinal IL-6 expression in a rat mononeuropathy model. Journal of interferon & cytokine research : the official journal of the International Society for Interferon and Cytokine Research, 16, 695.

DENK, F., CROW, M., DIDANGELOS, A., LOPES, D. M. & MCMAHON, S. B. 2016. Persistent Alterations in Microglial Enhancers in a Model of Chronic Pain. Cell reports, 15, 1771.

DENK, F. & MCMAHON, S. B. 2012. Chronic pain: emerging evidence for the involvement of epigenetics. Neuron, 73, 435.

DENK, F. & MCMAHON, S. B. 2012. Chronic pain: emerging evidence for the

involvement of epigenetics. Neuron, 73, 435.

DENK, F., MCMAHON, S. B. & TRACEY, I. 2014. Pain vulnerability: a neurobiological perspective. Nature neuroscience, 17, 192.

DICKENSON, A. H., CHAPMAN, V. & GREEN, G. M. 1997. The pharmacology of excitatory and inhibitory amino acid-mediated events in the transmission and modulation of pain in the spinal cord. General pharmacology, 28, 633.

DOCQUIER, M. A., LAVAND'HOMME, P., COLLET, V. & DE KOCK, M. 2002. Spinal alpha(2)-adrenoceptors are involved in the MACbar-sparing effect of systemic clonidine in rats. Anesthesia and Analgesia, 95, 935.

DOMINGUEZ, E., RIVAT, C., POMMIER, B., MAUBORGNE, A. & POHL, M. 2008. JAK/STAT3 pathway is activated in spinal cord microglia after peripheral nerve injury and contributes to neuropathic pain development in rat. Journal of neurochemistry, 107, 50.

DUARTE, R., MCNEILL, A., DRUMMOND, G. & TIPLADY, B. 2008. Comparison of the sedative, cognitive, and analgesic effects of nitrous oxide, sevoflurane, and ethanol. British Journal of Anaesthesia, 100, 203.

DUBOVY, P., BRAZDA, V., KLUSAKOVA, I. & HRADILOVA-SVIZENSKA, I.

2013. Bilateral elevation of interleukin-6 protein and mRNA in both lumbar and cervical dorsal root ganglia following unilateral chronic compression injury of the sciatic nerve. Journal of neuroinflammation, 10, 55.

EGER, E. I., 2ND, LIAO, M., LASTER, M. J., WON, A., POPOVICH, J., RAINES, D. E., SOLT, K., DUTTON, R. C., COBOS, F. V., 2ND & SONNER, J. M. 2006. Contrasting roles of the N-methyl-D-aspartate receptor in the production of immobilization by conventional and aromatic anesthetics. Anesthesia and Analgesia, 102, 1397.

EISENACH, J. C., PAN, P. H., SMILEY, R., LAVAND'HOMME, P., LANDAU, R. & HOULE, T. T. 2008. Severity of acute pain after childbirth, but not type of delivery, predicts persistent pain and postpartum depression. Pain, 140, 87.

ELLENBERGER, E. A., LUCAS, H. L., RUSSO, J. M., MUELLER, J. L., BARRINGTON, P. L., TSENG, L. F. & QUOCK, R. M. 2003. An opioid basis for early-phase isoflurane-induced hypotension in rats. Life Sciences, 73, 2591.

EMMANOUIL, D. E., DICKENS, A. S., HECKERT, R. W., OHGAMI, Y., CHUNG, E., HAN, S. J. & QUOCK, R. M. 2008. Nitrous oxide-antinociception is mediated by opioid receptors and nitric oxide in the periaqueductal gray region of the midbrain. European Neuropsychopharmacology, 18, 194.

ERIKSSON, H., TENHUNEN, A. & KORTTILA, K. 1996. Balanced analgesia improves recovery and outcome after outpatient tubal ligation. Acta Anaesthesiologica Scandinavica, 40, 151.

EVANS, S. F., STRINGER, M., BUKHT, M. D., THOMAS, W. A. & TOMLIN, S. J. 1985. Nitrous oxide inhalation does not influence plasma concentrations of beta-endorphin or Met-enkephalin-like immunoreactivity. British journal of anaesthesia, 57, 624.

EVANS, S. F., STRINGER, M., BUKHT, M. D., THOMAS, W. A. & TOMLIN, S. J. 1985. Nitrous oxide inhalation does not influence plasma concentrations of beta-endorphin or Met-enkephalin-like immunoreactivity. British journal of anaesthesia, 57, 624.

FANG, F., GUO, T. Z., DAVIES, M. F. & MAZE, M. 1997. Opiate receptors in the periaqueductal gray mediate analgesic effect of nitrous oxide in rats. European journal of pharmacology, 336, 137.

FENDER, C., FUJINAGA, M. & MAZE, M. 2000. Strain differences in the antinociceptive effect of nitrous oxide on the tail flick test in rats. Anesthesia and Analgesia, 90, 195.

FENG, J., FOUSE, S. & FAN, G. 2007. Epigenetic regulation of neural gene

expression and neuronal function. Pediatric research, 61, 58R.

FENG, S., COKUS, S. J., ZHANG, X., CHEN, P. Y., BOSTICK, M., GOLL, M. G., HETZEL, J., JAIN, J., STRAUSS, S. H., HALPERN, M. E., UKOMADU, C., SADLER, K. C., PRADHAN, S., PELLEGRINI, M. & JACOBSEN, S. E. 2010. Conservation and divergence of methylation patterning in plants and animals. Proceedings of the National Academy of Sciences of the United States of America, 107, 8689.

FILEN, S., YLIKOSKI, E., TRIPATHI, S., WEST, A., BJORKMAN, M., NYSTROM, J., AHLFORS, H., COFFEY, E., RAO, K. V., RASOOL, O. & LAHESMAA, R. 2010. Activating transcription factor 3 is a positive regulator of human IFNG gene expression. Journal of immunology (Baltimore, Md.: 1950), 184, 4990.

FLOOD, P. & KRASOWSKI, M. D. 2000. Intravenous anesthetics differentially modulate ligand-gated ion channels. Anesthesiology, 92, 1418.

FRIESEN, R. H. & WILLIAMS, G. D. 2008. Anesthetic management of children with pulmonary arterial hypertension. Pediatric Anesthesia, 18, 208.

FROEBA, G., GEORGIEFF, M., LINDER, E. M., FOHR, K. J., WEIGT, H. U., HOLSTRATER, T. F., KOLLE, M. A. & ADOLPH, O. 2010. Intranasal

application of xenon: describing the pharmacokinetics in experimental animals and the increased pain tolerance within a placebo-controlled experimental human study. British Journal of Anaesthesia, 104, 351.

FU, E. S., ZHANG, Y. P., SAGEN, J., CANDIOTTI, K. A., MORTON, P. D., LIEBL, D. J., BETHEA, J. R. & BRAMBILLA, R. 2010. Transgenic inhibition of glial NF-kappa B reduces pain behavior and inflammation after peripheral nerve injury. Pain, 148, 509.

FUJINAGA, M. & MAZE, M. 2002. Neurobiology of nitrous oxide-induced antinociceptive effects. Molecular Neurobiology, 25, 167.

FUKUHARA, N., ISHIKAWA, T., KINOSHITA, H., XIONG, L. & NAKANISHI, O. 1998. Central noradrenergic mediation of nitrous oxide-induced analgesia in rats. Canadian journal of anaesthesia = Journal canadien d'anesthesie, 45, 1123.

GALBAVY, W., KACZOCHA, M., PUOPOLO, M., LIU, L. & REBECCHI, M. J. 2015. Neuroimmune and Neuropathic Responses of Spinal Cord and Dorsal Root Ganglia in Middle Age. PloS one, 10, e0134394.

GALBAVY, W., LU, Y., KACZOCHA, M., PUOPOLO, M., LIU, L. & REBECCHI, M. J. 2017. Transcriptomic evidence of a para-inflammatory state in the middle aged lumbar spinal cord. Immunity & ageing : I & A, 14, 9.

GALINKIN, J. L., JANISZEWSKI, D., YOUNG, C. J., KLAFTA, J. M., KLOCK, P. A., COALSON, D. W., APFELBAUM, J. L. & ZACNY, J. P. 1997. Subjective, psychomotor, cognitive, and analgesic effects of subanesthetic concentrations of sevoflurane and nitrous oxide. Anesthesiology, 87, 1082.

GAO, X., KIM, H. K., CHUNG, J. M. & CHUNG, K. 2005. Enhancement of NMDA receptor phosphorylation of the spinal dorsal horn and nucleus gracilis neurons in neuropathic rats. Pain, 116, 62.

GELFMAN, S., COHEN, N., YEARIM, A. & AST, G. 2013. DNA-methylation effect on cotranscriptional splicing is dependent on GC architecture of the exon-intron structure. Genome research, 23, 789.

GEORGIEV, S. K., WAKAI, A., KOHNO, T., YAMAKURA, T. & BABA, H. 2006. Actions of norepinephrine and isoflurane on inhibitory synaptic transmission in adult rat spinal cord substantia gelatinosa neurons. Anesthesia and Analgesia, 102, 124.

GIACALONE, M., ABRAMO, A., GIUNTA, F. & FORFORI, F. 2013. Xenon-related Analgesia A New Target for Pain Treatment. Clinical Journal of Pain, 29, 639.

GILCHRIST, M., THORSSON, V., LI, B., RUST, A. G., KORB, M., ROACH, J. C., KENNEDY, K., HAI, T., BOLOURI, H. & ADEREM, A. 2006. Systems

biology approaches identify ATF3 as a negative regulator of Toll-like receptor 4. Nature, 441, 173.

GILLMAN, M. A. 1986. Pharmacokinetic differences could explain the lack of reversal of nitrous oxide analgesia by low-dose naloxone. Anesthesiology, 65, 449.

GINHOUX, F., GRETER, M., LEBOEUF, M., NANDI, S., SEE, P., GOKHAN, S., MEHLER, M. F., CONWAY, S. J., NG, L. G., STANLEY, E. R., SAMOKHVALOV, I. M. & MERAD, M. 2010. Fate mapping analysis reveals that adult microglia derive from primitive macrophages. Science (New York, N.Y.), 330, 841.

GOLEBSKI, K., LUITEN, S., VAN EGMOND, D., DE GROOT, E., ROSCHMANN, K. I., FOKKENS, W. J. & VAN DRUNEN, C. M. 2014. High degree of overlap between responses to a virus and to the house dust mite allergen in airway epithelial cells. PloS one, 9, e87768.

GOLEMBIEWSKI, J., CHERNIN, E. & CHOPRA, T. 2005. Prevention and treatment of postoperative nausea and vomiting. American Journal of Health-System Pharmacy, 62, 1247.

GOTO, T., MAROTA, J. J. & CROSBY, G. 1994. Nitrous oxide induces preemptive

analgesia in the rat that is antagonized by halothane. Anesthesiology, 80, 409.

GRANT, M. C., LEE, H., PAGE, A. J., HOBSON, D., WICK, E. & WU, C. L. 2016. The Effect of Preoperative Gabapentin on Postoperative Nausea and Vomiting: A Meta-Analysis. Anesthesia and Analgesia, 122, 976.

GRIFFIN, R. S., COSTIGAN, M., BRENNER, G. J., MA, C. H., SCHOLZ, J., MOSS, A., ALLCHORNE, A. J., STAHL, G. L. & WOOLF, C. J. 2007. Complement induction in spinal cord microglia results in anaphylatoxin C5a-mediated pain hypersensitivity. The Journal of neuroscience : the official journal of the Society for Neuroscience, 27, 8699.

GRINDLAY, J. & BABL, F. E. 2009. Review article: Efficacy and safety of methoxyflurane analgesia in the emergency department and prehospital setting. Emergency Medicine Australasia, 21, 4.

GUO, J. U., MA, D. K., MO, H., BALL, M. P., JANG, M. H., BONAGUIDI, M. A., BALAZER, J. A., EAVES, H. L., XIE, B., FORD, E., ZHANG, K., MING, G. L., GAO, Y. & SONG, H. 2011. Neuronal activity modifies the DNA methylation landscape in the adult brain. Nature neuroscience, 14, 1345.

GUO, T. Z., POREE, L., GOLDEN, W., STEIN, J., FUJINAGA, M. & MAZE, M. 1996. Antinociceptive response to nitrous oxide is mediated by supraspinal

opiate and spinal alpha(2) adrenergic receptors in the rat. Anesthesiology, 85, 846.

GYULAI, F. E., FIRESTONE, L. L., MINTUN, M. A. & WINTER, P. M. 1997. In vivo imaging of nitrous oxide-induced changes in cerebral activation during noxious heat stimuli. Anesthesiology, 86, 538.

HAAKVANDERLELY, F., BURM, A. G. L., VANKLEEF, J. W., VANDENNIEUWENHUYZEN, M. C. O., SIEMENS, T. J., MULDER, S. M., BOVILL, J. G. & VLETTER, A. A. 1994. The Effect of Epidural Administration of Alfentanil on Intraoperative Intravenous Alfentanil Requirements during Nitrous-Oxide Oxygen Alfentanil Anesthesia for Lower Abdominal-Surgery. Anaesthesia, 49, 1034.

HAGIHIRA, S., TAENAKA, N. & YOSHIYA, I. 1997. Inhalation anesthetics suppress the expression of c-Fos protein evoked by noxious somatic stimulation in the deeper layer of the spinal cord in the rat. Brain Research, 751, 124.

HAI, T., WOLFORD, C. C. & CHANG, Y. S. 2010. ATF3, a hub of the cellular adaptive-response network, in the pathogenesis of diseases: is modulation of inflammation a unifying component? Gene expression, 15, 1.

HARA, S., GAGNON, M. J., QUOCK, R. M. & SHIBUYA, T. 1994. Effect of opioid

peptide antisera on nitrous oxide antinociception in rats. Pharmacology, biochemistry, and behavior, 48, 699.

HARA, S., KUHNS, E. R., ELLENBERGER, E. A., MUELLER, J. L., SHIBUYA, T., ENDO, T. & QUOCK, R. M. 1995. Involvement of Nitric-Oxide in Intracerebroventricular Beta-Endorphin-Induced Neuronal Release of Methionine-Enkephalin. Brain Research, 675, 190.

HASHIMOTO, T., MAZE, M., OHASHI, Y. & FUJINAGA, M. 2001. Nitrous oxide activates GABAergic neurons in the spinal cord in Fischer rats. Anesthesiology, 95, 463.

HINRICHS-ROCKER, A., SCHULZ, K., JARVINEN, I., LEFERING, R., SIMANSKI, C. & NEUGEBAUER, E. A. 2009. Psychosocial predictors and correlates for chronic post-surgical pain (CPSP) - a systematic review. European journal of pain (London, England), 13, 719.

HOCKER, J., BOHM, R., MEYBOHM, P., GRUENEWALD, M., RENNER, J., OHNESORGE, H., SCHOLZ, J. & BEIN, B. 2009. Interaction of morphine but not fentanyl with cerebral alpha(2)-adrenoceptors in alpha(2)-adrenoceptor knockout mice. Journal of Pharmacy and Pharmacology, 61, 901.

HOCKER, J., WEBER, B., TONNER, P. H., SCHOLZ, J., BRAND, P. A.,

OHNESORGE, H. & BEIN, B. 2008. Meperidine, remifentanil and tramadol but not sufentanil interact with alpha(2)-adrenoceptors in alpha(2A)-, alpha(2B)- and alpha(2C)-adrenoceptor knock out mice brain. European Journal of Pharmacology, 582, 70.

HODGES, B. L., GAGNON, M. J., GILLESPIE, T. R., BRENEISEN, J. R., O'LEARY, D. F., HARA, S. & QUOCK, R. M. 1994. Antagonism of nitrous oxide antinociception in the rat hot plate test by site-specific mu and epsilon opioid receptor blockade. The Journal of pharmacology and experimental therapeutics, 269, 596.

HODGES, B. L., GAGNON, M. J., GILLESPIE, T. R., BRENEISEN, J. R., O'LEARY, D. F., HARA, S. & QUOCK, R. M. 1994. Antagonism of nitrous oxide antinociception in the rat hot plate test by site-specific mu and epsilon opioid receptor blockade. The Journal of pharmacology and experimental therapeutics, 269, 596.

HOETZENECKER, W., ECHTENACHER, B., GUENOVA, E., HOETZENECKER, K., WOELBING, F., BRUCK, J., TESKE, A., VALTCHEVA, N., FUCHS, K., KNEILLING, M., PARK, J. H., KIM, K. H., KIM, K. W., HOFFMANN, P., KRENN, C., HAI, T., GHORESCHI, K., BIEDERMANN, T. & ROCKEN, M.

2011. ROS-induced ATF3 causes susceptibility to secondary infections during sepsis-associated immunosuppression. Nature medicine, 18, 128.

HOJSTED, J., NIELSEN, P. R., GULDSTRAND, S. K., FRICH, L. & SJOGREN, P. 2010. Classification and identification of opioid addiction in chronic pain patients. European journal of pain (London, England), 14, 1014.

HONORE, P., LUGER, N. M., SABINO, M. A., SCHWEI, M. J., ROGERS, S. D., MACH, D. B., O'KEEFE, P. F., RAMNARAINE, M. L., CLOHISY, D. R. & MANTYH, P. W. 2000. Osteoprotegerin blocks bone cancer-induced skeletal destruction, skeletal pain and pain-related neurochemical reorganization of the spinal cord. Nature medicine, 6, 521.

HORN-HOFMANN, C., BUSCHER, P., LAUTENBACHER, S. & WOLSTEIN, J. 2015. The effect of nonrecurring alcohol administration on pain perception in humans: a systematic review. Journal of Pain Research, 8, 175.

HUMBLE, S. R., DALTON, A. J. & LI, L. 2015. A systematic review of therapeutic interventions to reduce acute and chronic post-surgical pain after amputation, thoracotomy or mastectomy. European journal of pain (London, England), 19, 451.

IEZAKI, T., OZAKI, K., FUKASAWA, K., INOUE, M., KITAJIMA, S., MUNETA,

T., TAKEDA, S., FUJITA, H., ONISHI, Y., HORIE, T., YONEDA, Y., TAKARADA, T. & HINOI, E. 2016. ATF3 deficiency in chondrocytes alleviates osteoarthritis development. The Journal of pathology, 239, 426.

IYENGAR, B. R., CHOUDHARY, A., SARANGDHAR, M. A., VENKATESH, K. V., GADGIL, C. J. & PILLAI, B. 2014. Non-coding RNA interact to regulate neuronal development and function. Frontiers in cellular neuroscience, 8, 47.

JANISZEWSKI, D. J., GALINKIN, J. L., KLOCK, P. A., COALSON, D. W., PARDO, H. & ZACNY, J. P. 1999. The effects of subanesthetic concentrations of sevoflurane and nitrous oxide, alone and in combination, on analgesia, mood, and psychomotor performance in healthy volunteers. Anesthesia and Analgesia, 88, 1149.

JEVTOVIC-TODOROVIC, V., TODOROVIC, S. M., MENNERICK, S., POWELL, S., DIKRANIAN, K., BENSHOFF, N., ZORUMSKI, C. F. & OLNEY, J. W. 1998. Nitrous oxide (laughing gas) is an NMDA antagonist, neuroprotectant and neurotoxin. Nature medicine, 4, 460.

JIN, S. X., ZHUANG, Z. Y., WOOLF, C. J. & JI, R. R. 2003. P38 Mitogen-Activated Protein Kinase is Activated After a Spinal Nerve Ligation in Spinal Cord Microglia and Dorsal Root Ganglion Neurons and Contributes to the

Generation of Neuropathic Pain. The Journal of neuroscience : the official journal of the Society for Neuroscience, 23, 4017.

JINKS, S. L., CARSTENS, E. & ANTOGNINI, J. F. 2009. Nitrous Oxide-Induced Analgesia Does Not Influence Nitrous Oxide's Immobilizing Requirements. Anesthesia and Analgesia, 109, 1111.

JINKS, S. L., CARSTENS, E. & ANTOGNINI, J. F. 2009. Nitrous oxide-induced analgesia does not influence nitrous oxide's immobilizing requirements. Anesthesia and Analgesia, 109, 1111.

JOHANSEN, A., ROMUNDSTAD, L., NIELSEN, C. S., SCHIRMER, H. & STUBHAUG, A. 2012. Persistent postsurgical pain in a general population: prevalence and predictors in the Tromso study. Pain, 153, 1390.

JONES, P. A. 2012. Functions of DNA methylation: islands, start sites, gene bodies and beyond. Nature reviews.Genetics, 13, 484.

KALLIOMAKI, J., GRANMO, M. & SCHOUENBORG, J. 2003. Spinal NMDA-receptor dependent amplification of nociceptive transmission to rat primary somatosensory cortex (SI). Pain, 104, 195.

KAROUZAKIS, E., GAY, R. E., GAY, S. & NEIDHART, M. 2012. Increased

recycling of polyamines is associated with global DNA hypomethylation in rheumatoid arthritis synovial fibroblasts. Arthritis and Rheumatism, 64, 1809.

KAROUZAKIS, E., GAY, R. E., MICHEL, B. A., GAY, S. & NEIDHART, M. 2009. DNA hypomethylation in rheumatoid arthritis synovial fibroblasts. Arthritis and Rheumatism, 60, 3613.

KARPOVA, N. N., SALES, A. J. & JOCA, S. R. 2017. Epigenetic Basis of Neuronal and Synaptic Plasticity. Current topics in medicinal chemistry, 17, 771.

KATSURA, H., OBATA, K., MIZUSHIMA, T., SAKURAI, J., KOBAYASHI, K., YAMANAKA, H., DAI, Y., FUKUOKA, T., SAKAGAMI, M. & NOGUCHI, K. 2006. Activation of Src-family kinases in spinal microglia contributes to mechanical hypersensitivity after nerve injury. The Journal of neuroscience : the official journal of the Society for Neuroscience, 26, 8680.

KATZ, J. & SELTZER, Z. 2009. Transition from acute to chronic postsurgical pain: risk factors and protective factors. Expert review of neurotherapeutics, 9, 723.

KAWABATA, A. 2011. Prostaglandin E2 and pain--an update. Biological & pharmaceutical bulletin, 34, 1170.

KIERDORF, K., ERNY, D., GOLDMANN, T., SANDER, V., SCHULZ, C.,

PERDIGUERO, E. G., WIEGHOFER, P., HEINRICH, A., RIEMKE, P., HOLSCHER, C., MULLER, D. N., LUCKOW, B., BROCKER, T., DEBOWSKI, K., FRITZ, G., OPDENAKKER, G., DIEFENBACH, A., BIBER, K., HEIKENWALDER, M., GEISSMANN, F., ROSENBAUER, F. & PRINZ, M. 2013. Microglia emerge from erythromyeloid precursors via Pu.1- and Irf8-dependent pathways. Nature neuroscience, 16, 273.

KIM, D., KIM, M. A., CHO, I. H., KIM, M. S., LEE, S., JO, E. K., CHOI, S. Y., PARK, K., KIM, J. S., AKIRA, S., NA, H. S., OH, S. B. & LEE, S. J. 2007. A critical role of toll-like receptor 2 in nerve injury-induced spinal cord glial cell activation and pain hypersensitivity. The Journal of biological chemistry, 282, 14975.

KIM, D., KIM, M. A., CHO, I. H., KIM, M. S., LEE, S., JO, E. K., CHOI, S. Y., PARK, K., KIM, J. S., AKIRA, S., NA, H. S., OH, S. B. & LEE, S. J. 2007. A critical role of toll-like receptor 2 in nerve injury-induced spinal cord glial cell activation and pain hypersensitivity. The Journal of biological chemistry, 282, 14975.

KIM, M. K., YI, M. S., KANG, H. & CHOI, G. J. 2016. Effects of remifentanil versus nitrous oxide on postoperative nausea, vomiting, and pain in patients receiving

thyroidectomy: Propensity score matching analysis. Medicine, 95.

KINGERY, W. S., SAWAMURA, S., AGASHE, G. S., DAVIES, M. F., CLARK, J. D. & ZIMMER, A. 2001. Enkephalin release and opioid receptor activation does not mediate the antinociceptive or sedative/hypnotic effects of nitrous oxide. European Journal of Pharmacology, 427, 27.

KOMATSU, T., SHINGU, K., TOMEMORI, N., URABE, N. & MORI, K. 1981. Nitrous oxide activates the supraspinal pain inhibition system. Acta Anaesthesiologica Scandinavica, 25, 519.

KONG, Y. Y., FEIGE, U., SAROSI, I., BOLON, B., TAFURI, A., MORONY, S., CAPPARELLI, C., LI, J., ELLIOTT, R., MCCABE, S., WONG, T., CAMPAGNUOLO, G., MORAN, E., BOGOCH, E. R., VAN, G., NGUYEN, L. T., OHASHI, P. S., LACEY, D. L., FISH, E., BOYLE, W. J. & PENNINGER, J. M. 1999. Activated T cells regulate bone loss and joint destruction in adjuvant arthritis through osteoprotegerin ligand. Nature, 402, 304.

KONSTANTATOS, A. H., HOWARD, W., STORY, D., MOK, L. Y., BOYD, D. & CHAN, M. T. 2016. A randomised controlled trial of peri-operative pregabalin vs. placebo for video-assisted thoracoscopic surgery. Anaesthesia, 71, 192.

KOYAMA, T. & FUKUDA, K. 2009. Nociceptin receptor antagonist JTC-801 inhibits

nitrous oxide-induced analgesia in mice. Journal of Anesthesia, 23, 301.

KOYANAGI, S., HIMUKASHI, S., MUKAIDA, K., SHICHINO, T. & FUKUDA, K. 2008. Dopamine D(2)-like receptor in the nucleus accumbens is involved in the antinociceptive effect of nitrous oxide. Anesthesia and Analgesia, 106, 1904.

KRYSTAL, J. H., PETRAKIS, I. L., O'MALLEY, S., KRISHNAN-SARIN, S., PEARLSON, G. & YOON, G. 2017. NMDA glutamate receptor antagonism and the heritable risk for alcoholism: new insights from a study of nitrous oxide. The international journal of neuropsychopharmacology.

KUHLMANN, L., FOSTER, B. L. & LILEY, D. T. 2013. Modulation of functional EEG networks by the NMDA antagonist nitrous oxide. PloS one, 8, e56434.

KWON, J. W., KWON, H. K., SHIN, H. J., CHOI, Y. M., ANWAR, M. A. & CHOI, S. 2015. Activating transcription factor 3 represses inflammatory responses by binding to the p65 subunit of NF-kappaB. Scientific reports, 5, 14470.

LAIRD, P. W. 2010. Principles and challenges of genomewide DNA methylation analysis. Nature reviews.Genetics, 11, 191.

LAIRD, P. W. 2010. Principles and challenges of genomewide DNA methylation

analysis. Nature reviews.Genetics, 11, 191.

LARBIG, W. 1994. Eeg Correlates of Pain Control. Eeg-Emg-Zeitschrift Fur Elektroenzephalographie Elektromyographie Und Verwandte Gebiete, 25, 151.

LATREMOLIERE, A., MAUBORGNE, A., MASSON, J., BOURGOIN, S., KAYSER, V., HAMON, M. & POHL, M. 2008. Differential implication of proinflammatory cytokine interleukin-6 in the development of cephalic versus extracephalic neuropathic pain in rats. The Journal of neuroscience : the official journal of the Society for Neuroscience, 28, 8489.

LATREMOLIERE, A., MAUBORGNE, A., MASSON, J., BOURGOIN, S., KAYSER, V., HAMON, M. & POHL, M. 2008. Differential implication of proinflammatory cytokine interleukin-6 in the development of cephalic versus extracephalic neuropathic pain in rats. The Journal of neuroscience : the official journal of the Society for Neuroscience, 28, 8489.

LAURENT, G., BERTAUX, G., MARTEL, A., FRAISON, M., FROMENTIN, S., GONZALEZ, S., SAINT PIERRE, F. & WOLF, J. E. 2006. A randomized clinical trial of continuous flow nitrous oxide and nalbuphine infusion for sedation of patients during radiofrequency atrial flutter ablation. Pace-Pacing and Clinical Electrophysiology, 29, 351.

LI, Y., REDDY, M. A., MIAO, F., SHANMUGAM, N., YEE, J. K., HAWKINS, D., REN, B. & NATARAJAN, R. 2008. Role of the histone H3 lysine 4 methyltransferase, SET7/9, in the regulation of NF-kappaB-dependent inflammatory genes. Relevance to diabetes and inflammation. The Journal of biological chemistry, 283, 26771.

LINK, R. E., DESAI, K., HEIN, L., STEVENS, M. E., CHRUSCINSKI, A., BERNSTEIN, D., BARSH, G. S. & KOBILKA, B. K. 1996. Cardiovascular regulation in mice lacking alpha2-adrenergic receptor subtypes b and c. Science (New York, N.Y.), 273, 803.

LISANDER, B. 1993. Evaluation of the Analgesic Effect of Metoclopramide after Opioid-Free Analgesia. British Journal of Anaesthesia, 70, 631.

LIU, S., MI, W. L., LI, Q., ZHANG, M. T., HAN, P., HU, S., MAO-YING, Q. L. & WANG, Y. Q. 2015. Spinal IL-33/ST2 Signaling Contributes to Neuropathic Pain via Neuronal CaMKII-CREB and Astroglial JAK2-STAT3 Cascades in Mice. Anesthesiology, 123, 1154.

LIU, X., TIAN, Y., MENG, Z., CHEN, Y., HO, I. H., CHOY, K. W., LICHTNER, P., WONG, S. H., YU, J., GIN, T., WU, W. K., CHENG, C. H. & CHAN, M. T. 2015. Up-regulation of Cathepsin G in the Development of Chronic

Postsurgical Pain: An Experimental and Clinical Genetic Study. Anesthesiology, 123, 838.

LOKK, K., MODHUKUR, V., RAJASHEKAR, B., MARTENS, K., MAGI, R., KOLDE, R., KOLTSINA, M., NILSSON, T. K., VILO, J., SALUMETS, A. & TONISSON, N. 2014. DNA methylome profiling of human tissues identifies global and tissue-specific methylation patterns. Genome biology, 15, r54.

LONATI, C., SORDI, A., GIULIANI, D., SPACCAPELO, L., LEONARDI, P., CARLIN, A., OTTANI, A., GALANTUCCI, M., GRIECO, P., CATANIA, A. & GUARINI, S. 2012. Molecular changes induced in rat liver by hemorrhage and effects of melanocortin treatment. Anesthesiology, 116, 692.

LU, J., NELSON, L. E., FRANKS, N., MAZE, M., CHAMBERLIN, N. L. & SAPER, C. B. 2008. Role of endogenous sleep-wake and analgesic systems in anesthesia. Journal of Comparative Neurology, 508, 648.

LUCAS, D. N., SIEMASZKO, O. & YENTIS, S. M. 2000. Maternal hypoxaemia associated with the use of Entonox (R) in labour. International Journal of Obstetric Anesthesia, 9, 270.

LUGINBUEHL, M., ZBINDEN, A. M., ESCH, J. S. A., SCHOLZ, J. & TONNER, P. H. 2000. Nitrous oxide: Mechanisms of action.

MACMILLAN, L. B., HEIN, L., SMITH, M. S., PIASCIK, M. T. & LIMBIRD, L. E. 1996. Central hypotensive effects of the alpha2a-adrenergic receptor subtype. Science (New York, N.Y.), 273, 801.

MALASPINA, A., NGOH, S. F., WARD, R. E., HALL, J. C., TAI, F. W., YIP, P. K., JONES, C., JOKIC, N., AVERILL, S. A., MICHAEL-TITUS, A. T. & PRIESTLEY, J. V. 2010. Activation transcription factor-3 activation and the development of spinal cord degeneration in a rat model of amyotrophic lateral sclerosis. Neuroscience, 169, 812.

MALMBERG, A. B. & BASBAUM, A. I. 1998. Partial sciatic nerve injury in the mouse as a model of neuropathic pain: behavioral and neuroanatomical correlates. Pain, 76, 215.

MALMBERG, A. B., BRANDON, E. P., IDZERDA, R. L., LIU, H., MCKNIGHT, G. S. & BASBAUM, A. I. 1997. Diminished inflammation and nociceptive pain with preservation of neuropathic pain in mice with a targeted mutation of the type I regulatory subunit of cAMP-dependent protein kinase. The Journal of neuroscience : the official journal of the Society for Neuroscience, 17, 7462.

MALMBERG, A. B., BRANDON, E. P., IDZERDA, R. L., LIU, H., MCKNIGHT, G. S. & BASBAUM, A. I. 1997. Diminished inflammation and nociceptive pain

with preservation of neuropathic pain in mice with a targeted mutation of the type I regulatory subunit of cAMP-dependent protein kinase. The Journal of neuroscience : the official journal of the Society for Neuroscience, 17, 7462.

MARACAJA-NETO, L. F., SILVA, G. A. M., DE MOURA, R. S., TIBIRICA, E. & LESSA, M. A. 2012. Opioid Receptor Blockade Prevents Propofol-induced Hypotension in Rats. Journal of Neurosurgical Anesthesiology, 24, 191.

MASSART, R., DYMOV, S., MILLECAMPS, M., SUDERMAN, M., GREGOIRE, S., KOENIGS, K., ALVARADO, S., TAJERIAN, M., STONE, L. S. & SZYF, M. 2016. Overlapping signatures of chronic pain in the DNA methylation landscape of prefrontal cortex and peripheral T cells. Scientific reports, 6, 19615.

MATSUSHITA, Y., ISHIKAWA, M., ABE, K., UTSUNOMIYA, I., CHIKUMA, T., HOJO, H., HOSHI, K., QUOCK, R. M. & TAGUCHI, K. 2007. Involvement of the protein development of tolerance antinociception in mice. Neuroscience, 148, 541.

MAUNAKEA, A. K., CHEPELEV, I., CUI, K. & ZHAO, K. 2013. Intragenic DNA methylation modulates alternative splicing by recruiting MeCP2 to promote exon recognition. Cell research, 23, 1256.

MAWHINNEY, L. J., DE RIVERO VACCARI, J. P., ALONSO, O. F., JIMENEZ, C. A., FURONES, C., MORENO, W. J., LEWIS, M. C., DIETRICH, W. D. & BRAMLETT, H. M. 2012. Isoflurane/nitrous oxide anesthesia induces increases in NMDA receptor subunit NR2B protein expression in the aged rat brain. Brain research, 1431, 23.

MENNERICK, S., JEVTOVIC-TODOROVIC, V., TODOROVIC, S. M., SHEN, W., OLNEY, J. W. & ZORUMSKI, C. F. 1998. Effect of nitrous oxide on excitatory and inhibitory synaptic transmission in hippocampal cultures. The Journal of neuroscience : the official journal of the Society for Neuroscience, 18, 9716.

MICHOT, B., KAYSER, V., HAMON, M. & BOURGOIN, S. 2015. CGRP receptor blockade by MK-8825 alleviates allodynia in infraorbital nerve-ligated rats. European journal of pain (London, England), 19, 281.

MIKA, J., KOROSTYNSKI, M., KAMINSKA, D., WAWRZCZAK-BARGIELA, A., OSIKOWICZ, M., MAKUCH, W., PRZEWLOCKI, R. & PRZEWLOCKA, B. 2008. Interleukin-1 alpha has antiallodynic and antihyperalgesic activities in a rat neuropathic pain model. Pain, 138, 587.

MILLION, M., WANG, L., WANG, Y., ADELSON, D. W., YUAN, P. Q., MAILLOT, C., COUTINHO, S. V., MCROBERTS, J. A., BAYATI, A., MATTSSON, H.,

WU, V., WEI, J. Y., RIVIER, J., VALE, W., MAYER, E. A. & TACHE, Y. 2006. CRF2 receptor activation prevents colorectal distension induced visceral pain and spinal ERK1/2 phosphorylation in rats. Gut, 55, 172.

MOALEM, G. & TRACEY, D. J. 2006. Immune and inflammatory mechanisms in neuropathic pain. Brain Research Reviews, 51, 240.

MONTES, A., ROCA, G., SABATE, S., LAO, J. I., NAVARRO, A., CANTILLO, J., CANET, J. & GROUP, G. S. 2015. Genetic and Clinical Factors Associated with Chronic Postsurgical Pain after Hernia Repair, Hysterectomy, and Thoracotomy: A Two-year Multicenter Cohort Study. Anesthesiology, 122, 1123.

MOODY, E. J., MATTSON, M., NEWMAN, A. H., RICE, K. C. & SKOLNICK, P. 1989. Stereospecific reversal of nitrous oxide analgesia by naloxone. Life Sciences, 44, 703.

MORI, H. & MISHINA, M. 1995. Structure and function of the NMDA receptor channel. Neuropharmacology, 34, 1219.

MUELLER, J. L. & QUOCK, R. M. 1992. Contrasting Influences of 5-Hydroxytryptamine Receptors in Nitrous-Oxide Antinociception in Mice. Pharmacology Biochemistry and Behavior, 41, 429.

MURPHY, P. G., RAMER, M. S., BORTHWICK, L., GAULDIE, J., RICHARDSON, P. M. & BISBY, M. A. 1999. Endogenous interleukin-6 contributes to hypersensitivity to cutaneous stimuli and changes in neuropeptides associated with chronic nerve constriction in mice. The European journal of neuroscience, 11, 2243.

MURPHY, P. G., RAMER, M. S., BORTHWICK, L., GAULDIE, J., RICHARDSON, P. M. & BISBY, M. A. 1999. Endogenous interleukin-6 contributes to hypersensitivity to cutaneous stimuli and changes in neuropeptides associated with chronic nerve constriction in mice. The European journal of neuroscience, 11, 2243.

NAGASAKA, H., TAGUCHI, M., TSUCHIYA, M., MIZUMOTO, Y., HORI, K., HAYASHI, K., MATSUMOTO, I., HORI, T. & SATO, I. 1997. Effect of nitrous oxide on spinal dorsal horn WDR neuronal activity in cats. Masui.The Japanese journal of anesthesiology, 46, 1190.

NAGELE, P., METZ, L. B. & CROWDER, C. M. 2004. Nitrous oxide (N(2)O) requires the N-methyl-D-aspartate receptor for its action in Caenorhabditis elegans. Proceedings of the National Academy of Sciences of the United States of America, 101, 8791.

NAGELE, P., METZ, L. B. & CROWDER, C. M. 2005. Xenon acts by inhibition of non-N-methyl-D-aspartate receptor-mediated glutamatergic neurotransmission in Caenorhabditis elegans. Anesthesiology, 103, 508.

NAGELE, P., ZEUGSWETTER, B., WIENER, C., BURGER, H., HUPFL, M., MITTLBOCK, M. & FODINGER, M. 2008. Influence of methylenetetrahydrofolate reductase gene polymorphisms on homocysteine concentrations after nitrous oxide anesthesia. Anesthesiology, 109, 36.

NAKANO, K., WHITAKER, J. W., BOYLE, D. L., WANG, W. & FIRESTEIN, G. S. 2013. DNA methylome signature in rheumatoid arthritis. Annals of the Rheumatic Diseases, 72, 110.

NAKAO, S., NAGATA, A., MASUZAWA, M., MIYAMOTO, E., YAMADA, M., NISHIZAWA, N. & SHINGU, K. 2003. NMDA receptor antagonist neurotoxicity and psychotomimetic activity. Masui.The Japanese journal of anesthesiology, 52, 594.

NAKATA, Y., GOTO, T. & MORITA, S. 1999. Effects of xenon on hemodynamic responses to skin Incision in humans. Anesthesiology, 90, 406.

NGUYEN, C. T., KIM, E. H., LUONG, T. T., PYO, S. & RHEE, D. K. 2014. ATF3 confers resistance to pneumococcal infection through positive regulation of

cytokine production. The Journal of infectious diseases, 210, 1745.

NIKOLAJSEN, L., SORENSEN, H. C., JENSEN, T. S. & KEHLET, H. 2004. Chronic pain following Caesarean section. Acta Anaesthesiologica Scandinavica, 48, 111.

NIRAJ, G. & ROWBOTHAM, D. J. 2011. Persistent postoperative pain: where are we now? British journal of anaesthesia, 107, 25.

O'CONNOR, A. B. 2009. Neuropathic pain: quality-of-life impact, costs and cost effectiveness of therapy. PharmacoEconomics, 27, 95.

OGATA, J., SHIRAISHI, M., NAMBA, T., SMOTHERS, C. T., WOODWARD, J. J. & HARRIS, R. A. 2006. Effects of anesthetics on mutant N-methyl-D-aspartate receptors expressed in Xenopus oocytes. The Journal of pharmacology and experimental therapeutics, 318, 434.

OHARA, A., MASHIMO, T., ZHANG, P., INAGAKI, Y., SHIBUTA, S. & YOSHIYA, I. 1997. A comparative study of the antinociceptive action of xenon and nitrous oxide in rats. Anesthesia and Analgesia, 85, 931.

OHASHI, Y., GUO, T., ORII, R., MAZE, M. & FUJINAGA, M. 2003. Brain stem opioidergic and GABAergic neurons mediate the antinociceptive effect of

nitrous oxide in Fischer rats. Anesthesiology, 99, 947.

OHASHI, Y., STOWELL, J. M., NELSON, L. E., HASHIMOTO, T., MAZE, M. & FUJINAGA, M. 2002. Nitrous oxide exerts age-dependent antinociceptive effects in Fischer rats. Pain, 100, 7.

ORESTES, P., BOJADZIC, D., LEE, J., LEACH, E., SALAJEGHEH, R., DIGRUCCIO, M. R., NELSON, M. T. & TODOROVIC, S. M. 2011. Free radical signalling underlies inhibition of Ca(V)3.2 T-type calcium channels by nitrous oxide in the pain pathway. Journal of Physiology-London, 589, 135.

ORESTES, P., BOJADZIC, D., LEE, J., LEACH, E., SALAJEGHEH, R., DIGRUCCIO, M. R., NELSON, M. T. & TODOROVIC, S. M. 2011. Free radical signalling underlies inhibition of CaV3.2 T-type calcium channels by nitrous oxide in the pain pathway. The Journal of physiology, 589, 135.

ORII, R., OHASHI, Y., GUO, T., NELSON, L. E., HASHIMOTO, T., MAZE, M. & FUJINAGA, M. 2002. Evidence for the involvement of spinal cord alpha1 adrenoceptors in nitrous oxide-induced antinociceptive effects in Fischer rats. Anesthesiology, 97, 1458.

ORII, R., OHASHI, Y., HALDER, S., GIOMBINI, M., MAZE, M. & FUJINAGA, M. 2003. GABAergic interneurons at supraspinal and spinal levels differentially

modulate the antinociceptive effect of nitrous oxide in Fischer rats. Anesthesiology, 98, 1223.

PADMOS, R. C., HILLEGERS, M. H., KNIJFF, E. M., VONK, R., BOUVY, A., STAAL, F. J., DE RIDDER, D., KUPKA, R. W., NOLEN, W. A. & DREXHAGE, H. A. 2008. A discriminating messenger RNA signature for bipolar disorder formed by an aberrant expression of inflammatory genes in monocytes. Archives of General Psychiatry, 65, 395.

PARVINI, S., HAMANN, S. R. & MARTIN, W. R. 1993. Pharmacological Characteristics of a Medullary Hyperalgesic Center. Journal of Pharmacology and Experimental Therapeutics, 265, 286.

PERKINS, J. R., ANTUNES-MARTINS, A., CALVO, M., GRIST, J., RUST, W., SCHMID, R., HILDEBRANDT, T., KOHL, M., ORENGO, C., MCMAHON, S. B. & BENNETT, D. L. 2014. A comparison of RNA-seq and exon arrays for whole genome transcription profiling of the L5 spinal nerve transection model of neuropathic pain in the rat. Molecular pain, 10, 7.

PERKINS, T. N., SHUKLA, A., PEETERS, P. M., STEINBACHER, J. L., LANDRY, C. C., LATHROP, S. A., STEELE, C., REYNAERT, N. L., WOUTERS, E. F. & MOSSMAN, B. T. 2012. Differences in gene expression and cytokine

production by crystalline vs. amorphous silica in human lung epithelial cells. Particle and fibre toxicology, 9, 6.

PETRENKO, A. B., YAMAKURA, T., KOHNO, T., SAKIMURA, K. & BABA, H. 2010. Reduced immobilizing properties of isoflurane and nitrous oxide in mutant mice lacking the N-methyl-D-aspartate receptor GluR(epsilon)1 subunit are caused by the secondary effects of gene knockout. Anesthesia and Analgesia, 110, 461.

PETRENKO, A. B., YAMAKURA, T., KOHNO, T., SAKIMURA, K. & BABA, H. 2013. Increased brain monoaminergic tone after the NMDA receptor GluN2A subunit gene knockout is responsible for resistance to the hypnotic effect of nitrous oxide. European journal of pharmacology, 698, 200.

PETRENKO, A. B., YAMAKURA, T., SAKIMURA, K. & BABA, H. 2014. Defining the role of NMDA receptors in anesthesia: are we there yet? European journal of pharmacology, 723, 29.

QI, F., ZHOU, Y., XIAO, Y., TAO, J., GU, J., JIANG, X. & XU, G. Y. 2013. Promoter demethylation of cystathionine-beta-synthetase gene contributes to inflammatory pain in rats. Pain, 154, 34.

QI, F., ZHOU, Y., XIAO, Y., TAO, J., GU, J., JIANG, X. & XU, G. Y. 2013. Promoter

demethylation of cystathionine-beta-synthetase gene contributes to inflammatory pain in rats. Pain, 154, 34.

QUOCK, R. M., BEST, J. A., CHEN, D. C., VAUGHN, L. K., PORTOGHESE, P. S. & TAKEMORI, A. E. 1990. Mediation of nitrous oxide analgesia in mice by spinal and supraspinal kappa-opioid receptors. European journal of pharmacology, 175, 97.

QUOCK, R. M., BEST, J. A., CHEN, D. C., VAUGHN, L. K., PORTOGHESE, P. S. & TAKEMORI, A. E. 1990. Mediation of nitrous oxide analgesia in mice by spinal and supraspinal kappa-opioid receptors. European journal of pharmacology, 175, 97.

QUOCK, R. M., CURTIS, B. A., REYNOLDS, B. J. & MUELLER, J. L. 1993. Dose-dependent antagonism and potentiation of nitrous oxide antinociception by naloxone in mice. The Journal of pharmacology and experimental therapeutics, 267, 117.

QUOCK, R. M., EMMANOUIL, D. E., VAUGHN, L. K. & PRUHS, R. J. 1992. Benzodiazepine Receptor Mediation of Behavioral-Effects of Nitrous-Oxide in Mice. Psychopharmacology, 107, 310.

QUOCK, R. M. & GRACZAK, L. M. 1988. Influence of narcotic antagonist drugs

upon nitrous oxide analgesia in mice. Brain research, 440, 35.

QUOCK, R. M., KOUCHICH, F. J. & TSENG, L. F. 1985. Does nitrous oxide induce release of brain opioid peptides? Pharmacology, 30, 95.

QUOCK, R. M., KOUCHICH, F. J. & TSENG, L. F. 1986. Influence of nitrous oxide upon regional brain levels of methionine-enkephalin-like immunoreactivity in rats. Brain research bulletin, 16, 321.

QUOCK, R. M. & MUELLER, J. 1991. Protection by U-50,488h against Beta-Chlornaltrexamine Antagonism of Nitrous-Oxide Antinociception in Mice. Brain Research, 549, 162.

QUOCK, R. M., MUELLER, J. L. & VAUGHN, L. K. 1993. Strain-dependent differences in responsiveness of mice to nitrous oxide (N2O) antinociception. Brain research, 614, 52.

QUOCK, R. M., WALCZAK, C. K., HENRY, R. J. & CHEN, D. C. 1990. Effect of subtype-selective opioid receptor blockers on nitrous oxide antinociception in rats. Pharmacological research, 22, 351.

RABBEN, T., SKJELBRED, P. & OYE, I. 1999. Prolonged analgesic effect of ketamine, an N-methyl-D-aspartate receptor inhibitor, in patients with chronic

pain. The Journal of pharmacology and experimental therapeutics, 289, 1060.

RAMANI, R. & WARDHAN, R. 2008. Understanding anesthesia through functional imaging. Current Opinion in Anesthesiology, 21, 530.

RAMER, M. S., MURPHY, P. G., RICHARDSON, P. M. & BISBY, M. A. 1998. Spinal nerve lesion-induced mechanoallodynia and adrenergic sprouting in sensory ganglia are attenuated in interleukin-6 knockout mice. Pain, 78, 115.

RAMSAY, D. S., OMACHI, K., LEROUX, B. G., SEELEY, R. J., PRALL, C. W. & WOODS, S. C. 1999. Nitrous oxide-induced hypothermia in the rat: Acute and chronic tolerance. Pharmacology Biochemistry and Behavior, 62, 189.

RANCE, N. E., KRAJEWSKI, S. J., SMITH, M. A., CHOLANIAN, M. & DACKS, P. A. 2010. Neurokinin B and the hypothalamic regulation of reproduction. Brain research, 1364, 116.

RANFT, A., KURZ, J., BECKER, K., DODT, H. U., ZIEGLGANSBERGER, W., RAMMES, G., KOCHS, E. & EDER, M. 2007. Nitrous oxide (N2O) pre- and postsynaptically attenuates NMDA receptor-mediated neurotransmission in the amygdala. Neuropharmacology, 52, 716.

RICHARDSON, K. J. & SHELTON, K. L. 2015. N-methyl-D-aspartate receptor

channel blocker-like discriminative stimulus effects of nitrous oxide gas. The Journal of pharmacology and experimental therapeutics, 352, 156.

SACERDOTE, P., FRANCHI, S., TROVATO, A. E., VALSECCHI, A. E., PANERAI, A. E. & COLLEONI, M. 2008. Transient early expression of TNF-alpha in sciatic nerve and dorsal root ganglia in a mouse model of painful peripheral neuropathy. Neuroscience letters, 436, 210.

SAMACO, R. C., FRYER, J. D., REN, J., FYFFE, S., CHAO, H. T., SUN, Y., GREER, J. J., ZOGHBI, H. Y. & NEUL, J. L. 2008. A partial loss of function allele of methyl-CpG-binding protein 2 predicts a human neurodevelopmental syndrome. Human molecular genetics, 17, 1718.

SANDKUHLER, J. 2009. Models and mechanisms of hyperalgesia and allodynia. Physiological Reviews, 89, 707.

SATO, Y., KOBAYASHI, E., MURAYAMA, T., MISHINA, M. & SEO, N. 2005. Effect of N-methyl-D-aspartate receptor epsilon1 subunit gene disruption of the action of general anesthetic drugs in mice. Anesthesiology, 102, 557.

SAWADA, Y., HOSOKAWA, H., MATSUMURA, K. & KOBAYASHI, S. 2008. Activation of transient receptor potential ankyrin 1 by hydrogen peroxide. The European journal of neuroscience, 27, 1131.

SAWAMURA, S., KINGERY, W. S., DAVIES, M. F., AGASHE, G. S., CLARK, J. D., KOBILKA, B. K., HASHIMOTO, T. & MAZE, M. 2000. Antinociceptive action of nitrous oxide is mediated by stimulation of noradrenergic neurons in the brainstem and activation of alpha(2B) adrenoceptors. Journal of Neuroscience, 20, 9242.

SAWAMURA, S., OBARA, M., TAKEDA, K., MAZE, M. & HANAOKA, K. 2003. Corticotropin-releasing factor mediates the antinociceptive action of nitrous oxide in rats. Anesthesiology, 99, 708.

SAWAMURA, S., OBARA-NAWATA, M., TAKEDA, K. & HANAOKA, K. 2004. General anesthetics inhibit the nitrous-oxide-induced activation of corticotropin releasing factor containing neurons in rats. European Journal of Pharmacology, 503, 49.

SCHMIDT, P. C., RUCHELLI, G., MACKEY, S. C. & CARROLL, I. R. 2013. Perioperative gabapentinoids: choice of agent, dose, timing, and effects on chronic postsurgical pain. Anesthesiology, 119, 1215.

SCHOLZ, J., BROOM, D. C., YOUN, D. H., MILLS, C. D., KOHNO, T., SUTER, M. R., MOORE, K. A., DECOSTERD, I., COGGESHALL, R. E. & WOOLF, C. J. 2005. Blocking caspase activity prevents transsynaptic neuronal apoptosis

and the loss of inhibition in lamina II of the dorsal horn after peripheral nerve injury. The Journal of neuroscience : the official journal of the Society for Neuroscience, 25, 7317.

SCHOLZ, J. & WOOLF, C. J. 2007. The neuropathic pain triad: neurons, immune cells and glia. Nature neuroscience, 10, 1361.

SHAN, X., WANG, L., HOFFMASTER, R. & KRUGER, W. D. 1999. Functional characterization of human methylenetetrahydrofolate reductase in Saccharomyces cerevisiae. The Journal of biological chemistry, 274, 32613.

SHELTON, K. L. & NICHOLSON, K. L. 2010. GABA(A) positive modulator and NMDA antagonist-like discriminative stimulus effects of isoflurane vapor in mice. Psychopharmacology, 212, 559.

SHINGU, K., OSAWA, M., OMATSU, Y., KOMATSU, T., URABE, N. & MORI, K. 1981. Naloxone does not antagonize the anesthetic-induced depression of nociceptor-driven spinal cord response in spinal cats. Acta Anaesthesiologica Scandinavica, 25, 526.

SIMPSON, V. J. & JOHNSON, T. E. 1996. Genetic models in the study of anesthetic drug action. International Review of Neurobiology, Vol 39, 39, 223.

SMITH, R. A., WILSON, M. & MILLER, K. W. 1978. Naloxone has no effect on nitrous oxide anesthesia. Anesthesiology, 49, 6.

SOLT, K. & FORMAN, S. A. 2007. Correlating the clinical actions and molecular mechanisms of general anesthetics. Current Opinion in Anesthesiology, 20, 300.

SONG, X. S., CAO, J. L., XU, Y. B., HE, J. H., ZHANG, L. C. & ZENG, Y. M. 2005. Activation of ERK/CREB pathway in spinal cord contributes to chronic constrictive injury-induced neuropathic pain in rats. Acta Pharmacologica Sinica, 26, 789.

STEVENS, J. E., OSHIMA, E. & MORI, K. 1983. Effects of nitrous oxide on the epileptogenic property of enflurane in cats. British journal of anaesthesia, 55, 145.

STEYAERT, A. & DE KOCK, M. 2012. Chronic postsurgical pain. Current opinion in anaesthesiology, 25, 584.

STIGLITZ, D. K., AMARATUNGE, L. N., KONSTANTATOS, A. H. & LINDHOLM, D. E. 2010. Intraoperative nitrous oxide as a preventive analgesic. Anaesthesia and Intensive Care, 38, 890.

STOVER, J. F., SAKOWITZ, O. W., KROPPENSTEDT, S. N., THOMALE, U. W., KEMPSKI, O. S., FLUGGE, G. & UNTERBERG, A. W. 2004. Differential effects of prolonged isoflurane anesthesia on plasma, extracellular, and CSF glutamate, neuronal activity, 125I-Mk801 NMDA receptor binding, and brain edema in traumatic brain-injured rats. Acta Neurochirurgica, 146, 819.

SUGAI, N., MARUYAMA, H. & GOTO, K. 1982. Effect of nitrous oxide alone or its combination with fentanyl on spinal reflexes in cats. British journal of anaesthesia, 54, 567.

SUKENAGA, N., IKEDA-MIYAGAWA, Y., TANADA, D., TUNETOH, T., NAKANO, S., INUI, T., SATOH, K., OKUTANI, H., NOGUCHI, K. & HIROSE, M. 2016. Correlation Between DNA Methylation of TRPA1 and Chronic Pain States in Human Whole Blood Cells. Pain medicine (Malden, Mass.), 17, 1906.

SURPRENANT, A., HORSTMAN, D. A., AKBARALI, H. & LIMBIRD, L. E. 1992. A point mutation of the alpha 2-adrenoceptor that blocks coupling to potassium but not calcium currents. Science (New York, N.Y.), 257, 977.

SUZUKI, M., TSUEDA, K., LANSING, P. S., TOLAN, M. M., FUHRMAN, T. M., IGNACIO, C. I. & SHEPPARD, R. A. 1999. Small-dose ketamine enhances

morphine-induced analgesia after outpatient surgery. Anesthesia and Analgesia, 89, 98.

SUZUKI, M. M. & BIRD, A. 2008. DNA methylation landscapes: provocative insights from epigenomics. Nature reviews.Genetics, 9, 465.

TAJERIAN, M., ALVARADO, S., MILLECAMPS, M., DASHWOOD, T., ANDERSON, K. M., HAGLUND, L., OUELLET, J., SZYF, M. & STONE, L. S. 2011. DNA methylation of SPARC and chronic low back pain. Molecular pain, 7, 65.

TAMBOLI, R. A., HAJRI, T., JIANG, A., MARKS-SHULMAN, P. A., WILLIAMS, D. B., CLEMENTS, R. H., MELVIN, W., BOWEN, B. P., SHYR, Y., ABUMRAD, N. N. & FLYNN, C. R. 2011. Reduction in inflammatory gene expression in skeletal muscle from Roux-en-Y gastric bypass patients randomized to omentectomy. PloS one, 6, e28577.

TANGA, F. Y., NUTILE-MCMENEMY, N. & DELEO, J. A. 2005. The CNS role of Toll-like receptor 4 in innate neuroimmunity and painful neuropathy. Proceedings of the National Academy of Sciences of the United States of America, 102, 5856.

TODOROVIC, S. M., JEVTOVIC-TODOROVIC, V., MENNERICK, S., PEREZ-

REYES, E. & ZORUMSKI, C. F. 2001. Ca(v)3.2 channel is a molecular substrate for inhibition of T-type calcium currents in rat sensory neurons by nitrous oxide. Molecular pharmacology, 60, 603.

TRANG, T., BEGGS, S., WAN, X. & SALTER, M. W. 2009. P2X4-receptor-mediated synthesis and release of brain-derived neurotrophic factor in microglia is dependent on calcium and p38-mitogen-activated protein kinase activation. The Journal of neuroscience : the official journal of the Society for Neuroscience, 29, 3518.

TSUDA, M., SHIGEMOTO-MOGAMI, Y., KOIZUMI, S., MIZOKOSHI, A., KOHSAKA, S., SALTER, M. W. & INOUE, K. 2003. P2X4 receptors induced in spinal microglia gate tactile allodynia after nerve injury. Nature, 424, 778.

TSUJINO, H., KONDO, E., FUKUOKA, T., DAI, Y., TOKUNAGA, A., MIKI, K., YONENOBU, K., OCHI, T. & NOGUCHI, K. 2000. Activating transcription factor 3 (ATF3) induction by axotomy in sensory and motoneurons: A novel neuronal marker of nerve injury. Molecular and cellular neurosciences, 15, 170.

TURAN, A., BELLEY-COTE, E. P., VINCENT, J., SESSLER, D. I., DEVEREAUX, P. J., YUSUF, S., VAN OOSTVEEN, R., CORDOVA, G., YARED, J. P., YU, H., LEGARE, J. F., ROYSE, A., ROCHON, A., NASR, V., AYAD, S.,

QUANTZ, M., LAMY, A. & WHITLOCK, R. P. 2015. Methylprednisolone Does Not Reduce Persistent Pain after Cardiac Surgery. Anesthesiology, 123, 1404.

ULMANN, L., HATCHER, J. P., HUGHES, J. P., CHAUMONT, S., GREEN, P. J., CONQUET, F., BUELL, G. N., REEVE, A. J., CHESSELL, I. P. & RASSENDREN, F. 2008. Up-regulation of P2X4 receptors in spinal microglia after peripheral nerve injury mediates BDNF release and neuropathic pain. The Journal of neuroscience : the official journal of the Society for Neuroscience, 28, 11263.

ULTENIUS, C., LINDEROTH, B., MEYERSON, B. A. & WALLIN, J. 2006. Spinal NMDA receptor phosphorylation correlates with the presence of neuropathic signs following peripheral nerve injury in the rat. Neuroscience letters, 399, 85.

UNKEL, W. & PETERS, J. 1998. Postoperative nausea and emesis: Mechanisms and treatment. Anasthesiologie Intensivmedizin Notfallmedizin Schmerztherapie, 33, 533.

VALDES-SOCIN, H., RUBIO ALMANZA, M., TOME FERNANDEZ-LADREDA, M., DEBRAY, F. G., BOURS, V. & BECKERS, A. 2014. Reproduction, smell, and neurodevelopmental disorders: genetic defects in different

hypogonadotropic hypogonadal syndromes. Frontiers in endocrinology, 5, 109.

VALLEJO, R., TILLEY, D. M., CEDENO, D. L., KELLEY, C. A., DEMAEGD, M. & BENYAMIN, R. 2016. Genomics of the Effect of Spinal Cord Stimulation on an Animal Model of Neuropathic Pain. Neuromodulation : journal of the International Neuromodulation Society, 19, 576.

VAUGHN, L. K. & PRUHS, R. J. 1995. Strain-Dependent Variability in Nitrous-Oxide Withdrawal Seizure Frequency. Life Sciences, 57, 1125.

VERGE, G. M., MILLIGAN, E. D., MAIER, S. F., WATKINS, L. R., NAEVE, G. S. & FOSTER, A. C. 2004. Fractalkine (CX3CL1) and fractalkine receptor (CX3CR1) distribution in spinal cord and dorsal root ganglia under basal and neuropathic pain conditions. The European journal of neuroscience, 20, 1150.

VERRI, W. A., JR., CUNHA, T. M., PARADA, C. A., POOLE, S., CUNHA, F. Q. & FERREIRA, S. H. 2006. Hypernociceptive role of cytokines and chemokines: targets for analgesic drug development? Pharmacology & therapeutics, 112, 116.

VIET, C. T., YE, Y., DANG, D., LAM, D. K., ACHDJIAN, S., ZHANG, J. & SCHMIDT, B. L. 2011. Re-expression of the methylated EDNRB gene in oral squamous cell carcinoma attenuates cancer-induced pain. Pain, 152, 2323.

VOTTA-VELIS, E. G., PIEGELER, T., MINSHALL, R. D., AGUIRRE, J., BECK-SCHIMMER, B., SCHWARTZ, D. E. & BORGEAT, A. 2013. Regional anaesthesia and cancer metastases: the implication of local anaesthetics. Acta Anaesthesiologica Scandinavica, 57, 1211.

WAN, G., YANG, K., LIM, Q., ZHOU, L., HE, B. P., WONG, H. K. & TOO, H. P. 2010. Identification and validation of reference genes for expression studies in a rat model of neuropathic pain. Biochemical and biophysical research communications, 400, 575.

WANG, H., SUN, H., DELLA PENNA, K., BENZ, R. J., XU, J., GERHOLD, D. L., HOLDER, D. J. & KOBLAN, K. S. 2002. Chronic neuropathic pain is accompanied by global changes in gene expression and shares pathobiology with neurodegenerative diseases. Neuroscience, 114, 529.

WANG, X., FAN, J., ZHANG, M., SUN, Z. & XU, G. 2013. Gene expression changes under cyclic mechanical stretching in rat retinal glial (Muller) cells. PloS one, 8, e63467.

WANG, X. S., MENDOZA, T. R., GAO, S. Z. & CLEELAND, C. S. 1996. The Chinese version of the Brief Pain Inventory (BPI-C): its development and use in a study of cancer pain. Pain, 67, 407.

WANG, Y., LIU, C., GUO, Q. L., YAN, J. Q., ZHU, X. Y., HUANG, C. S. & ZOU, W. Y. 2011. Intrathecal 5-azacytidine inhibits global DNA methylation and methyl- CpG-binding protein 2 expression and alleviates neuropathic pain in rats following chronic constriction injury. Brain research, 1418, 64.

WANG, Z. F., LI, Q., LIU, S. B., MI, W. L., HU, S., ZHAO, J., TIAN, Y., MAO-YING, Q. L., JIANG, J. W., MA, H. J., WANG, Y. Q. & WU, G. C. 2014. Aspirin-triggered Lipoxin A4 attenuates mechanical allodynia in association with inhibiting spinal JAK2/STAT3 signaling in neuropathic pain in rats. Neuroscience, 273, 65.

WATSON, C. J., BAGHDOYAN, H. A., LYDIC, R., HUDETZ, A. & PEARCE, R. 2010. A Neurochemical Perspective on States of Consciousness.

WEI, X. H., NA, X. D., LIAO, G. J., CHEN, Q. Y., CUI, Y., CHEN, F. Y., LI, Y. Y., ZANG, Y. & LIU, X. G. 2013. The up-regulation of IL-6 in DRG and spinal dorsal horn contributes to neuropathic pain following L5 ventral root transection. Experimental neurology, 241, 159.

WEISBERG, I., TRAN, P., CHRISTENSEN, B., SIBANI, S. & ROZEN, R. 1998. A second genetic polymorphism in methylenetetrahydrofolate reductase (MTHFR) associated with decreased enzyme activity. Molecular genetics and

metabolism, 64, 169.

WERNER, M. U. & KONGSGAARD, U. E. 2014. I. Defining persistent post-surgical pain: is an update required? British journal of anaesthesia, 113, 1.

WILDER-SMITH, O. H. G., TASSONYI, E., CRUL, B. J. P. & ARENDT-NIELSEN, L. 2003. Quantitative sensory testing and human surgery - Effects of analgesic management on postoperative neuroplasticity. Anesthesiology, 98, 1214.

WILLER, J. C., BERGERET, S., GAUDY, J. H. & DAUTHIER, C. 1985. Failure of naloxone to reverse the nitrous oxide-induced depression of a brain stem reflex: an electrophysiologic and double-blind study in humans. Anesthesiology, 63, 467.

WILLS, V. L. & HUNT, D. R. 2000. Pain after laparoscopic cholecystectomy. British Journal of Surgery, 87, 273.

WILSON, S. D. & HORNE, D. W. 1986. Effect of nitrous oxide inactivation of vitamin B12 on the levels of folate coenzymes in rat bone marrow, kidney, brain, and liver. Archives of Biochemistry and Biophysics, 244, 248.

WOOD, C. & BIOY, A. 2008. Hypnosis and pain in children. Journal of Pain and Symptom Management, 35, 437.

WOOLF, C. J. 2011. Central sensitization: implications for the diagnosis and treatment of pain. Pain, 152, S2.

WOUTERS, J., STAS, M., GOVAERE, O., VAN DEN EYNDE, K., VANKELECOM, H. & VAN DEN OORD, J. J. 2012. Gene expression changes in melanoma metastases in response to high-dose chemotherapy during isolated limb perfusion. Pigment cell & melanoma research, 25, 454.

WU, Y. P., CAO, C., WU, Y. F., LI, M., LAI, T. W., ZHU, C., WANG, Y., YING, S. M., CHEN, Z. H., SHEN, H. H. & LI, W. 2017. Activating transcription factor 3 represses cigarette smoke-induced IL6 and IL8 expression via suppressing NF-kappaB activation. Toxicology letters, 270, 17.

XING, G. G., LIU, F. Y., QU, X. X., HAN, J. S. & WAN, Y. 2007. Long-term synaptic plasticity in the spinal dorsal horn and its modulation by electroacupuncture in rats with neuropathic pain. Experimental neurology, 208, 323.

XU, J. Y. & CHEN, C. 2015. Endocannabinoids in synaptic plasticity and neuroprotection. The Neuroscientist : a review journal bringing neurobiology, neurology and psychiatry, 21, 152.

YANG, J. C., CLARK, W. C. & NGAI, S. H. 1980. Antagonism of nitrous oxide analgesia by naloxone in man. Anesthesiology, 52, 414.

YANG, J. C., CLARK, W. C. & NGAI, S. H. 1980. Antagonism of nitrous oxide analgesia by naloxone in man. Anesthesiology, 52, 414.

YANG, Y. K., LU, X. B., WANG, Y. H., YANG, M. M. & JIANG, D. M. 2014. Identification crucial genes in peripheral neuropathic pain induced by spared nerve injury. European review for medical and pharmacological sciences, 18, 2152.

YU, E. H. Y., TRAN, D. H. D., LAM, S. W. & IRWIN, M. G. 2016. Remifentanil tolerance and hyperalgesia: short-term gain, long-term pain? Anaesthesia, 71, 1347.

YU, L., YANG, F., LUO, H., LIU, F. Y., HAN, J. S., XING, G. G. & WAN, Y. 2008. The role of TRPV1 in different subtypes of dorsal root ganglion neurons in rat chronic inflammatory nociception induced by complete Freund's adjuvant. Molecular pain, 4, 61.

YU, L. N., ZHOU, X. L., YU, J., HUANG, H., JIANG, L. S., ZHANG, F. J., CAO, J. L. & YAN, M. 2012. PI3K contributed to modulation of spinal nociceptive information related to ephrinBs/EphBs. PloS one, 7, e40930.

ZHANG, C., DAVIES, M. F., GUO, T. Z. & MAZE, M. 1999. The analgesic action of nitrous oxide is dependent on the release of norepinephrine in the dorsal horn

of the spinal cord. Anesthesiology, 91, 1401.

ZHANG, H. H., HU, J., ZHOU, Y. L., QIN, X., SONG, Z. Y., YANG, P. P., HU, S., JIANG, X. & XU, G. Y. 2015. Promoted Interaction of Nuclear Factor-kappaB With Demethylated Purinergic P2X3 Receptor Gene Contributes to Neuropathic Pain in Rats With Diabetes. Diabetes, 64, 4272.

ZHANG, Z. B., RUAN, C. C., CHEN, D. R., ZHANG, K., YAN, C. & GAO, P. J. 2016. Activating transcription factor 3 SUMOylation is involved in angiotensin II-induced endothelial cell inflammation and dysfunction. Journal of Molecular and Cellular Cardiology, 92, 149.

ZHAO, Y., WU, X., QIAN, L., GUO, L., LIAO, J. & WU, X. 2017. Activating transcription factor 3 protects mice against pseudomonas aeruginosa-induced acute lung injury by interacting with lipopolysaccharide binding protein. Molecular immunology, 90, 27.

ZHOU, X. L., YU, L. N., WANG, Y., TANG, L. H., PENG, Y. N., CAO, J. L. & YAN, M. 2014. Increased methylation of the MOR gene proximal promoter in primary sensory neurons plays a crucial role in the decreased analgesic effect of opioids in neuropathic pain. Molecular pain, 10, 51.

ZHUANG, Z. Y., GERNER, P., WOOLF, C. J. & JI, R. R. 2005. ERK is sequentially

activated in neurons, microglia, and astrocytes by spinal nerve ligation and contributes to mechanical allodynia in this neuropathic pain model. Pain, 114, 149.

ZHUANG, Z. Y., GERNER, P., WOOLF, C. J. & JI, R. R. 2005. ERK is sequentially activated in neurons, microglia, and astrocytes by spinal nerve ligation and contributes to mechanical allodynia in this neuropathic pain model. Pain, 114, 149.

ZHUO, M. 2011. Cortical plasticity as a new endpoint measurement for chronic pain. Molecular pain, 7, 54.

ZILLER, M. J., GU, H., MULLER, F., DONAGHEY, J., TSAI, L. T., KOHLBACHER, O., DE JAGER, P. L., ROSEN, E. D., BENNETT, D. A., BERNSTEIN, B. E., GNIRKE, A. & MEISSNER, A. 2013. Charting a dynamic DNA methylation landscape of the human genome. Nature, 500, 477.

ZMUDA, E. J., VIAPIANO, M., GREY, S. T., HADLEY, G., GARCIA-OCANA, A. & HAI, T. 2010. Deficiency of Atf3, an adaptive-response gene, protects islets and ameliorates inflammation in a syngeneic mouse transplantation model. Diabetologia, 53, 1438.

ZORUMSKI, C. F., NAGELE, P., MENNERICK, S. & CONWAY, C. R. 2015.

Treatment-Resistant Major Depression: Rationale for NMDA Receptors as Targets and Nitrous Oxide as Therapy. Frontiers in psychiatry, 6, 172.

ZUNIGA, J., JOSEPH, S. & KNIGGE, K. 1987. Nitrous oxide analgesia: partial antagonism by naloxone and total reversal after periaqueductal gray lesions in the rat. European journal of pharmacology, 142, 51.

ZUNIGA, J. R., JOSEPH, S. A. & KNIGGE, K. M. 1987. The effects of nitrous oxide on the central endogenous pro-opiomelanocortin system in the rat. Brain research, 420, 57.

ZUNIGA, J. R., KNIGGE, K. K. & JOSEPH, S. A. 1986. Central beta-endorphin release and recovery after exposure to nitrous oxide in rats. Journal of oral and maxillofacial surgery : official journal of the American Association of Oral and Maxillofacial Surgeons, 44, 714.

PART V APPENDIX

Appendix 1. Significantly enriched transcription factors among nitrous oxide-sensitive differentially expressed genes

Fraction	motif	TF	q-value	N_2/Sham	N_2O/Sham	N_2/CCI	N_2O/CCI
0.256039	ARI5B_MOUSE.H10MO.C	Arid5b	0.04872	9.02208	9.59790	9.93324	9.35535
0.676329	TBX20_MOUSE.H10MO.C	Tbx20	0.04785	0.00000	0.01120	0.00000	0.00000
0.502415	NR6A1_MOUSE.H10MO.B	Nr6a1	0.04574	1.43352	1.49217	1.77941	1.49423
0.690821	RFX1_MOUSE.H10MO.C	Rfx1	0.04125	3.12675	3.41932	3.35177	3.37847
0.840580	PLAG1_MOUSE.H10MO.D	Plag1	0.03620	1.33979	1.38968	1.35726	1.35839
0.425121	NFAC4_MOUSE.H10MO.C	Nfatc4	0.03180	0.32934	0.38909	0.33667	0.50387
0.712560	IKZF1_MOUSE.H10MO.C	Ikzf1	0.02948	1.73225	1.58072	3.81560	3.53290
0.241546	PIT1_MOUSE.H10MO.C	Pou1f1	0.02770	0.01234	0.00000	0.02004	0.01247
0.205314	CDX1_MOUSE.H10MO.C	Cdx1	0.02325	0.00000	0.03226	0.04134	0.02577
0.178744	MSX3_MOUSE.H10MO.D	Msx3	0.01768	0.02318	0.01648	0.03926	0.04221
0.550725	ELK3_MOUSE.H10MO.D	Elk3	0.01485	3.48945	3.42861	4.88107	4.42880
0.142512	HNF1A_MOUSE.H10MO.A	Hnf1a	0.01390	0.01653	0.00507	0.02016	0.00418
0.514493	ETV5_MOUSE.H10MO.D	Etv5	0.01358	12.3681	12.6701	13.6340	13.1933
0.403382	PRGR_MOUSE.H10MO.S	Pgr	0.01063	3.46651	2.90296	3.13554	3.02460
0.746377	CTCF_MOUSE.H10MO.A	Ctcf	0.01008	16.9265	16.8335	17.9931	17.8484
0.504831	PEBB_MOUSE.H10MO.C	Cbfb	0.00986	10.5172	10.0886	13.3033	12.4894
0.608696	HEY2_MOUSE.H10MO.D	Hey2	0.00825	8.75459	7.79499	7.67054	7.93660

0.763285	ZFX_MOUSE.H10MO.C	Zfx	0.00784	5.31905	5.33871	5.22969	5.02074
0.265700	GATA4_MOUSE.H10MO.B	Gata4	0.00743	0.00887	0.00000	0.00000	0.00000
0.678744	NR0B1_MOUSE.H10MO.D	Nr0b1	0.00631	0.03092	0.02194	0.07660	0.11586
0.695652	MAFA_MOUSE.H10MO.D	Mafa	0.00385	7.20154	9.99260	7.24799	8.95528
0.369565	IRF9_MOUSE.H10MO.C	Irf9	0.00366	11.0934	10.6792	13.7586	12.1787
0.458937	NR2E3_MOUSE.H10MO.C	Nr2e3	0.00329	0.07093	0.05848	0.09765	0.20521
0.809179	ZIC1_MOUSE.H10MO.B	Zic1	0.00289	13.3918	13.8674	13.4472	14.8173
0.176329	CDC5L_MOUSE.H10MO.D	Cdc5l	0.00284	32.3702	31.9459	31.5090	31.5402
0.384058	FOXO4_MOUSE.H10MO.C	Foxo4	0.00205	17.7728	17.6862	17.0111	17.435
0.214976	PO2F2_MOUSE.H10MO.B	Pou2f2	0.00188	1.42867	1.34416	3.17440	2.78394
0.164251	ALX1_MOUSE.H10MO.B	Alx1	0.00093	0.00000	0.00000	0.00000	0.00000
0.502415	RUNX3_MOUSE.H10MO.B	Runx3	0.00083	0.02061	0.00000	0.06133	0.08034
0.741546	REST_MOUSE.H10MO.A	Rest	0.00062	3.04484	3.10116	3.53656	2.99255
0.700483	AP2D_MOUSE.H10MO.D	Tfap2d	0.00060	0.00000	0.00000	0.00000	0.00000
0.289855	HIF1A_MOUSE.H10MO.A	Hif1a	0.00026	38.8596	38.0828	43.8090	39.7680
0.328502	MAX_MOUSE.H10MO.A	Max	0.00010	32.4092	31.4256	32.2940	35.2969
0.712560	RXRG_MOUSE.H10MO.C	Rxrg	9.00E-05	4.96248	4.41150	3.77372	4.39921
0.169082	LHX3_MOUSE.H10MO.C	Lhx3	8.61E-05	0.66514	0.45218	0.58304	0.56100
0.649758	MYOG_MOUSE.H10MO.C	Myog	4.69E-05	0.00000	0.02768	0.01779	0.01115
0.637681	HTF4_MOUSE.H10MO.C	Tcf12	3.71E-05	14.9983	14.6833	14.5231	15.3693
0.736715	HEN1_MOUSE.H10MO.C	Nhlh1	3.51E-05	0.27960	0.45199	0.19388	0.43489
0.277778	EVI1_MOUSE.H10MO.B	Mecom	2.34E-05	3.14068	3.11769	2.54744	2.70306

0.340580	HXD10_MOUSE.H10MO.D	Hoxd10	1.04E-05	27.0465	25.4409	25.7274	24.9084
0.463768	NRF1_MOUSE.H10MO.A	Nrf1	9.28E-06	4.27258	4.39387	5.11615	5.21437
0.396135	ELK4_MOUSE.H10MO.B	Elk4	8.28E-06	4.59070	4.92844	5.08400	5.09923
0.154589	MEF2C_MOUSE.H10MO.B	Mef2c	6.38E-06	4.63603	4.87615	5.76377	5.77446
0.536232	RUNX2_MOUSE.H10MO.B	Runx2	6.33E-06	0.31924	0.39408	0.30159	0.32824
0.736715	SMAD1_MOUSE.H10MO.D	Smad1	1.75E-06	9.91493	10.2449	11.1420	10.4436
0.444444	ERG_MOUSE.H10MO.A	Erg	1.35E-06	4.14290	4.77704	4.04282	3.97320
0.550725	SMAD4_MOUSE.H10MO.C	Smad4	1.05E-06	15.9724	15.5427	16.0818	16.5526
0.323671	FOXC1_MOUSE.H10MO.C	Foxc1	1.01E-06	1.73044	1.91896	2.02407	2.08295
0.567633	MXI1_MOUSE.H10MO.C	Mxi1	6.10E-07	29.6523	28.7762	29.3427	29.1707
0.466184	MYC_MOUSE.H10MO.A	Myc	2.54E-07	1.92893	1.70057	3.66323	2.97326
0.205314	TEF_MOUSE.H10MO.D	Tef	2.37E-07	53.9717	58.5285	55.8915	58.7207
0.780193	KLF6_MOUSE.H10MO.D	Klf6	2.27E-07	2.97322	3.30653	3.84323	3.99098
0.429952	FOXA1_MOUSE.H10MO.B	Foxa1	1.30E-07	0.00000	0.03137	0.00000	0.01105
0.671498	MYF6_MOUSE.H10MO.C	Myf6	6.57E-08	0.00000	0.00000	0.00000	0.01722
0.654589	KLF3_MOUSE.H10MO.D	Klf3	5.39E-08	7.65265	6.63239	8.11603	7.50887
0.620773	ELF3_MOUSE.H10MO.D	Elf3	3.04E-08	0.00000	0.03622	0.01088	0.00000
0.734300	RXRA_MOUSE.H10MO.C	Rxra	2.12E-08	18.6930	18.8472	19.0367	17.9222
0.439614	FOXA3_MOUSE.H10MO.C	Foxa3	1.58E-08	0.15279	0.13263	0.24818	0.23152
0.403382	GCR_MOUSE.H10MO.S	Nr3c1	1.13E-08	18.5905	18.0477	16.9697	16.8552
0.403382	GCR_MOUSE.H10MO.S	Nr3c1	1.13E-08	22.1050	20.2019	19.2332	19.1577
0.710145	MYOD1_MOUSE.H10MO.C	Myod1	1.11E-08	0.12050	0.09585	0.11838	0.05712

0.241546	PROP1_MOUSE.H10MO.D	Prop1	8.86E-09	0.00000	0.00000	0.00000	0.00000
0.171498	ZFHX3_MOUSE.H10MO.D	Zfhx3	5.12E-09	1.16202	1.25390	1.44684	1.27027
0.357488	NANOG_MOUSE.H10MO.A	Nanog	5.01E-09	0.00000	0.00000	0.01040	0.00000
0.222222	MEF2D_MOUSE.H10MO.C	Mef2d	4.73E-09	22.1460	22.6896	21.6869	23.1072
0.620773	PRDM1_MOUSE.H10MO.A	Prdm1	2.34E-09	0.13179	0.09427	0.24563	0.16597
0.637681	SMAD3_MOUSE.H10MO.C	Smad3	1.81E-09	3.22522	3.14552	3.40939	3.49086
0.514493	FEV_MOUSE.H10MO.C	Fev	1.31E-09	0.07960	0.04850	0.08060	0.01278
0.642512	SMAD2_MOUSE.H10MO.D	Smad2	5.84E-10	9.69274	10.0325	9.95566	10.2836
0.422705	ELK1_MOUSE.H10MO.B	Elk1	3.62E-10	9.92604	10.0281	11.3815	11.6909
0.239130	FOXP3_MOUSE.H10MO.D	Foxp3	3.44E-10	0.68792	0.58801	0.78943	0.69129
0.821256	KLF1_MOUSE.H10MO.C	Klf1	5.57E-11	0.49233	0.49932	0.55166	0.60516
0.202899	PO3F2_MOUSE.H10MO.D	Pou3f2	4.74E-11	12.0087	11.5671	10.8275	11.4345
0.425121	ELF5_MOUSE.H10MO.D	Elf5	4.68E-11	0.25884	0.27148	0.19030	0.22163
0.342995	FOXA2_MOUSE.H10MO.B	Foxa2	4.14E-11	0.01059	0.05518	0.03002	0.02209
0.632850	EGR3_MOUSE.H10MO.D	Egr3	1.54E-11	0.91795	1.29380	0.79818	1.02654
0.516908	UBIP1_MOUSE.H10MO.D	Ubp1	1.36E-11	22.3939	23.5119	23.9579	22.5487
0.644928	E2F1_MOUSE.H10MO.A	E2f1	1.24E-11	4.04758	4.33441	4.94665	4.83045
0.350242	HXC6_MOUSE.H10MO.D	Hoxc6	4.95E-12	8.78232	7.92331	9.87306	9.81940
0.613527	STAT3_MOUSE.H10MO.B	Stat3	3.99E-12	30.9625	30.4769	43.7674	39.7823
0.227053	MEF2A_MOUSE.H10MO.B	Mef2a	1.89E-12	13.0488	13.1492	14.2723	13.9348
0.205314	CDX2_MOUSE.H10MO.C	Cdx2	7.56E-13	0.00000	0.00000	0.03442	0.00000
0.657005	ARNT2_MOUSE.H10MO.D	Arnt2	2.60E-13	32.0113	33.3678	30.9106	31.8179

0.246377	HMGA1_MOUSE.H10MO.D	Hmga1	2.31E-13	176.609	162.335	167.283	172.926
0.623188	GABP1_MOUSE.H10MO.C	Gabpb1	1.95E-13	7.64983	7.52386	8.20102	8.57115
0.632850	GABPA_MOUSE.H10MO.A	Gabpa	1.40E-13	6.81241	7.18930	7.92446	7.62051
0.618357	EHF_MOUSE.H10MO.A	Ehf	1.33E-13	0.01998	0.00000	0.00000	0.00000
0.277778	ONEC2_MOUSE.H10MO.D	Onecut2	6.38E-14	0.39535	0.56969	0.43622	0.26247
0.449275	FOXO3_MOUSE.H10MO.B	Foxo3	2.52E-14	13.3631	13.7506	13.6999	14.0902
0.792271	KLF4_MOUSE.H10MO.C	Klf4	9.78E-15	2.47071	2.25028	2.60453	2.84421
0.657005	GCR_MOUSE.H10MO.C	Nr3c1	2.78E-15	18.5905	18.0477	16.9697	16.8552
0.657005	GCR_MOUSE.H10MO.C	Nr3c1	2.78E-15	22.1050	20.2019	19.2332	19.1577
0.555556	IRF2_MOUSE.H10MO.C	Irf2	6.78E-16	11.7372	10.2247	11.3866	12.2304
0.770531	ELF2_MOUSE.H10MO.C	Elf2	5.13E-16	11.0557	10.3840	11.6165	11.4226
0.507246	IRF7_MOUSE.H10MO.C	Irf7	3.44E-16	3.41984	3.88739	3.92000	3.47615
0.437198	FOXD3_MOUSE.H10MO.D	Foxd3	3.25E-16	2.87120	2.31696	2.00279	2.51778
0.640097	NFYA_MOUSE.H10MO.D	Nfya	6.77E-17	5.53683	4.91463	7.10354	5.74073
0.434783	FOXJ2_MOUSE.H10MO.C	Foxj2	4.45E-17	7.18814	7.38185	7.64568	6.93043
0.801932	EGR2_MOUSE.H10MO.C	Egr2	4.33E-17	0.01001	0.05628	0.03939	0.04637
0.637681	ELF1_MOUSE.H10MO.B	Elf1	2.71E-17	4.42639	4.50306	5.72196	5.22384
0.698068	FLI1_MOUSE.H10MO.A	Fli1	1.54E-17	2.18380	2.04033	3.99383	2.99127
0.224638	NKX31_MOUSE.H10MO.C	Nkx3-1	6.65E-18	0.15049	0.33991	0.21132	0.14354
0.830918	EGR4_MOUSE.H10MO.D	Egr4	3.38E-18	0.08307	0.21396	0.42203	0.21504
0.814010	TFE2_MOUSE.H10MO.A	Tcf3	2.96E-18	8.89525	8.58655	9.77540	9.54925
0.867150	KLF15_MOUSE.H10MO.D	Klf15	1.29E-18	7.06205	7.87000	7.54050	8.39886

0.681159	EGR1_MOUSE.H10MO.A	Egr1	2.10E-19	6.57053	7.10668	8.94657	8.07585
0.821256	SP2_MOUSE.H10MO.C	Sp2	1.56E-19	6.16842	6.42795	6.73224	6.41250
0.731884	ETV4_MOUSE.H10MO.B	Etv4	5.49E-20	6.43609	5.80415	5.88882	5.68570
0.821256	SRBP2_MOUSE.H10MO.B	Srebf2	4.25E-20	45.4352	44.8390	44.0486	44.3666
0.640097	ETS1_MOUSE.H10MO.B	Ets1	1.01E-20	4.96770	4.52966	4.90357	5.10549
0.753623	SPI1_MOUSE.H10MO.A	Spi1	8.65E-21	4.63653	4.82476	13.7204	12.0679
0.521739	FOXO1_MOUSE.H10MO.C	Foxo1	4.44E-21	5.81823	6.60318	5.88550	6.99088
0.594203	IRF1_MOUSE.H10MO.C	Irf1	2.02E-22	2.70110	2.81850	3.87515	3.59927
0.654589	SPIB_MOUSE.H10MO.B	Spib	1.85E-22	0.10110	0.04932	0.07447	0.09310
0.753623	ETS2_MOUSE.H10MO.C	Ets2	1.14E-22	11.0857	11.9168	13.3950	12.7324
0.828502	SP4_MOUSE.H10MO.D	Sp4	5.25E-23	3.76684	4.09776	4.43558	3.72511
0.519324	FOXJ3_MOUSE.H10MO.S	Foxj3	5.12E-23	18.6611	18.4368	17.7291	18.2958
0.181159	TBP_MOUSE.H10MO.C	Tbp	3.97E-23	7.76776	7.35905	7.56931	7.99425
0.463768	FOXF1_MOUSE.H10MO.D	Foxf1	2.60E-23	0.91425	0.77190	0.79964	0.74067
0.516908	FOXM1_MOUSE.H10MO.D	Foxm1	1.07E-23	1.36591	1.44714	2.74142	2.36971
0.840580	E2F6_MOUSE.H10MO.A	E2f6	1.66E-24	22.1729	21.7485	22.6060	21.9942
0.678744	IRF5_MOUSE.H10MO.D	Irf5	9.19E-25	5.78213	6.26597	11.0049	9.85624
0.801932	E2F4_MOUSE.H10MO.C	E2f4	1.11E-25	17.2434	16.7950	18.7095	18.0164
0.657005	IRF3_MOUSE.H10MO.C	Irf3	3.52E-26	26.0503	22.8005	26.5443	24.8185
0.698068	IRF8_MOUSE.H10MO.D	Irf8	1.32E-28	5.05749	5.71808	15.8936	13.8399
0.487923	FOXJ3_MOUSE.H10MO.A	Foxj3	6.18E-31	18.6611	18.4368	17.7291	18.2958
0.908213	PURA_MOUSE.H10MO.D	Pura	6.01E-31	30.9938	32.3783	33.5288	29.2456

0.673913	EPAS1_MOUSE.H10MO.D	Epas1	5.46E-31	66.2661	69.8308	66.3898	67.1890
0.886473	SP1_MOUSE.H10MO.S	Sp1	1.17E-31	5.98500	5.97818	6.54885	5.79186
0.487923	FUBP1_MOUSE.H10MO.D	Fubp1	2.67E-34	22.2332	21.3640	24.5641	21.6392
0.942029	MAZ_MOUSE.H10MO.D	Maz	2.42E-35	46.8118	49.4945	48.9226	50.7451
0.702899	STAT2_MOUSE.H10MO.B	Stat2	2.25E-37	14.1095	13.4814	17.5381	15.9360
0.449275	ARI3A_MOUSE.H10MO.D	Arid3a	9.54E-40	1.63253	1.37340	1.88491	1.65878
0.893720	SP3_MOUSE.H10MO.B	Sp3	2.25E-40	15.8647	14.6358	15.4297	15.9981
0.867150	RREB1_MOUSE.H10MO.D	Rreb1	8.95E-42	1.14037	1.20566	1.41914	1.40838
0.828502	WT1_MOUSE.H10MO.D	Wt1	4.35E-42	0.10583	0.09062	0.07556	0.08772
0.920290	SP1_MOUSE.H10MO.A	Sp1	5.11E-43	5.98500	5.97818	6.54885	5.79186
0.874396	IRF4_MOUSE.H10MO.C	Irf4	3.02E-60	0.13893	0.21040	0.19779	0.19812
0.898551	STAT1_MOUSE.H10MO.A	Stat1	5.19E-64	18.9949	20.5911	24.0655	22.0935

Appendix 2. Gene otology analysis of differentially expressed genes between N_2/CCI and N_2O/CCI

TERM	COUNT	%	PVALUE	GENES	FOLD ENRICH-MENT	BONFER RONI	BENJAM INI	FDR
GO:0015671~OXYGEN TRANSPORT	4	4.938	$5.63E^{-05}$	LOC689064, HBA2, HBA1, HBB	51.956	0.032	0.032	0.083
GO:0030890~POSITIVE REGULATION OF B CELL PROLIFERATION	4	4.938	$7.89E^{-04}$	CD38, PTPRC, CARD11, CD74	21.7489	0.370	0.206	1.155
GO:0034097~RESPONSE TO CYTOKINE	5	6.173	$8.13E^{-04}$	CD38, CORO1A, SERPINA3N, PTGS2, SOCS3	11.808	0.378	0.147	1.189
GO:0010942~POSITIVE REGULATION OF CELL DEATH	4	4.938	0.002	PTGS2, HBA2, HBA1, HBB	17.319	0.593	0.201	2.233

GO:0032355~RESPONSE TO ESTRADIOL	6	7.408	0.002	CD38, ARPC1B, PTGS2, SOCS3, VIM, HBA2	6.979	0.608	0.171	2.327
GO:0030728~OVULATION	3	3.704	0.003	TNFAIP6, PTGS2, IL4R	38.967	0.778	0.222	3.721
GO:0042744~HYDROGEN PEROXIDE CATABOLIC PROCESS	3	3.704	0.003	HBA2, HBA1, HBB	38.967	0.778	0.222	3.721
GO:0042102~POSITIVE REGULATION OF T CELL PROLIFERATION	4	4.938	0.003	PTPRC, ITGAL, CARD11, CORO1A	14.170	0.798	0.204	3.941
GO:0048821~ERYTHROCYTE DEVELOPMENT	3	3.704	0.005	HBA2, HBA1, HBB	29.225	0.931	0.284	6.514
GO:0007159~LEU	3	3.704	0.005	PTPRC,	28.056	0.945	0.276	7.043

KOCYTE CELL-CELL ADHESION				ITGAL, ITGAM				
GO:0045776~NEGATIVE REGULATION OF BLOOD PRESSURE	3	3.704	0.012	HBA2, HBA1, APLN	17.535	0.999	0.517	16.722
GO:0051930~REGULATION OF SENSORY PERCEPTION OF PAIN	3	3.704	0.015	HBA2, HBA1, FCGR3A	15.941	1.000	0.548	19.733
GO:0010332~RESPONSE TO GAMMA RADIATION	3	3.704	0.016	PTPRC, APOBEC1, SOCS3	15.248	1.000	0.547	21.286
GO:0010043~RESPONSE TO ZINC ION	3	3.704	0.019	APOBEC1, VIM, MT1	14.028	1.000	0.576	24.470
GO:0055114~OXIDATION-	8	9.876543	0.019775	LOC681458, PTGS2,	2.873	1.000	0.566	25.470

REDUCTION PROCESS				CH25H, ALOX5AP, RRM2, KMO, CP, ALDH1L2				
GO:0006955~IMMUNE RESPONSE	5	6.17284	0.026358	RT1-A2, RT1-CE16, IL4R, WAS, CD74	4.378	1.000	0.647	32.507
GO:0032570~RESPONSE TO PROGESTERONE	3	3.703704	0.026564	CD38, SOCS3, NR1H3	11.690	1.000	0.626	32.716
GO:0006935~CHEMOTAXIS	3	3.703704	0.029932	C3AR1, HMGB2, CMKLR1	10.959	1.000	0.649	36.062
GO:0032496~RESPONSE TO LIPOPOLYSACCHARIDE	5	6.17284	0.030647	HMGB2, SERPINA3N, PTGS2, SOCS3, CSF2RB	4.175	1.000	0.636	36.753
GO:0006954~INFLAMMATORY RESPONSE	5	6.17284	0.036847	C3AR1, SERPINA3N, PTGS2, IL4R,	3.936	1.000	0.685	42.452

				PARP4				
GO:0006265~DNA TOPOLOGICAL CHANGE	2	2.469136	0.041419	HMGB2, TOP2A	46.760	1.000	0.710	46.345
GO:0045577~REGULATION OF B CELL DIFFERENTIATION	2	2.469136	0.041419	PTPRC, CARD11	46.760	1.000	0.710	46.345
GO:0042542~RESPONSE TO HYDROGEN PEROXIDE	3	3.703704	0.042942	HBA2, HBA1, HBB	8.992	1.000	0.710	47.586
GO:0045059~POSITIVE THYMIC T CELL SELECTION	2	2.469136	0.049498	PTPRC, CD74	38.967	1.000	0.741	52.629
GO:0050798~ACTIVATED T CELL PROLIFERATION	2	2.469136	0.049498	ITGAL, ITGAM	38.967	1.000	0.741	52.629

Appendix 3. Methylated DNA immunoprecipitation sequencing-sequencing reads statistics

Sample Name	Read length (bp)	Clean Reads	Clean bases	Q20 (%)	GC (%)
N_2/CCI-1	100	43352954	4335295400	99.18;98.26	49.97
N_2/CCI-2	100	43263852	4326385200	99.17;98.03	50.18
N_2/CCI-3	100	51536562	5153656200	99.12;98.05	49.88
N_2O/CCI-1	100	59262074	5926207400	99.12;98.09	50.01
N_2O/CCI-2	100	69690558	6969055800	99.19;98.31	50.20
N_2O/CCI-3	100	50221354	5022135400	99.19;98.32	50.16
N_2O/Sham-1	100	44201536	4420153600	99.14;98.22	49.84
N_2O/Sham-2	100	58684116	5868411600	99.21;98.50	50.16
N_2O/Sham-3	100	55555664	5555566400	99.19;98.32	50.10
N_2/Sham-1	100	61326086	6132608600	99.18;98.38	49.92
N_2/Sham-2	100	70528172	7052817200	99.19;98.25	49.98
N_2/Sham-3	100	55019848	5501984800	99.19;98.32	49.82

Appendix 4. List of activating transcription factor 3 (Atf3) motif enriched genes

GENE	N_2/Sham	N_2O/Sham	N_2/CCI	N_2O/CCI
AABR06031050.1	0.9578	1.9436	2.1268	1.9436
AABR06089048.1	63.6120	82.2380	89.7470	82.2381
AABR06097983.1	2.0005	0.9498	1.7877	0.9499
AABR06098457.2	5.7703	4.5805	6.2011	4.5805
Abca1	3.9959	4.1798	4.7923	4.1798
Abcd1	4.5629	5.5500	6.1152	5.5500
Abcg2	18.4400	15.7960	14.1070	15.7960
Acsl5	19.8160	23.8320	25.5510	23.8318
Adcy4	1.5997	1.8080	2.0678	1.8080
Aif1	35.2200	85.3650	95.1800	85.3648
Alox5ap	2.9601	5.1609	7.6926	5.1609
Anxa3	53.5890	138.2700	164.4300	138.2660
Aoah	0.1909	0.8840	0.7501	0.8840
Apln	25.6730	23.8720	17.9510	23.8717
Arhgap19	2.6532	2.6907	3.4229	2.6907
Asf1b	0.2004	2.3083	2.5884	2.3083
Aspm	0.3295	0.8762	0.9715	0.8762
Atf3	0.6761	8.3258	16.0130	8.3258
Aurkb	1.8176	4.2858	5.0552	4.2858
B3gnt9	2.2777	2.4357	1.6465	2.4357
B4galt1	1.5352	2.7105	2.7858	2.7105
Bdnf	1.3471	1.8295	2.0355	1.8295
Bin2	7.1622	14.6910	17.7710	14.6911
Blnk	4.0202	8.7166	10.8370	8.7166
Brca1	0.5928	0.7355	0.9317	0.7355
C1rl	0.6768	1.6266	1.8010	1.6266
C1s	4.9530	5.9270	7.1132	5.9270
C5ar1	1.7418	4.4429	5.5528	4.4429
C5ar2	0.9591	2.6447	2.4278	2.6447
Calca	98.2430	84.1750	89.2006	84.1748
Card9	3.3556	6.1878	6.5744	6.1878
Casp8	0.9232	1.4805	1.6135	1.4805
Ccl2	0.4913	5.8003	7.9619	5.8003
Ccna2	0.7686	4.0064	5.4838	4.0064

Ccr5	9.1380	13.0190	14.1657	13.0186
Cd180	2.5970	5.7947	7.1865	5.7947
Cd1d1	1.1764	1.5350	1.8841	1.5350
Cd300a	1.5398	3.7414	5.0113	3.7414
Cd33	8.1037	17.4993	20.7951	17.4993
Cd37	6.9309	11.4199	13.0759	11.4199
Cdc20	1.6035	4.6280	4.5413	4.6280
Cdc45	0.7862	1.2988	1.6082	1.2988
Cdca2	0.2851	0.5974	0.9046	0.5974
Cdca7l	1.1797	1.9017	2.1449	1.9017
Cdca8	1.7548	3.8253	4.6386	3.8253
Cebpb	11.0015	18.0718	17.1933	18.0718
Cenpa	0.1548	2.0782	1.8810	2.0782
Cenpe	0.6557	1.0107	1.2875	1.0107
Cenpw	0.1502	0.9867	0.9927	0.9867
Cfh	12.4561	19.1903	21.8306	19.1903
Ch25h	2.3831	4.6259	7.8207	4.6259
Chaf1a	4.1881	4.4184	5.0578	4.4184
Cks1b	2.7358	4.0312	4.2130	4.0312
Cmtm3	2.5614	3.8688	4.3503	3.8688
Cmtm6	7.2737	10.1567	10.9892	10.1567
Colgalt1	11.3928	15.9317	18.0170	15.9317
Creld2	10.5358	13.8733	14.9025	13.8733
Crh	0.6698	2.2762	2.7490	2.2762
Csf2ra	2.6923	4.3507	5.7913	4.3507
Csf3r	1.5551	4.4897	5.2367	4.4897
Ddx39a	10.0248	11.1397	12.2845	11.1397
Dguok	21.8623	17.6417	16.2570	17.6417
Dna2	0.7081	0.9253	1.1608	0.9253
Dnase1l1	6.9117	7.6209	8.4636	7.6209
Dock2	1.2763	2.8105	3.3873	2.8105
Dock8	1.4788	3.3296	4.1711	3.3296
Dsn1	0.9193	1.5799	1.9278	1.5799
Dtl	0.1982	0.6991	0.8774	0.6991
E2f2	0.9961	1.9729	1.7962	1.9729
Ebf2	2.0251	2.8309	2.4825	2.8309
Ebf3	11.6086	14.1970	12.0340	14.1970

Egr1	6.5705	8.0759	8.9466	8.0759
Elk3	3.4895	4.4288	4.8811	4.4288
Erp29	76.2282	93.3062	97.2308	93.3062
Exo5	3.0533	4.4403	4.8604	4.4403
F10	0.2654	1.3159	1.5224	1.3159
Fabp7	274.9420	273.7100	315.0390	273.7100
Fam64a	0.5622	1.9643	2.9387	1.9643
Fam96a	15.4034	19.3378	21.2382	19.3378
Fancd2	0.8905	1.4786	1.6521	1.4786
Fgl2	5.9814	6.8298	8.3632	6.8298
Fhod1	2.2354	3.4484	4.1531	3.4484
Fli1	2.1838	2.9913	3.9938	2.9913
Fosb	0.2617	0.6857	1.0566	0.6857
Frmpd4	6.2720	6.3861	5.7316	6.3861
Gareml	7.7491	7.7070	6.2385	7.7070
Gfap	882.8350	1454.7600	1713.6700	1454.7600
Gk5	1.7871	2.1027	2.3386	2.1027
Glipr1	1.8093	5.7722	5.6472	5.7722
Glipr2	10.6991	15.2542	18.8391	15.2542
Gpnmb	6.5694	6.9728	8.5160	6.9728
Gpr160	1.1212	1.9154	2.6774	1.9154
H2afz	169.4800	222.3960	233.4820	222.3960
Hebp1	7.7873	10.2571	11.4184	10.2571
Hexb	62.4973	72.7913	75.3934	72.7913
Hist1h4b	0.0000	0.0000	0.0000	0.0000
Hist1h4b	0.2239	0.1569	0.0000	0.1569
Hist1h4b	15.2929	25.7766	16.1199	25.7766
Hist1h4b	1.6799	1.9930	2.0836	1.9930
Hist1h4b	1.6799	2.5077	2.0415	2.5077
Hist1h4b	5.3906	3.9675	2.9435	3.9675
Hist1h4b	5.9303	6.2931	7.9167	6.2931
Hjurp	0.6120	1.2756	1.3896	1.2756
Hk2	2.7408	4.0945	4.4602	4.0945
Hpcal4	17.8030	24.5438	21.0012	24.5438
Hspa5	162.5670	178.7870	200.0860	178.7870
Ifit1	0.4391	0.3975	2.2242	0.3975
Ifitm3	18.5436	22.9414	26.3760	22.9414

Ifngr1	28.8008	36.0090	38.2261	36.0090
Igf2	9.1011	8.5565	7.8675	8.5565
Igfbp2	35.0077	25.5312	23.1669	25.5312
IL16	0.7971	1.6257	1.7594	1.6257
IL21r	0.4194	1.4812	1.5965	1.4812
IL6	0.0828	0.7634	1.2689	0.7634
Iqgap3	0.5013	1.0835	1.2575	1.0835
Irf5	5.7821	9.8562	11.0049	9.8562
Irgm	2.5924	3.8781	3.7717	3.8781
Itgb2	4.7391	11.5817	13.2113	11.5817
Itgb3	1.1186	1.3357	1.8963	1.3357
Itih3	215.6620	280.9860	320.7850	280.9860
Itpripl1	1.5749	1.9022	2.4373	1.9022
Itpripl2	1.2763	1.5196	1.9559	1.5196
Junb	9.9262	11.4295	14.5028	11.4295
Kif15	0.7439	1.0745	1.2854	1.0745
Kif18a	0.3453	0.6656	0.8690	0.6656
Kif4a	0.3607	1.0449	1.3031	1.0449
Kifc1	1.0876	3.1255	3.6687	3.1255
Kpna2	10.5565	14.8845	16.1774	14.8845
Laptm5	16.9348	28.3463	34.2434	28.3463
Lat2	5.3309	13.6632	17.1886	13.6632
Lcp2	2.4281	4.3885	5.3891	4.3885
Ldha	65.8533	82.8879	90.6442	82.8879
Lgmn	97.6214	118.8510	128.6490	118.8510
Lmnb1	4.1785	7.5288	8.4106	7.5288
LOC100359539	2.5442	5.7217	6.5788	5.7217
LOC100360087	17.0202	19.9449	22.6780	19.9449
LOC100360977	35.7056	34.4981	34.0468	34.4981
LOC100909521	64.2320	79.1706	84.6701	79.1706
LOC100910384	7.5096	5.9348	5.3962	5.9348
LOC100910474	0.0000	0.0000	0.0000	0.0000
LOC100910474	114.7720	116.4570	113.5860	116.4570
LOC100911372	39.9978	47.5368	50.0421	47.5368
LOC257642	0.0000	0.0000	0.0000	0.0000
LOC257642	0.0000	0.0000	0.0000	0.0000
LOC257642	100.6580	101.6240	85.2608	101.6240

LOC257642	1.4737	6.8573	3.1427	6.8573
LOC680329	0.0750	0.2452	0.0000	0.2452
LOC681458	3.2808	3.5965	2.2103	3.5965
LOC685186	6.1731	7.1953	6.3708	7.1953
LOC688459	1.8043	2.1089	2.9707	2.1089
LOC691909	1.0860	1.5468	1.8986	1.5468
Lrrc25	0.2157	1.7120	1.9844	1.7120
Lyc2	0.0227	0.1073	0.2227	0.1073
Lyc2	30.3928	40.8013	46.4464	40.8013
Lyn	5.4320	10.9277	13.5549	10.9277
Man2b1	15.5229	16.3908	18.3864	16.3908
Mapkapk2	23.7324	29.4886	30.7712	29.4886
Mastl	0.6587	0.9703	1.2014	0.9703
Mcm2	3.1312	5.8252	6.4913	5.8252
Mcm4	7.4162	8.7860	9.9897	8.7860
Mcm5	1.1874	4.6154	5.6750	4.6154
Mcm6	2.4305	5.2447	6.6663	5.2447
MGC112715	23.9032	28.5338	31.1065	28.5338
Mlxipl	0.3223	0.0677	0.4783	0.0677
Mlxipl	3.9965	5.3081	6.2499	5.3081
Mmp19	1.7813	2.5083	3.0908	2.5083
Ms4a6a	1.7248	4.0821	5.4469	4.0821
Mt1	0.9616	1.9814	2.5007	1.9814
Mt1	28.4930	44.4945	66.1744	44.4945
Mx1	1.0336	2.3577	3.0331	2.3577
Myh6	2.5070	1.7065	2.0751	1.7065
Nbea	32.0413	31.9833	26.6268	31.9833
Ncf1	7.2834	9.7059	10.8416	9.7059
Neb	0.9106	0.5636	0.6528	0.5636
Nlrc4	0.7743	1.4215	1.4043	1.4215
Nmi	8.0695	10.1780	10.7401	10.1780
Nmu	4.2840	8.4515	7.4764	8.4515
Nt5e	7.2788	8.8470	10.3877	8.8470
Nuf2	1.2811	2.6361	3.0254	2.6361
Nusap1	0.5652	3.1083	3.5194	3.1083
Pabpc1	57.2534	74.0510	80.8532	74.0510
Parp4	9.8354	8.5599	11.1670	8.5599

Parvg	1.6000	3.6416	4.4382	3.6416
Pclo	3.7684	4.0503	4.0080	4.0503
Pcna	49.5355	59.6716	65.2612	59.6716
Pdlim1	4.9810	5.5475	6.7519	5.5475
Pdlim4	23.9078	31.4744	36.7527	31.4744
Pdpn	18.2372	22.0629	26.4197	22.0629
Pex11a	9.2418	6.5244	9.3334	6.5244
Pik3cg	1.6275	3.1005	3.4648	3.1005
Pla2g4a	5.6951	9.2182	9.8290	9.2182
Pld5	12.2670	9.5382	8.9192	9.5382
Plk1	0.6099	2.3530	2.7619	2.3530
Pnma1	0.9035	1.3228	0.6792	1.3228
Pot1b	2.1605	1.8147	3.1436	1.8147
Psmb10	19.2459	25.5140	26.5872	25.5140
Psmb8	3.6915	6.6409	10.0446	6.6409
Ptk7	3.1331	4.3969	4.8165	4.3969
Ptprc	1.7278	3.8288	4.9535	3.8288
PVR	1.8309	2.0509	2.9904	2.0509
Rab32	4.1089	7.3071	9.2286	7.3071
Rbm3	58.0436	67.4283	71.8630	67.4283
Rcan1	24.0423	27.6578	30.4241	27.6578
RGD1310335	0.1389	0.3886	0.7673	0.3886
Rn50_6_1241.2	2.1714	2.8749	3.0777	2.8749
Rn50_6_1241.2	3.0488	3.8066	4.5156	3.8066
Rpl36al	14.2283	16.5995	17.5068	16.5995
Rpl36al	237.2630	226.1470	233.0180	226.1470
RT1-CE7	8.2074	14.2265	13.5927	14.2265
Sass6	0.9624	1.7217	1.3787	1.7217
Sass6	1.2363	1.4656	1.4630	1.4656
Scg2	163.8420	210.2140	210.0000	210.2140
Scpep1	20.0110	26.7512	28.9354	26.7512
Sdc1	1.6072	2.1548	2.4417	2.1548
Serp1	59.6478	66.0427	69.6627	66.0427
Serpina3n	1.3939	5.8061	8.0145	5.8061
Sh2d1b	5.1810	9.2774	9.3695	9.2774
Sh3bp2	2.3748	3.0018	3.7610	3.0018
Shc1	8.6028	11.2553	11.9758	11.2553

Shcbp1	1.4504	2.8060	3.7605	2.8060
Shisa8	5.1573	8.0577	6.0376	8.0577
Sirpa	39.1963	46.5503	50.0504	46.5503
Slc14a1	32.5553	39.4237	40.3985	39.4237
Slc15a3	2.4931	3.6845	4.0822	3.6845
Slc38a2	71.0499	73.8181	58.2383	73.8181
Slc38a5	2.5157	4.7960	7.0034	4.7960
Slc5a7	61.1163	44.1452	42.4633	44.1452
Snrpg	64.5916	72.8048	80.1057	72.8048
Soat1	7.2762	10.1884	10.8938	10.1884
Sorbs1	34.7735	38.7941	42.0500	38.7941
Sox11	0.8648	1.7699	1.9813	1.7699
Sp140	0.9298	2.4721	2.7394	2.4721
Spi1	4.6365	12.0679	13.7204	12.0679
Sst	204.5510	254.0750	226.5340	254.0750
Stat1	18.9949	22.0935	24.0655	22.0935
Stat3	30.9625	39.7823	43.7674	39.7823
Stat6	3.3581	4.6231	5.4362	4.6231
Steap4	0.3375	0.5797	0.6007	0.5797
Susd3	2.6600	3.4171	3.9577	3.4171
Tac1	43.6217	77.3739	70.3226	77.3739
Tac3	26.7070	37.3271	28.6323	37.3271
Tagap	0.3547	1.0377	1.3243	1.0377
Tal1	1.8660	2.2929	2.5337	2.2929
Tax1bp3	9.5466	14.2174	15.0235	14.2174
Tbxas1	0.9515	2.6113	2.9133	2.6113
Tgm2	6.0752	6.8921	8.6524	6.8921
Thrsp	10.7524	10.5931	11.5503	10.5931
Tle3	7.8970	9.4573	10.2128	9.4573
Tlr6	1.0277	1.5652	1.5775	1.5652
Tmem156	0.3227	0.6743	0.9021	0.6743
Tmem216	16.8607	18.2700	16.3220	18.2700
Tmsb4x	1927.8300	2217.3100	2336.4000	2217.3100
Tnfaip8l2	4.0980	8.2667	8.9378	8.2667
Trim45	5.0656	3.9237	3.7284	3.9237
Trim55	0.3877	0.7638	1.0288	0.7638
Troap	0.3026	1.4084	1.5568	1.4084

Tspan8	4.8876	4.0234	5.5684	4.0234
Tubb6	3.6819	4.4953	5.6913	4.4953
Tyrobp	27.7210	80.3660	94.3939	80.3660
Uba7	1.6844	2.3505	2.5070	2.3505
Ube2t	0.4700	1.6088	1.3861	1.6088
Uhrf1	1.2675	3.0532	3.5670	3.0532
Unc13d	0.9427	1.4972	1.6500	1.4972
Upp1	6.2525	8.6105	11.3379	8.6105
Was	1.3190	2.6434	3.8992	2.6434
Wdhd1	1.6900	2.1384	2.3196	2.1384
Wsb1	61.9521	63.3685	71.2862	63.3685
Xbp1	41.0026	45.5079	53.1682	45.5079
Zgrf1	0.5705	0.6637	0.7160	0.6637